EPA

Research and Development

Application of Pollution Prevention
Techniques to Reduce Indoor Air Emissions
From Aerosol Consumer Products

Prepared for

Office of Prevention, Pesticides, and Toxic Substances

And

Office of Radiation and Indoor Air

Prepared by

National Risk Management
Research Laboratory
Research Triangle Park, NC 27711

Foreword

The U.S. Environmental Protection Agency is charged by Congress with protecting the Nation's land, air, and water resources. Under a mandate of national environmental laws, the Agency strives to formulate and implement actions leading to a compatible balance between human activities and the ability of natural systems to support and nurture life. To meet this mandate, EPA's research program is providing data and technical support for solving environmental problems today and building a science knowledge base necessary to manage our ecological resources wisely, understand how pollutants affect our health, and prevent or reduce environmental risks in the future.

The National Risk Management Research Laboratory (NRMRL) is the Agency's center for investigation of technological and management approaches for preventing and reducing risks from pollution that threaten human health and the environment. The focus of the Laboratory's research program is on methods and their cost-effectiveness for prevention and control of pollution to air, land, water, and subsurface resources, protection of water quality in public water systems; remediation of contaminated sites, sediments and ground water; prevention and control of indoor air pollution; and restoration of ecosystems. NRMRL collaborates with both public and private sector partners to foster technologies that reduce the cost of compliance and to anticipate emerging problems. NRMRL's research provides solutions to environmental problems by: developing and promoting technologies that protect and improve the environment; advancing scientific and engineering information to support regulatory and policy decisions; and providing the technical support and information transfer to ensure implementation of environmental regulations and strategies at the national, state, and community levels.

This publication has been produced as part of the Laboratory's strategic long-term research plan. It is published and made available by EPA's Office of Research and Development to assist the user community and to link researchers with their clients.

E. Timothy Oppelt, Director
National Risk Management Research Laboratory

EPA REVIEW NOTICE

APPLICATION OF POLLUTION PREVENTION TECHNIQUES TO REDUCE INDOOR AIR EMISSIONS FROM AEROSOL CONSUMER PRODUCTS

By

Charlene W. Bayer
Electro-Optics, Environment & Materials Laboratory
Georgia Tech Research Institute
Atlanta, Georgia 30332-0820

Richard A. Browner and Stacy Ho
School of Chemistry & Biochemistry
Georgia Institute of Technology
Atlanta, Georgia 30332-0400

Leslie L. Christianson, Ling Ying Zhao, Per Heiselberg, Mike E. Tumbleson, and Michael M. Cui
Biochemical Engineering Research Laboratory
University of Illinois at Urbana-Champaign
1304 W. Pennsylvania Avenue
Urbana, Illinois 61801

Abstract

Aerosol consumer products potentially are amenable to pollution prevention strategies that reformulate or redesign products, substitute raw materials, or improve consumer use procedures. A basic understanding of the behavior of aerosol consumer products is essential in the development of pollution prevention strategies, which may reduce occupant exposures and guide manufacturers in the development of more efficacious, less toxic products. This research project was undertaken to develop tools and methodologies to measure aerosol chemical and particle dispersion through space. EPA's National Risk Management Research Laboratory sponsored a cooperative agreement with the Georgia Tech Research Institute (GTRI), and the University of Illinois (UI) to develop tools and methodologies to measure aerosol chemical composition and particle dispersion through space. These tools can be used to devise pollution prevention strategies that could reduce occupant chemical exposures and guide manufacturers in formulating more efficacious products. The GTRI researchers built an Aerosol Mass Spectral Interface (AMSI), which is interfaced with a mass spectrometer (MS), that chemically characterizes aerosol consumer products through space. The UI researchers developed techniques for measuring aerosol movement indoors by tracking particle size changes via particle velocity measurements using particle image velocimetry (PIV). A group of Industry Partners participated in this research project to ensure that the technologies developed would be useful to industry.

The AMSI was designed, constructed, and optimized to transfer a focused beam of aerosol particles into a mass spectrometer for chemical analysis. It was shown experimentally during this project that the AMSI can quantitatively detect compositional changes as the aerosol travels through space. These data provide important information for the formulating of aerosol consumer products for pollution prevention strategies. The PIV system demonstrated a correlation between the material properties of the aerosol components and the spray pattern. These data were used to develop a model for prediction of the major characteristics of aerosol spray patterns. The model can be a useful guide for developing pollution prevention strategies.

This report was submitted in fulfillment of grant number CR822007 under the sponsorship of US EPA. This report covers a period from July 1994 to September 1997, and was completed as of December 31, 1997.

Table of Contents

Contents (Cont.)

List of Tables

List of Figures

Figures (Cont.)

Acknowledgments

1.0 Introduction

1.1 Background

The U.S. EPA has identified indoor air quality (IAQ) as one of the most important environmental risks to the Nation's health (1 & 2). IAQ mitigation approaches generally have focused on techniques such as ventilation and source elimination or removal. In the Pollution Prevention Act of 1990 (3 & 4), Congress declared that pollution should be prevented or reduced at the source whenever feasible. Modification of equipment, processes, and procedures; reformulations or redesign of products; substitution of raw materials; and/or improvements in use procedures may accomplish source reduction.

The U.S. chemical specialties industry is a $50 billion industry employing more than a million people (5). The products provided by the chemical specialties industry include aerosol consumer products for such uses as personal care, household cleaning, laundry, pest control, and automotive maintenance. Aerosol consumer products are an important segment of this industry. Since the development of the aerosol packaging system during World War II, aerosol consumer product usage has advanced in the U.S. to nearly three billion aerosol products used each year and more than 1500 individual aerosol products (5).

Aerosol consumer products potentially are amenable to pollution prevention strategies that reformulate or redesign products, substitution of raw materials, and improvement in use procedures. For example, the tools developed under this project may provide the manufacturers with data showing that products can be reformulated, thereby reducing the required amount of active ingredient. For example, if 50% more of the active ingredient is reaching the use site than is needed for efficacy, the manufacturer may be able to reduce the amount of active ingredient in the product accordingly.

A basic understanding of the behavior of aerosol consumer products can be used to develop pollution prevention strategies, which may reduce occupant exposures and guide manufacturers in the development of more efficacious products. This research project was undertaken to develop tools and methodologies to measure aerosol chemical and particle dispersion through space. EPA's National Risk Management Research Laboratory sponsored a cooperative agreement with the Georgia Tech Research Institute (GTRI), and the University of Illinois (UI) to develop tools and methodologies to measure aerosol chemical composition and particle dispersion through space. These tools can be used to devise pollution prevention strategies that could reduce occupant chemical exposures and guide manufacturers in formulating more efficacious products. The GTRI researchers built an Aerosol Mass Spectral Interface (AMSI), which is interfaced with a mass spectrometer, that chemically characterizes aerosol consumer products through space. The AMSI/MS is unique in that it measures the spatial chemical composition of the aerosol stream, rather than the more conventional technique of measuring the chemical composition of single aerosol particles. The UI researchers developed techniques for measuring aerosol indoors by tracking particle size changes via particle velocity measurements using particle image velocimetry (PIV). This technique was used to develop a model to predict the major characteristics of aerosol spray patterns. A group of Industry Partners participated in this research project to ensure that the technologies developed would be useful to industry.

1.2 Traditional Aerosol Analysis

An aerosol (aerodispersed system) consists of a gas (dispersion medium) in which liquids or solid substances may be dispersed (6). An aerosol is an unstable system, changing its concentration and particle-size distribution with volume and time. Aerosols can also change their state from solid to liquid and vice versa (6). The transient nature of an aerosol makes aerosol characterization an analytical challenge.

In the aerosol package, a gas is put under enough pressure to liquefy the gas. When the package nozzle system is activated, the pressure is relieved, and vaporization occurs. An aerosol can is kept closed by a stem gasket, which seals the opening under the nozzle button. This gasket is held in place by a spring inside a housing. When the nozzle button is pressed, it pushes the valve stem down against the spring, relieving the pressure and keeping the gasket sealed. When the seal opens, the higher pressure inside the can pushes the product through the dip tube and out of the valve. A controlled amount of propellant in the product vaporizes as it leaves the can, creating the aerosol spray. A small amount of the liquefied propellant still in the container also vaporizes, maintaining the pressure constant. The combination of product and propellant is finely tuned to produce the correct concentration, spray pattern, and particle size for an effective product. The spray nozzle system is developed for each product. Similar products, such as aerosol deodorizers with different scents, must each have the spray nozzle system developed for each scent for effective delivery of the product to the use-site.

Aerosol analysis has traditionally focused on both particle size and distribution measurement or the chemical analysis by collecting a time-weighted average sample of the aerosol (7). The aerosol industry usually determines aerosol particle size via measurement of the spray particle-size distribution via forward light scattering (8). A Malvern Particle Sizer is usually the instrument used for this particle-sizing time-averaging analytical technique (8 & 9). The Malvern system uses particle light scattering as its detection technique and has an accurate particle-size range of 1.2 – 1000 µm. The light scattering angle is inversely proportional to the particle size. This method provides no data about the chemical composition of the measured aerosol.

Aerosol chemical composition by the indoor research community traditionally has focused on collecting a time-weighted average sample of the aerosol on a filter, which is then extracted and analyzed by a chromatographic, MS, or other analytical technique (7 & 10). The industry primarily uses two different methods for determining the volatile content in aerosol formulation. The first is a vacuum distillation method that is applicable to anhydrous aerosols that do not contain methylene chloride or volatile active ingredients (11). This method evaporates away, under vacuum, the propellant and other volatile components from an aliquot of the aerosol liquid, which has been withdrawn from the aerosol package. The remaining nonvolatile residue is weighed, and the total percent of nonvolatile components is calculated.

The second method, the Densimetric Method, is applicable for the determination of the volatile content of essentially anhydrous aerosol products with nonflammable propellants, which do not contain solids at low temperature (12). This method is based on the fact that, under isothermal conditions, the density of an aerosol formulation is almost a linear function of the volatile or nonvolatile content. This method is primarily used for production control procedures. The aerosol consumer product sample is chilled to approximately $-3O^{\circ}C$. The dispenser is punctured, and the contents of the package are poured into a chilled hydrometer. The density is recorded. The composition is calculated from the density by comparing the sample results with those from a series of known standards via linear regression analysis.

The analysis of aerosol dispersion and fate in rooms traditionally has been conducted by crude analytical techniques. Spray cone analysis, depiction of the three-dimensional analysis of the liquid particles, has been done typically by using indicator paper as a target for a sprayer actuated at a specified distance (13). When the spray hits the target indicator paper, a two-

dimensional image is formed, which indicates the relative cone pattern and density. It has been recognized for some time that real-time, on-line analytical methods are necessary to accurately understand the environmental and human exposure impacts of aerosol products, but to date these methods do not exist.

The focus on real-time methodology development for aerosol products for environmental impact assessment, to date, has been on outdoor aerosols. Several different analytical systems for single particle aerosol analysis have been under investigation. The integration of MS and laser desorption techniques, particularly time-of-flight (TOF) MS has received considerable attention (14-18). This integrated system has been successfully used for the elemental analysis of single aerosol particles. The system is capable of measuring the aerodynamic size and chemical composition of the particles *in situ*. This type of system is used for outdoor aerosol analysis since these aerosols are generally less complex and much more dilute than the aerosols produced by consumer products.

2.0 Conclusions

The tools and methodologies developed under this research project can be used to better understand aerosol consumer product behavior. Once this understanding is achieved, then effective pollution prevention strategies can be designed. Potential pollution prevention strategies include product reformulation, raw materials substitution or more pure raw materials use, and clearer instructions to end users. The tools developed under this project may provide the manufacturers with data showing that products can be reformulated reducing the required amount of active ingredient.

The primary objective of this research project was to develop tools and methodologies to characterize aerosol consumer products in space, which could then be used to develop pollution prevention strategies.   In order for pollution prevention strategies to be devised, it is necessary to understand the basic behavior of aerosol consumer products during use. This aim was accomplished successfully by the design and construction of the AMSI for measuring aerosol particle chemical compositional changes during dispersion through space and the PIV for measuring dispersion of aerosol particles through space via velocity measurements.

2.1 Chemical Composition

The AMSI can be used by the industry, to determine the chemical composition of aerosol particles through space. Knowing the chemical composition and the changes in the chemical composition during particle dispersion through space may guide the industry to make more efficacious products and devise pollution prevention strategies through product reformulation.

The AMSI was designed, constructed, and optimized to transfer a focused aerosol beam of particles into a mass spectrometer for chemical analysis. It was shown experimentally that the AMSI could detect compositional changes through space, and that the AMSI was transferring aerosol particles into the mass spectrometer.   The data obtained in this project indicate that the AMSI/MS has the potential for quantitative analysis, but further study is required to confirm this.

An additional experiment was conducted to ascertain that the AMSI was transferring aerosol particles in the MS. One function of the AMSI is to strip the propellant solvent from the aerosol particles prior to transference of the particle into the MS. It was necessary to show that aerosol particles remain after this stripping occurs. This was done using a Helium/Neon laser to cause forward off-angle light scattering with photodiode array detection of scattered light. The detection of light energy above baseline indicates the presence of particles while gases do not scatter light. Increased light intensity above baseline from particles exiting the AMSI nozzle while spraying two of the surrogate aerosols (see section 5.1) into the AMSI indicated that aerosol particles were exiting the AMSI and being transferred into the MS.

One important finding from the chemical compositional research was the importance of the purity of the starting materials to make the aerosols. A contaminant was found in the sodium lauryl sulfate (SLS) used to make the test aerosols. This contaminant was also detected in each of the test aerosols containing SLS. This shows the importance of pure starting materials. This type of data, which can be determined with the AMSI/MS, can help the industry to formulate the most pure and least polluting products.

2.2 Particulate Behavior

Particle size changes are an important aspect of aerosol consumer product behavior and performance. Changes in particle size indicate aerosol agglomeration, resulting in increasing particle size and slower velocities, or component evaporation, resulting in decreasing particle size and increasing velocities. Aerosol agglomeration can prevent the transport of the particles to the use site, reducing product efficacy since gravitation fall-out of particles is greater for larger sized particles. The evaporation of components from the aerosol during travel to the use site can prevent active components from reaching the use site and can result in increased pollutant transference from the liquid medium to the airborne medium. An understanding of these ongoing phenomena can provide pollution prevention strategies for product reformulation.

The PIV system was developed to measure particle size via velocity measurements during aerosol dispersion through space. This camera system allows for the non-intrusive, whole field measurement of aerosol particle dispersion through space. Particle velocities and the spatial structure of the particle movements were measured. Additionally the effects of ventilation on the transport of the particles were determined. This is an important parameter for source control via ventilation pollution prevention strategies in the indoor environment.

A PIV system was used to determine the particulate characteristics of the spray cone of aerosol consumer products. The PIV was used to measure particle concentrations and velocity distributions. These techniques were used in an environmental chamber to investigate the effect of localized air flow patterns on particle concentration distributions as the aerosols are transported through space in the indoor environment.

The results from this research project showed that particle transport in room airflow is influenced primarily by gravitation, convection, and eddy diffusion resulting from turbulent velocities.   These forces generate differences in particle concentration and particle size distribution throughout a room. Particle movement depends on characteristics of the local airflow conditions.

Important findings about the particulate behavior of aerosol consumer products were that compressed gas propellants appeared to result in a wider distribution of particle sizes than hydrocarbon propellants, and the velocity of the aerosol particles decreased with increasing distance from the aerosol spray nozzle. More than 90% of the particles were found to be greater than 25 μm in size. It was also found that room air ventilation did have an effect on aerosol particle concentration distribution. The particle distribution was stratified so that the particles were densest in the lower portion of the room and more dilute in the upper portions of the room.

A simplified engineering model was developed to predict the mass, momentum, and energy flux over space of aerosol consumer products – critical factors for evaluation of aerosol consumer product efficacy. The velocity of the aerosol particles in the hydrocarbon propellant driven sprays appeared to be increasing near the spray nozzle. This may have been caused by evaporation of the liquid propellants near the spray nozzle. The velocity peaked at a distance of 20 mm from the nozzle, and then decreased as the distance from the nozzle increased, probably due to air drag. This mechanism appeared to control the atomization process near the spray nozzle.

3.0 Recommendations

The tools and methodologies developed under this research project can be used to better understand aerosol consumer product behavior. Once this understanding is achieved, effective pollution prevention strategies can be designed. The tools developed under this project may provide the manufacturers with data showing that products can be reformulated reducing the required amount of active ingredient. For example, if 50% more of the active ingredient is reaching the use site than is needed for efficacy, the manufacturer can reduce the amount of active ingredient in the product by 50%. This information can be obtained using the tools developed during this research project.

The primary recommendation resulting from this project is that the manufacturers begin using these tools to study their products. The products can be studied to determine the chemical composition of the products when they reach the use site and determine the minimum amount of active ingredients necessary for efficacy. The manufacturers can investigate the effects of product dispersion, and the effects of room air movement on dispersion, to better guide consumers on actual use conditions. An understanding of the dispersion chemically can aid in reformulations that minimize cross-media transference during use.

3.1 Technology Costs

Since the AMSI is not commercially available and must be machined, the costs are dependent upon the individual machine shop. In general, the cost of the AMSI should be below $1000. The AMSI, in its current form, must be interfaced with a MS with PB or electrospray (or ion spray) capabilities and preferably with MS/MS capabilities. These systems range from $150,000 to $500,000, depending on the sophistication. Once the AMSI/MS is operating the analytical costs will range from a few tens to a few hundreds of dollars per sample. Analysis requires a few minutes of time per sample. Data interpretation requires the greatest amount of time and is dependent upon the skill and knowledge of the operator. As a laboratory builds a database of aerosol products, data interpretation can be cut down to a few minutes of time per sample.

The final costs of the PIV system are dependent on the particular instrument manufacturer and features of the component parts. Generally the cost of a system to measure aerosol dispersion through space is about $75,000 to $90,000. The time requirements for measurement of aerosol dispersion are considerable since the data interpretation is a labor-intensive process. Characterization of the aerosol spray pattern requires approximately one hour for data collection, approximately six hours to calculate concentrations, and approximately 12 hours to calculate the velocity distributions.

3.2 Technology Limitations

There are limitations to the tools developed under this project. The majority of these limitations can be overcome with additional research.

The AMSI is only applicable to aerosols that exit the nozzle in a spray form, using either propellant or pump spray systems. Aerosols that are ejected as foams or gels cannot be introduced into the MS by the AMSI. Also, high viscosity aerosols that are released primarily as dry particles, such as spray powders or paints, will quickly contaminate the AMSI and MS during analysis. This limitation will be extremely difficult to overcome, and probably cannot be

eliminated with the current AMSI design. These types of products will require a different type of sample introduction method.

Particle size selection with the AMSI is not currently calibrated. It was shown experimentally that the numbers of smaller particle being transferred into the MS from the AMSI are reduced, but it is not possible to give the range of particles that are being transferred into the MS.

The developed PIV system allows for the determination of two-dimensional structures of full-scale room air flows and particle concentration. Two cameras or holograms are required to measure particle dispersion in three-dimensional space. The current system measures particle velocities within 5% accuracy for particles greater than 100 μm in size. A newer and faster PIV system would increase speed and simplify fate and transport measurements, thus allowing for smaller particles to be measured with increased accuracy.

4.0 Technical Approach

Spatial dispersion of aerosols through space can be divided into two different components: chemical compositional behavior and particulate dispersional behavior. The GTRI researchers primarily focused on development of the chemical compositional behavior tools, and the UI researchers focused on the particulate dispersional behavior tools. The Industry Partners provided invaluable guidance and assistance assuring that the approaches used by the university researchers would result in useful methodologies and tools. Over a four-year period, ten meetings were held with the Industry Partners to maintain interaction and guidance among the researchers, U.S. EPA, and the Industry Partners. Additional discussions were held with individual Industry Partners during the project via telephone, e-mail, and meetings. A final meeting was held in December 1997, at the annual meeting of the Chemical Specialties Manufacturers Association, to report on the results of the project to the industry. The Industry Partners met once without the university researchers or the U.S. EPA project officer to develop a scheme to allow the researchers to investigate the many types of aerosol products without having to investigate hundreds of products. Also to maintain the objectivity of the project, the Industry Partners wanted to avoid using actual products to develop the methodology since this could put a few manufacturers at risk. The Industry Partners developed a scheme of surrogate aerosols to represent the many types of aerosol consumer products without testing of actual products (discussed in Section 5.1). These surrogate aerosols were formulated and provided to the university researchers as needed by the Industry Partners upon request by the university researchers. The Industry Partners also provided GTRI with four blinded aerosol consumer products that were actual products to test their chemical characterization system on real products.

Aerosol chemistry has the possibility to result in chemical compositional changes as the aerosol disperses through space. These changes can be the result of chemical reactions, chemical decomposition, particle agglomeration, and/or solvent evaporation. These changes will be occurring dynamically as the aerosol travels through space. The GTRI researchers developed the AMSI to be interfaced with a MS so that these changes could be measured (discussed in Section 5.2). Two types of MS's were used. One with a particle beam (PB) liquid chromatographic (LC) interface, and one with an atmospheric interface. It was necessary to introduce the aerosol spray into the MS system as an aerosol; therefore, the MS design had to be capable of handling this type of sample form. The AMSI was designed to transfer a focused aerosol beam into the MS separating the propellant from the remainder of the aerosol droplets. By using MS/MS techniques, it was possible to separate the complex mixture into its component parts, in a manner similar to a chromatographic separation. The separation is performed by MS/MS using multiple quadrupoles in series so that the ions passing through the quadrupole mass filters the ions are separated.

The UI researchers used PIV and modeling to develop particulate dispersional behavior tools (discussed in Section 5.3). The PIV system was used to determine the three-dimensional, constantly changing spray cone characteristics by measuring the particle concentrations and velocity distributions. The characteristics of the spray cone as the liquid particles are ejected from the spray nozzle are a major factor in the behavior of the aerosol as it is dispersed through space. Localized airflow patterns also can affect the dispersion of the aerosol through space; therefore, the PIV system, in conjunction with an environmental chamber, was used to investigate the influence of localized airflow patterns on aerosol spatial dispersion. The PIV data were then used to develop a model for predicting the major characteristics of aerosol spray patterns.

5.0 Methods, Results, and Discussion

A description of the Surrogate Aerosols is given in Section 5.1. The chemical compositional methods and results are discussed in Section 5.2. The particle spatial dispersion methods and results are covered in Section 5.3.

5.1 Surrogate Aerosols

The "World of Aerosols" is immense. In 1993, 340 new products were introduced (19). A major task was the development of a classification scheme representative of most of the industry, yet which would divide the industry into a manageable size for meaningful data. Also to maintain the scientific integrity of the project and full cooperation of the Industry Partners, it was important that the research focus on generic products rather than any specific manufacturers' formulations. Since the purpose of the project was to develop generic tools and methods that could be used by the industry as a whole to develop pollution prevention strategies, it was important to focus on the end-use of products rather than specific formulations. Aerosol consumer products are formulated and packaged so that their dispersion results in the products properly reaching the use site in the appropriate physical form and chemical concentration. For example, a hair spray is designed to disperse in very fine droplets with a wide spray cone. A pesticide is designed with a minimally dispersed spray cone for a maximum amount of product stream reaching the use site over a distance of several feet.

Based on this information, it was decided that to develop effective tools and methods on aerosol dispersional behavior, the aerosol classification scheme should focus on product uses since this would have the greatest influence on spatial dispersion. Furthermore, it was decided that generic products could be used in this project, since there was no value added by using specific products. A list of twelve surrogate aerosols was developed by the Industry Partners, representing common formulations and uses: 1) surface wipe aerosols, 2) surface non-wipe aerosols, 3) and air aerosols. The latter two further subdivided into the categories of liquefied hydrocarbon propellant and compressed gas propellant aerosols, since the propellant system could have an influence on aerosol spatial dispersion; and therefore, could be important in the design of pollution prevention strategies. Also, the surface wipe and surface non-wipe surrogates were tested both as pressurized and pump delivery systems. Pump delivery systems were included since these also could influence aerosol spatial dispersion and could be important in pollution prevention strategies. It is important to realize that pump delivery systems are not true aerosol consumer products since the product is not a liquefied product under pressure (5). Table 1 outlines the surrogate formulation matrix. The seven surrogate aerosols were designed, prepared, and supplied by the Industry Partners.

Table 1. Description of the surrogate aerosols.

Type	Water	Volatile Solvent	Nonvolatile Solvent	Propellant
Surface Wipe Aerosol (SWA)	QS[a]	Butyl Cellosolve[®b] 5%	SLS[c] 2%	A31[d] 10%
Surface Wipe Pump (SWP)	QS[a]	Butyl Cellosolve[®b] 5%	SLS[c] 2%	Trigger
Surface Non-wipe 1 (SNW1)	0%	Ethanol 67.5%	Silicone 7.5%	A46[d] 25%
Surface Non-wipe 2 (SNW2)	0%	Ethanol 92.5%	Silicone 7.5%	QS[a]-CO_2[e]
Surface Non-wipe Pump (SNWP)	0%	Ethanol 92.5%	Silicone 7.5%	Fine mister
Air Aerosol 1 (AA1)	70%	Ethanol 10%	0%	A46[d] 20%
Air Aerosol 2 (AA2)	90%	Ethanol 10%	0%	QS[a]-CO_2[e]

[a]   QS = Quantity sufficient to bring to volume

[b]   Butyl Cellosolve[®] = BC

[c]   SLS = Sodium lauryl sulfate (a surfactant)

[d]   A31 and A46 = liquefied hydrocarbon propellant mixtures of propane and isobutane

[e]   Compressed gas propellant

The surrogate aerosols were formulated to be representative of three common aerosol product classifications. The surface wipe aerosols represent products such as household cleaners, dusting aids, and disinfectants. The only difference between SWA and SWP is that SWA is aerosolized via a hydrocarbon propellant, and SWA is aerosolized via a pump trigger nozzle. There were three different surface non-wipe surrogate aerosols: 1) SNW1 using a hydrocarbon propellant, 2) SNW2 using a compressed gas propellant, and 3) SNWP using a pump mister nozzle. These three surrogate aerosols represent such products as personal care products, pan no-stick sprays, paints, and adhesives. Two surrogate aerosols were representative of aerosols such as air fresheners and insecticides: AA1 and AA2. The only difference between AA1 and AA2 was the propellant. AA1 used a hydrocarbon propellant, and AA2 used a compressed gas propellant.

Also important in the formulation of the aerosol consumer product systems and in the design of the surrogate aerosols is the delivery of the aerosol to the site to its use site, the chemical composition, and the chemical composition and form of the product at its use site. The efficacy of the product is dependent on how and in what form it arrives at its use site. For example, a hairspray must be delivered to the hair as a gentle, wide spray that cannot bounce back off of the hair or it will not meet the user's needs. An insecticide must be delivered in a hard, tight spray that will reach the pest with a maximum quantity of product. The surrogate

aerosols were designed to represent the three common aerosol product classifications so that the importance of the aerosol delivery system as related to its intended use could be determined during the transport in room studies. Pollution prevention strategies formulated must account for the requirements of the end-use of the product.

5.2 Chemical Composition

The analytical strategy for aerosol chemical characterization was to design and construct an aerosol inlet interface, which would allow introduction of aerosols into a MS for aerosol chemical composition determination. The aerosol interface/MS system had to be able to measure the transient and complex chemical nature of the aerosol stream in real-time. Chromatographic separation of the components was not a feasible technique for separation of the chemical components of the aerosol products, since real-time analysis could not be achieved by chromatographic analysis. Therefore, MS/MS techniques were preferable. The MS/MS uses quadrupole mass analyzers in series. Ion separations can be achieved by ion filtering with the quadrupole mass analyzers.

The aerosol inlet interface developed had to provide quantitative data about the chemical compositional changes related to the distance of the aerosol particles from the aerosol spray nozzle (spatial chemical compositional changes) and chemical composition versus particle size distribution of the aerosol spray. Additionally, it was found during the course of this project that the aerosol inlet interface had to be able to cope with large sample quantities.

5.2.1 Aerosol Mass Spectral Interface

A PB approach (20 & 21) was used. The AMSI was designed, constructed, and optimized to collect and sort the aerosol particles from the aerosol consumer product and transfer a focused aerosol beam into a MS for compositional analysis (22). The AMSI is a portable inlet system for aerosol chemical analysis by MS. The aerosol product is analyzed in real-time using the MS to perform separations and chemical compositional analysis. Using a gas flow to steer the particles away from a straight-line trajectory (steering gas), the AMSI can be operated so that the aerosol particle-size distribution entering the MS can be controlled. The amount of smaller particles transferring into the MS is decreased with increasing steering gas flow. When no steering gas is applied, the entire distribution of particle sizes passes into the MS. When the steering gas is applied, fewer of the smaller size particles enter the MS; only the larger sized particles pass into the MS. By looking at the results obtained with no steering gas, and those with increasing amounts of steering gas, it is possible to use pattern recognition subtraction techniques to determine the chemical composition based on particle size (23-26). The development of these techniques for this application and the calibration of the particle size distribution as related to the amount of steering gas flow have not been done in this research project due to funding limitations. These are additional research avenues for pursuit.

The AMSI is essentially the momentum separator portion of a PB interface (20) (Figure 1). The PB interface is designed to couple a LC to a MS so that the eluting analyte and mobile

11

Figure 1. Detailed schematic of AMSI.
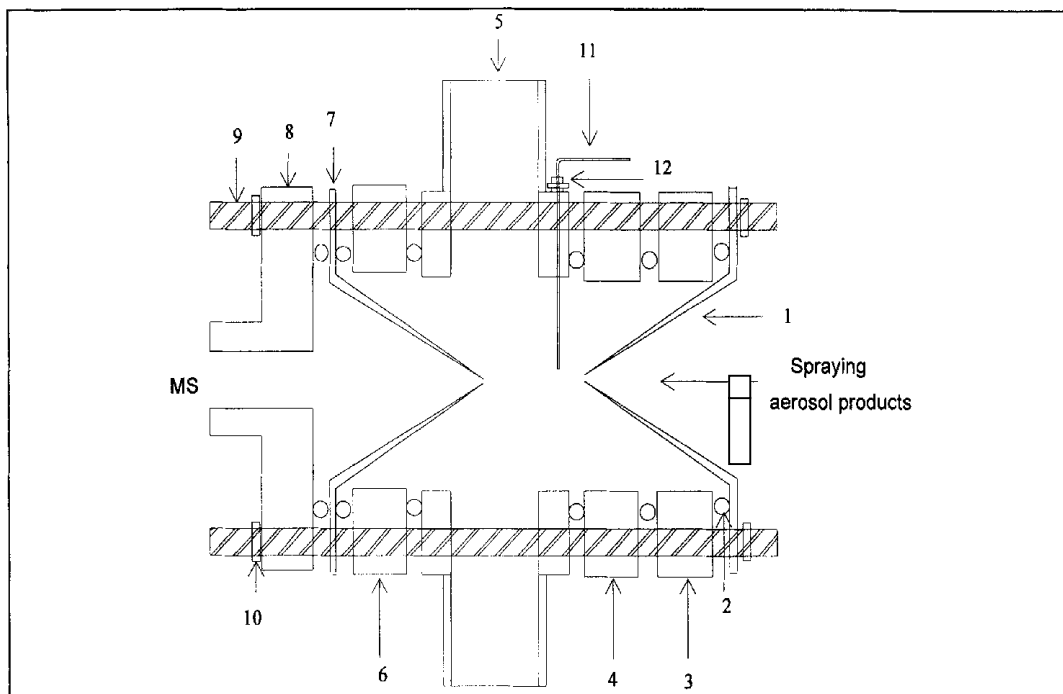
1. Nozzle. 2. O-ring. 3, 4, 6, Spacer. 5. Pump-out unit, for connecting vacuum hose. 7. Skimmer. 8. Connector, connects the AMSI to the MS. 9. Connecting rod. 10. Screw. 11. Gas line. 12. Swagelok® fitting.

phase mixture exiting the chromatograph can be converted to a form that can be analyzed by the MS. In the PB interface, the eluding mixture is nebulized by mixing with an inert gas, vaporized, and separated into the aerosol particles minus the mobile phase. Only the aerosol particles enter the MS. The momentum separator is the chamber in which the aerosol particles are separated from the mobile phase. The AMSI serves the function of the momentum separator separating the aerosol particles from the propellants. The AMSI functions like a two-stage jet separator. The separator is divided into two chambers, the first between the nozzle and the skimmer(s). The primary role of the skimmers is to sample only those aerosols moving in a straight trajectory, thereby focusing the aerosol beam. The aerosol consumer product package nebulizes the aerosol as it is ejected by mixing the ingredients with the propellant as it leaves the aerosol package; therefore, the nebulizer of the PB is unnecessary to the AMSI. Immediately after the aerosol beam formation by the AMSI nozzle, a stream of gas perpendicular to the beam axis is introduced to size-sort the particles based on their resistance to the steering gas flow. The AMSI is interfaced directly with a MS so that the aerosols are analyzed without sample collection or chromatographic separation. Two types of MS's were used; both designed for use with LC systems. One of the MS's was a quadrupole MS with a LC/PB inlet system. The second MS was a triple quadrupole system (MS/MS) designed with an atmospheric inlet system (API). The PBMS was used because it is a commonly available MS in many laboratories. This system is designed to handle a PB inlet system; therefore is readily adaptable to the AMSI. The API was selected because of its atmospheric inlet system (27 & 28). The atmospheric inlet allows for direct sampling of the aerosols from the AMSI. Early in the project, the aerosols were sprayed directly into the API. This method was unsuccessful since the direct introduction of the aerosols severely overloaded and contaminated the MS. The API is designed for ultratrace analysis and was unable to handle the large sample load introduced by the aerosol spray. The API triple quadrupole system allowed for sample separation to be done by the MS rather than the more conventional chromatographic system (27 & 29).

An experiment was done to ascertain that the AMSI was transferring aerosol particles into the MS even though it was known that PB technology passes "dry" aerosol particles into the MS from previous work (20 & 30). This was done using a 2-mm watt helium/neon laser to cause forward off-angle light scattering by the aerosol particles using photodiode array detection of scattered light. The detection of light energy above baseline indicates the presence of particles since gases do not scatter light. The laser was focused on the particles exiting the first sample stage immediately after the AMSI nozzle. The laser was set five degrees off-axis in order to detect forward-scattering light using a photodiode detector. Increased light intensity was detected above baseline from particles exiting the AMSI nozzle while spraying both SWA and AA1 into the AMSI, indicating that aerosol particles were exiting the AMSI and being transferred into the MS.

A number of issues and parameters had to be addressed during the development of the AMSI: 1) generation of standard aerosols, 2) analysis of the total aerosol product without propellant removal, 3) optimization of the AMSI design, 4) MS analysis of the surrogate aerosols and selection of identification and quantitation ions, 5) confirmation of the ability to quantitatively analyze aerosol chemical compositions through space, and 6) development of the particle distribution sizing system for relating aerosol particle chemical composition to particle size distribution. These six issues are discussed individually below,

5.2.2 Generation of Standard Aerosols

It was necessary to be able to generate aerosols of a standard size and composition. The standardized aerosol generation system was required for evaluation of the chemical characterization system under design, and for quantitation of detected chemical components. An oscillating capillary nebulizer (OCN) (patent pending), which generates aerosols with size distributions from 10 μm to $\leq$ 0.1 μm, was used to generate standardized aerosols (30 & 31). The OCN is a type of vibrating-orifice generator. Vibrating-orifice generators are designed to produce highly monodisperse aerosols and are considered to be primary particle-size aerosol generators (32). Standard aerosols, for this project, were generated using authentic standard mixtures resulting in standards of known compositions and concentrations over a range of liquid flows (1 μL/min to 1 mL/min).

Standard aerosols were generated for analysis of the surrogate aerosols using both authentic standards obtained from commercial chemical suppliers and bulk samples obtained from the Industry Partners. The bulk samples obtained from the Industry Partners were the compounds used to make the surrogate aerosols. Bulk samples were obtained as individual compounds and as the liquid mixtures used to prepare the surrogate aerosols.

5.2.3 Total Aerosol Consumer Product Analysis

The AMSI is designed to separate the aerosol particles from the propellant so that the non-propellant portions of the aerosol are enriched for MS detection. In many aerosol consumer products, the propellant is used as the solvent system or a major component of the solvent system.   The high concentration of propellants in the aerosol products versus the active ingredients was expected to mask the presence of the components of interest.   The Industry Partners did state that there were times when they wanted to be able to detect the propellants also. Therefore, the early analyses of the surrogate aerosols were done without the AMSI.

Initially the surrogate aerosols were sprayed directly into the API atmospheric inlet. However, the MS was too sensitive for this method of sample introduction, since the MS was designed for ultratrace analysis. The API was severely overloaded and contaminated by this

method of analysis. The API is designed to be unable to detect hydrocarbons, but it was possible to detect the hydrocarbon propellants with the API when the surrogate aerosols were sprayed directly into the atmospheric inlet. This probably was due to the large amount of sample entering the MS. When SWA was analyzed, only BC was detected. When AA1, AA2, SNW1, and SNW2 were analyzed, only the molecular ion for ethanol was detected. Only one or two sprays of the surrogate aerosols could be sprayed into the API before the system was excessively contaminated and had to be shutdown for maintenance. Both the ion spray and the heated nebulizer modes were tried with the same results. Then it was decided that the API was inappropriate for direct analysis of the aerosols without the AMSI.

The PBMS was then used for direct analysis of the surrogate aerosols. This method was successfully used for direct analysis of the aerosols when the nebulizing portion of the PB was removed so that the aerosols were sprayed directly into the expansion region of the interface (31). The mass spectrometer used for this series of experiments was an Extrel Benchmark™ MS equipped with a ThermaBeam interface (the Extrel version of the PB). The source temperature was set at 285°C. The system was operated in EI mode scanning from 35 to 550 amu. The surrogate aerosols were sprayed individually into the PBMS system with a continuous spray of approximately 8-9 seconds.

Initially the surrogate aerosol cans were held near the instrument inlet and sprayed. The width of the spray cone resulted in contamination of the outside of the MS. Over time the aerosol liquid was running down the instrument contaminating the system. A Plexiglas ™ box was designed to prevent the overspray from reaching the instrument. The spraying box was constructed of 0.64 cm thick Plexiglas™ with the dimensions of 396 cm length x 457 cm width x 366 cm height and open on one side. The open side is where the aerosol can is held for spraying. A hole the size of the MS inlet was drilled in the side opposite the open side. The spraying box was regularly cleaned to prevent cross-contamination from the analyses. The aerosol was held so that the spray was centered at the entrance hole from the box.

Large differences in response were found for the different types of surrogate aerosols when using this type of MS analysis. AA1 and AA2 contained no non-volatile components and gave the poorest signals. The aerosols containing silicone, SNW1, SNW2, and SNWP, gave the strongest signals. This probably is due to the high transport efficiency of silicone, which is probably the reason that silicone is used in the aerosol products. Unfortunately the silicone also severely contaminated the MS ion source resulting in frequent shutdowns for cleaning and maintenance. Aerosols that were more dispersive, such as the surface wipe aerosols, were less concentrated when reaching the MS; while the more direct aerosols, such as the air aerosols, were more concentrated when reaching the MS.

As can be seen in Figure 2, the MS of the air aerosols primarily showed the presence of ethanol. The hydrocarbon propellants are the primary compounds shown in the spectra of SWA (Figure 3) and SWP (Figure 4). It is possible, with careful MS interpretation, to determine the presence of the non-propellant components from these spectra (Table 2), but analysis of the non-propellant compounds is simpler when the AMSI interface is used.

14

Figure 2. PBMS of AA1. M/z 45 is the molecular ion of ethanol.
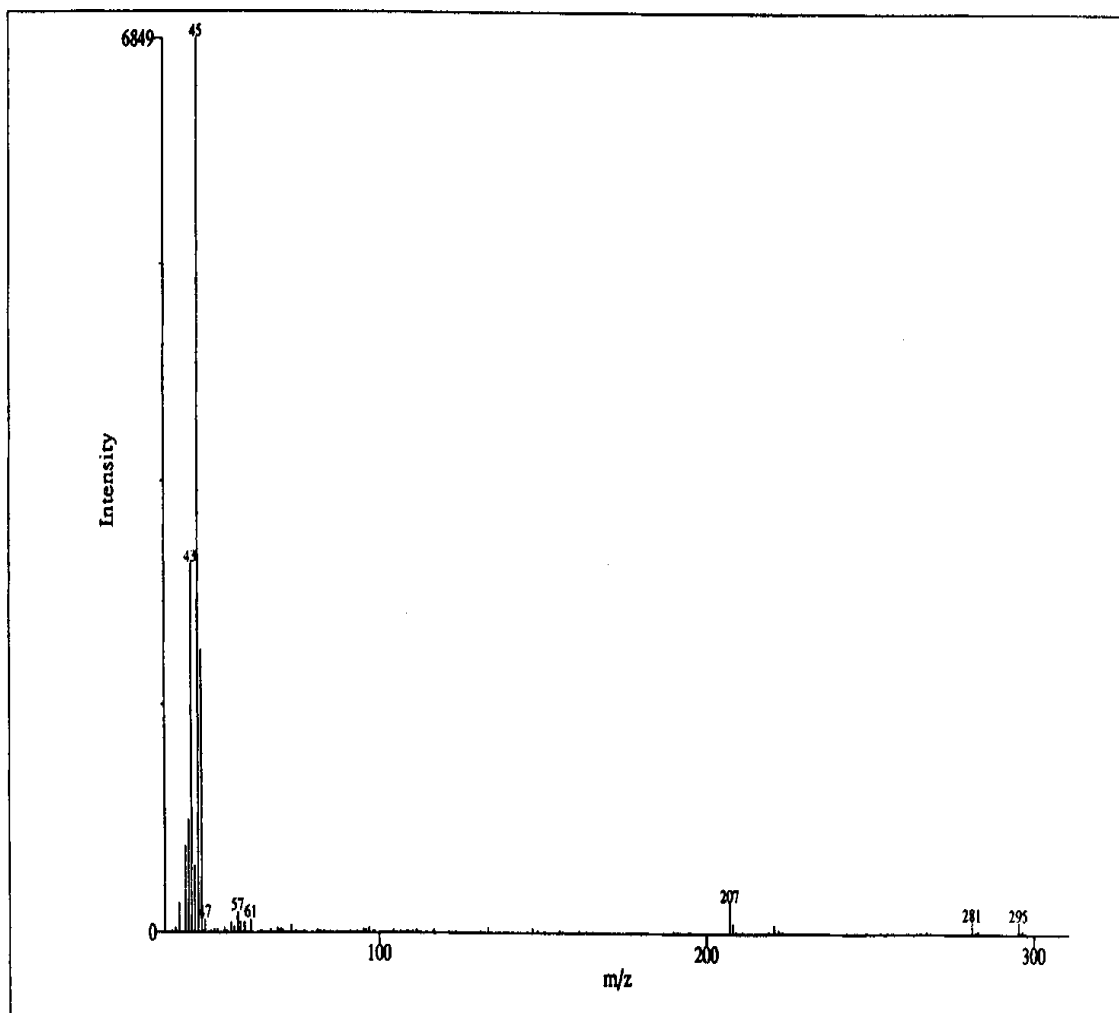
Figure 3. PBMS of SWA. M/z 43, 57, and 83 are major hydrocarbon ions. M/z 207, 221, 281,
295, and 355 are several ion/molecule reaction adducts with silicone in the aerosol
spray (to be discussed later in the report). M/z 168 is the SLS ion.
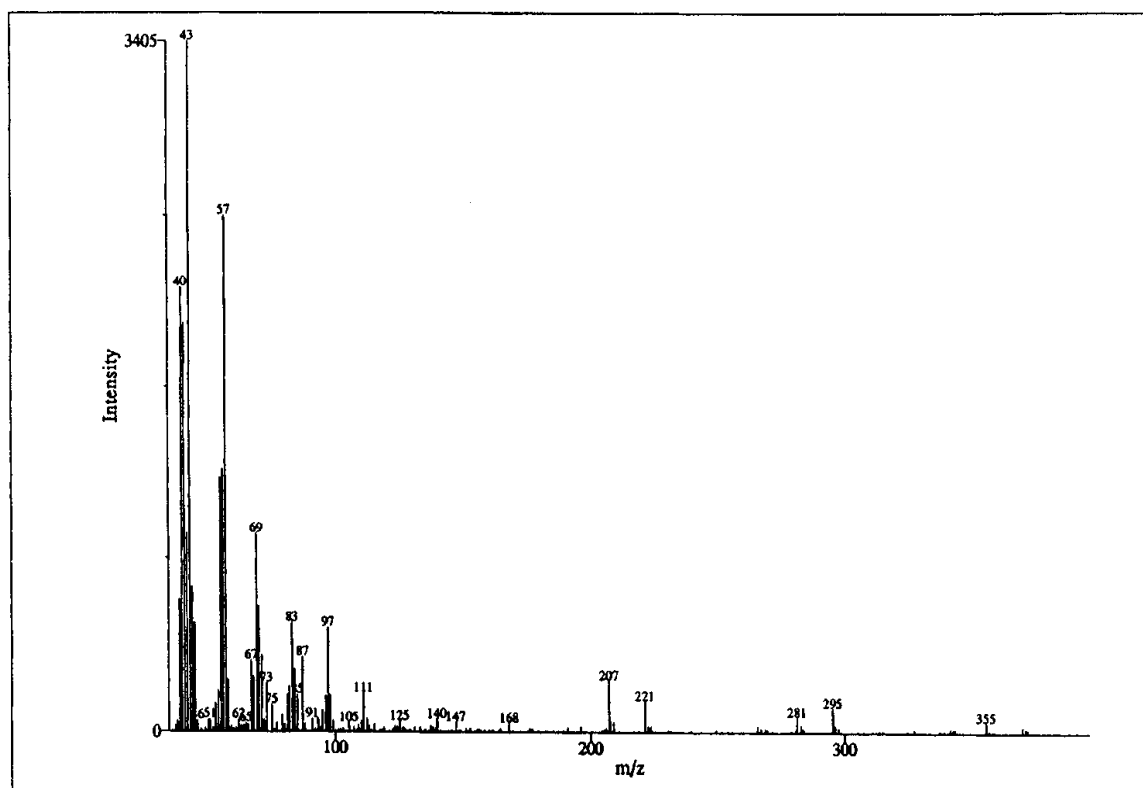
Table 2. Peak assignments for SWP and SWA analyzed by PBMS without the AMSI

Surrogate Aerosol	m/z	Fragment Assignment	Originating Compound
SWP & SWA	43	$C_3H_7^+$	Hydrocarbon propellant
SWP & SWA	45	$HOCH_2CH_2^+$	BC
SWP & SWA	57	$C_4H_9^+$	Hydrocarbon propellant
SWP & SWA	69	$HOCH_2CH_2O$	BC
SWP & SWA	41	$C_3H_5^+$	BC and/or SLS
SWP & SWA	83	$C_5H_{11}^+$	Hydrocarbon propellant
SWP & SWA	85	$C_6H_{13}^+$	SLS
SWP & SWA	87	$CH_2OC_4H_9^+$	BC
SWP & SWA	97	$CH_3C_4H_8CH=CH^+$	SLS
SWP & SWA	100	$BC-H_2O$	BC
SWP & SWA	111	$C_8H_{15}^+$	SLS
SWA	140	$C_{10}H_{20}^+$	SLS
SWA	147	$[(BC-H_2O) \bullet (BC-OC_4H_9)]^+$	BC
SWP & SWA	168	$C_{12}H_{24}$	SLS
SWA	207	$[(BC + OH) + C_5H_{12}]$	SLS & BC
SWA	221	$[(BC + OH) + C_6H_{14}]$	SLS & BC
SWA	281	$[(BC + H_2O) + C_9H_{20}]$	SLS & BC
SWA	295	$[(BC + H_2O) + C_{10}H_{22}]$	SLS & BC
SWA	355	$[(BC + H_2O) + C_{13}H_{28}]$	SLS impurity & BC

16

Figure 4. PBMS of SWP. M/z 43, 57, and 83 are primary hydrocarbon ions. M/z 168 is SLS ion.
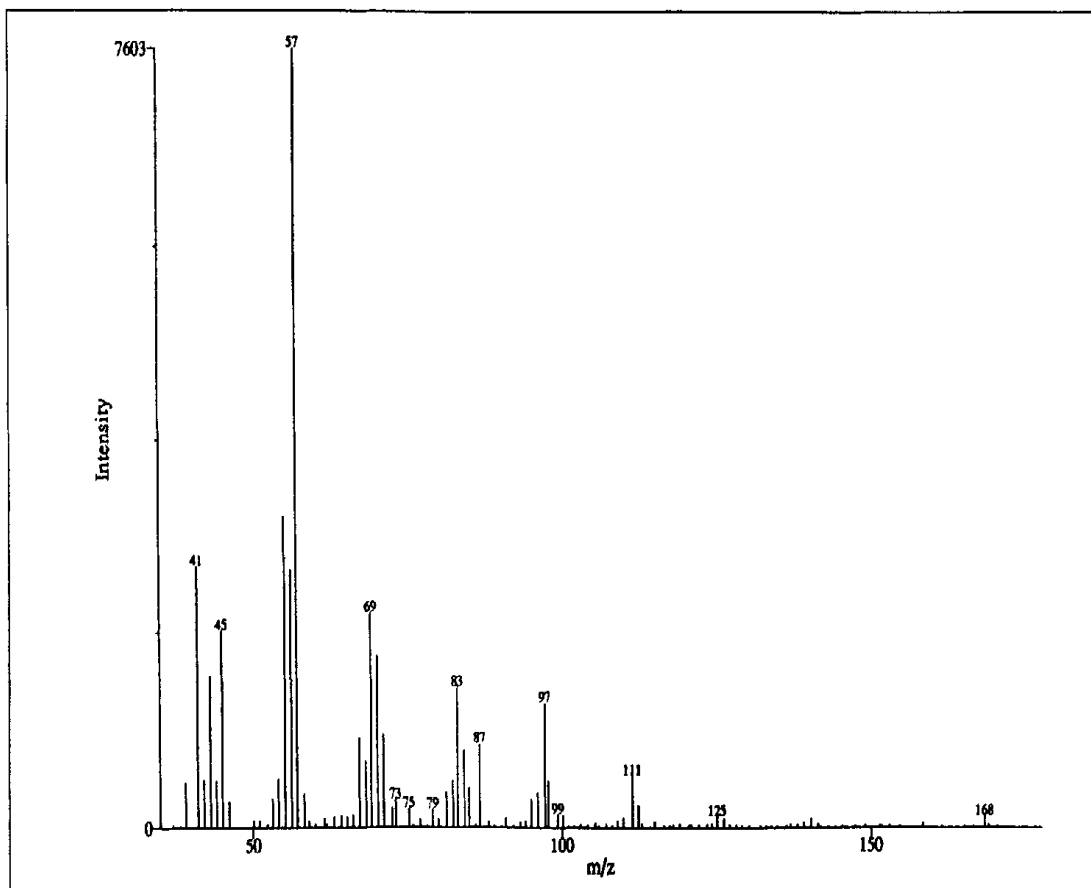
5.2.4 Optimization of AMSI

The optimization of the AMSI looked at several different parameters: 1) vacuum pumping of the AMSI, 2) reproducibility, and 3) bore size and shape of the skimmers.

5.2.4.1   Vacuum Application to AMSI

The need for a vacuum on the AMSI was investigated by examining the sensitivity of the system with and without the vacuum pump operating using SWP. The pump sprays presented the greater challenge to the AMSI since these did not have the aerosol propellant to add force to the particles moving them into and through the AMSI. The analytical sensitivity was much greater (approximately 64%) when a small vacuum was applied after the nozzle of the AMSI, as can be seen in Figure 5. The amount of vacuum was only a few torr and was optimized for maximum signal height. The vacuum had to be small enough to prevent interference with the MS vacuum.

17

Figure 5. Comparison of PBCI response of SWP with and without vacuum pump connected to AMSI.
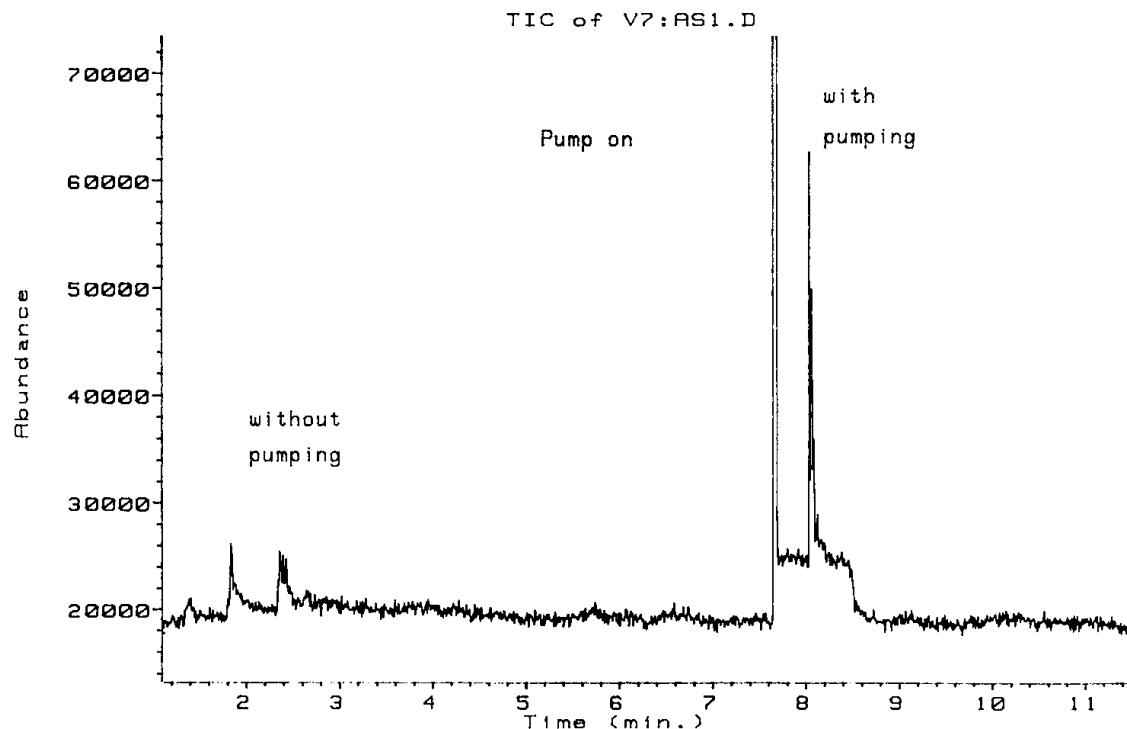
5.2.4.2   Reproducibility

In order for the AMSI/MS to be useful for quantitative analyses, the response must be reproducible. Reproducibility was tested by repeatedly spraying a surrogate aerosol into the AMSI/MS and examining repeatability of signal. Using the Model A AMSI, which uses no skimmers after the nozzle, the reproducibility was poor, particularly with the pump-triggered sprays. When a skimmer was added after the nozzle (Figure 1) (AMSI Model B), a reproducibility of five percent of the standard deviation from the mean was achieved (Figure 6). As can be seen in Figure 6, repeated spraying of SWP gave reproducible signal intensities. The primary variance is the operator pressing on the aerosol actuator. The reproducibility is dependent on the ability to repeatedly spray the aerosol in a reproducible manner. Variations in the duration of time the actuator is pressed and the amount of pressure applied to the actuator change the amount of sample ejected form the aerosol container into the AMSI; and therefore, the changes in signal intensity. Automatic spraying systems are available for laboratory use, but these were not used in this project, since the variations in actuating the aerosol actuator has a significant influence on the impact of the aerosol consumer product on the environment. Understanding this impact and differences that occur during actuator activation can provide important data for product use instructions for pollution prevention strategies.

18

Figure 6. Reproducibility of mass spectral response with skimmer added (AMSI Model B).
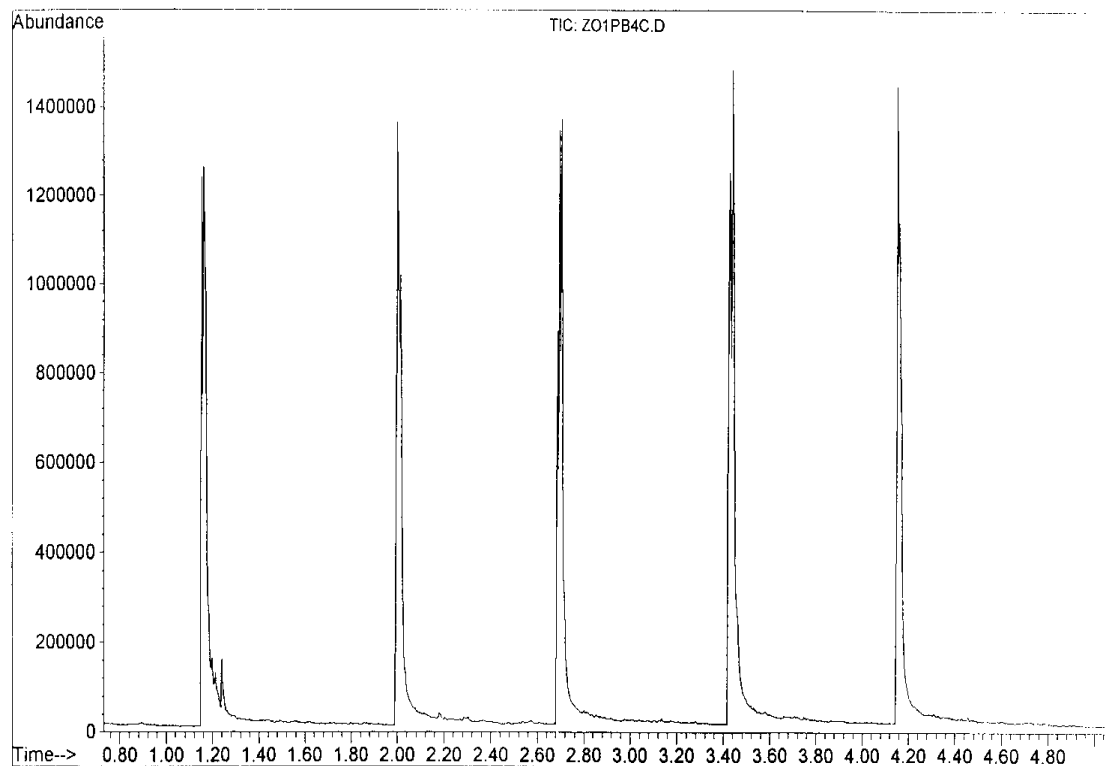
5.2.4.3   Skimmer Design

The primary role of the skimmer in the AMSI is to sample the aerosol particles moving in a straight trajectory, and to exclude the particles deviating from the straight line between the nozzle and the skimmer. This is critical for particle-size distribution selection by the steering gas, since the steering gas will force the smaller particles, those less able to withstand the force of the gas flow, away from the straight-line trajectory. The size of the entrance hole in the skimmer will affect the ability of the skimmer to operate properly. Too large of a bore size will allow the skimmer to sample particles not moving in a straight trajectory. Too small of a hole will reduce the analytical sensitivity due to signal loss. The shape of the skimmer can also affect its ability to function correctly. Four skimmer shapes were tested with varying bore hole sizes. The four skimmer shapes tested are shown in Figure 7, and a detailed list of the skimmers tested is given in Table 3. The different skimmer shapes were chosen to look at extremes.

Types A and B are convergent skimmers with 60° and 160° angles, respectively. Types C are concave skimmers with a 145° angle. The height of the cylindrical portion of Type C is 2.54 cm. Type D skimmers were comprised of a, b, and c three pieces with threads. When a, b, and c are screwed together, the Type D skimmers are concave skimmers similar to the Type C skimmers with an angle of 145°. When b is removed, convergent skimmers result, which are similar to Types A and B.

19

Figure 7. Different types of skimmers. A: 60° angle. B: 160° angle. C-D: 145° angle. In group D: a, b, and c are joined together to form concave skimmers as in C. Alternatively, a and c are joined to form skimmers A and B.

(A) SK1-SK5

(C) SKD, SKE

(B) SK I, SK II, SK III

(D) SKA, SKB, SKC, SKF
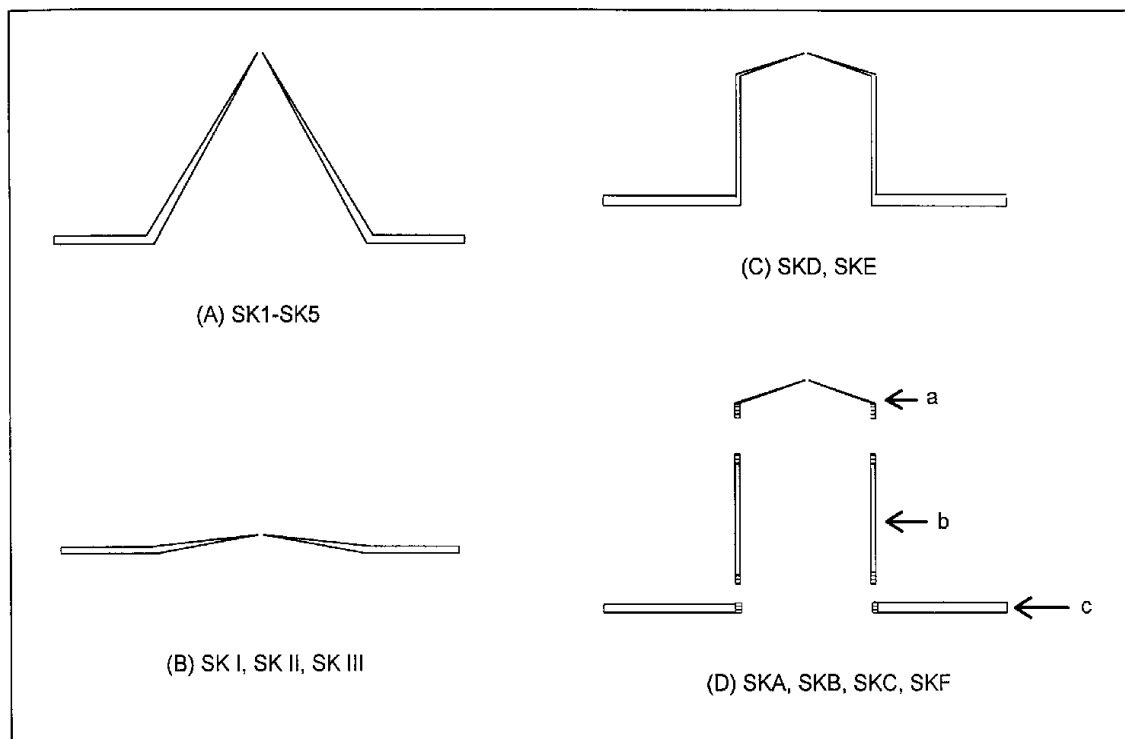
As can be seen in Table 3, the Type A, SK4 skimmer with a 0.076-cm bore size produced the optimum results. The trend of responses was Type 1 (convergent) > Type B, C, D (cone only, the convergent configuration) > Type D (concave configuration). The 60° angle produced better results than the 145° or the 160°. For the Type D skimmers, the responses of the convergent configurations for SKA, SKC, and SKF were one order of magnitude higher than the concave configurations. For the SKB Type D skimmer, the response of the convergent and the concave configurations were approximately the same and the standard deviations were high. This probably is the result of the turbulence created by this skimmer reducing the amount of sample passing through the skimmer. The conic shape of the convergent skimmer minimizes the turbulence resulting in a higher sample efficiency and greater instrumental response. The effect of the angle can be seen in Figure 8, which compares a 60° nozzle angle with a 160° nozzle angle. As can be seen in this figure, a good response is obtained with the 60° nozzle angle.

Bore size results were less conclusive. The differences in bore sizes appeared to be more of a difference in the machine shop's ability to make the skimmer than the actual bore sizes. Smoothness of the hole appeared to have the greatest effect on the response. Comparing SK4 with SK5, the bore size of SK4 is 40% that of SK5. SK4 had a signal response that was 2.5 times larger than SK5 with a standard deviation of only 8.91%, while the standard deviation of SK5 was 68.66%. Similar results were found for SKI and SKII. The bore size of SKI was almost two times greater than that of SKII, but the signal intensities were similar. SKII and SKIII were identical in bore size and shape, but SKIII was not as smooth as SKII. SKII gave more reproducible results. SKD and SKC also were identical in bore size and shape, but SKD gave more reproducible and sensitive results, since SKD was much smoother than SKC. The smoother surface results in less

20

Figure 8. Comparison of SWP response with nozzle angles of 60° and 160°.
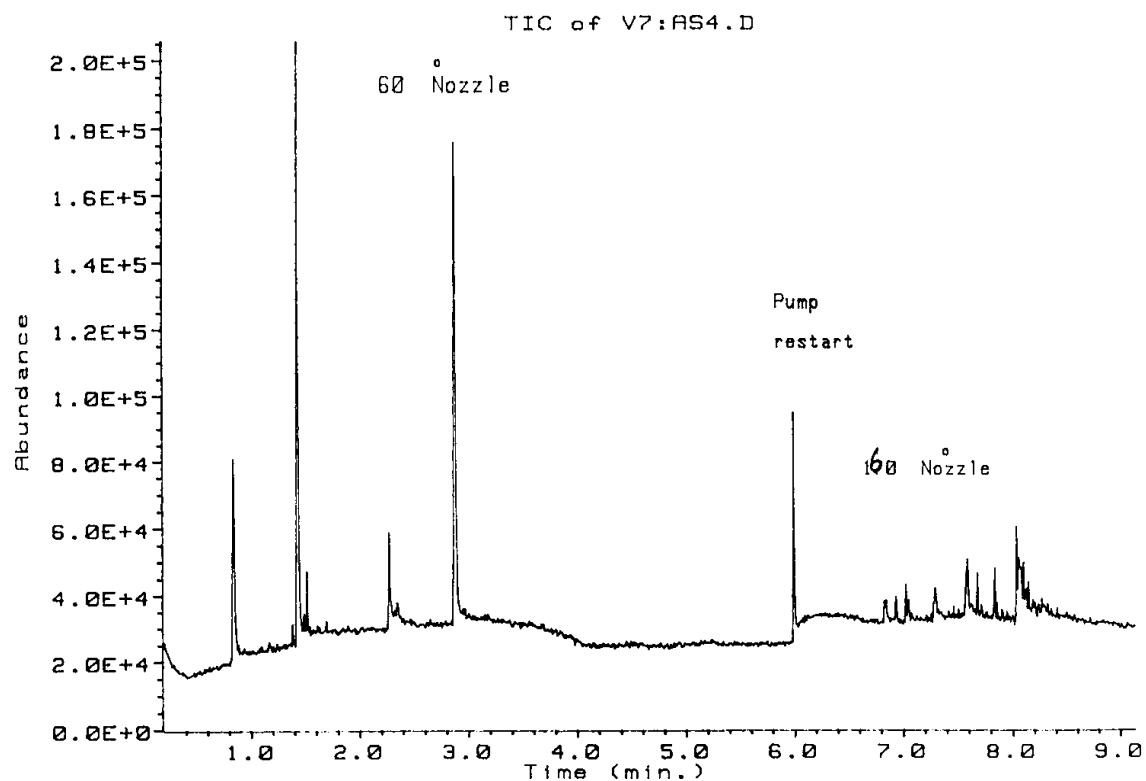
turbulence to the aerosol beam as it passes through the skimmer. Reducing turbulence appears to increase sensitivity and reproducibility.

The SK4 skimmer, with the 60° angle and 0.076 cm bore size, was chosen as the optimum skimmer. It was the one used in all subsequent analyses. A schematic of this skimmer is shown in Figure 9.

Table 3. Results of AMSI skimmer optimization

	Nozzle				Distance (mm)[b]	Normalized Response[c]	% Relative Standard Deviation
	Skimmer ID	Outer Angle (degrees)	Bore Size (cm)	Material[a]			
Type A	SK1	60	0.060	Al	10	3.36×10^6	17.57
	SK2	60	0.061	Al	10	5.86×10^6	23.06
	SK3	60	0.064	Al	--	--	--
	SK4	60	0.076	Al	10	11.87×10^6	8.91
	SK5	60	0.190	Al	10	4.78×10^6	68.66
Type B	SKI	159	0.096	Al	22	2.80×10^6	16.07
	SKII	160	0.051	Al	22	2.35×10^6	15.41
	SKIII	160	0.051	Al	22	2.93×10^6	40.91
Type C	SKD, concave	145	0.034	SS	15	3.41×10^6	8.38
	SKE, concave	145	0.032	SS	15	0.51×10^6	12.57
Type D	SKA, cone only	144	0.127	Al	11	8.01×10^6	11.06
	SKB, cone only	145	0.094	Al	11	3.89×10^6	27.54
	SKC, cone only	145	0.033	Al	11	1.25×10^6	17.61
	SKF, cone only	145	<0.028	Al	11	2.55×10^6	32.24
	SKA, concave	144	0.127	Al	15	0.84×10^6	8.22
	SKB, concave	145	0.094	Al	15	3.91×10^6	35.52
	SKC, concave	145	0.033	Al	15	0.46×10^6	9.98
	SKF, concave	145	<0.028	Al	15	0.09×10^6	33.28

[a] Al = aluminum; SS = stainless steel; [b] Measured between the nozzle tips and SK3; [c] Average of five replicates and normalized.

Figure 9. Optimum skimmer design schematic.

5.2.5 AMSI/MS Analysis

AMSI/MS analysis was done by PBMS and with API. The API had MS/MS capabilities that allowed for more extensive MS interpretation. The MS/MS capabilities were not as important for analysis of the surrogate aerosols as they were for the analysis of actual aerosol consumer products. The components of the surrogate aerosols were known. It is likely that the components of real products may not be known.

5.2.5.1   Particle Beam Mass Spectrometer (PBMS)

A HP 5989B LC/MS equipped with a HP 59980A PB interface was used in both the electron impact (EI) and chemical ionization (CI) modes with the AMSI. The source and quadrupole temperatures were set at 260°C and 100°C, respectively, and the PB desolvation chamber temperature was set at 55°C. When the system was operated in the CI mode, the source pressure was maintained at 2.2 X 10^{-4} torr in the positive CI mode and 1.5 X 10^{-4} torr in the negative CI mode. Isobutane was used as the ionization gas. The system was initially calibrated according to manufacturer's instructions, and then optimized for the aerosol products by tuning to SLS and BC via flow injections with the oscillating nebulizer.

The AMSI was coupled with the PB interface (Figure 10) through 0.5 mm o.d. Teflon®
tubing. The two-second spray of the aerosol was drawn into the PB desolvation chamber by a
vacuum pump drawing from behind the nozzle of the AMSI. The spraying box was used to direct
the aerosol into the AMSI. A 0.5 mm o.d. glass tube was used to connect the spraying box to the
AMSI. Helium was used as the steering gas for particle size selection since helium does not
interfere with MS operation.

Figure 10. Schematic of AMSI coupled to PBMS.
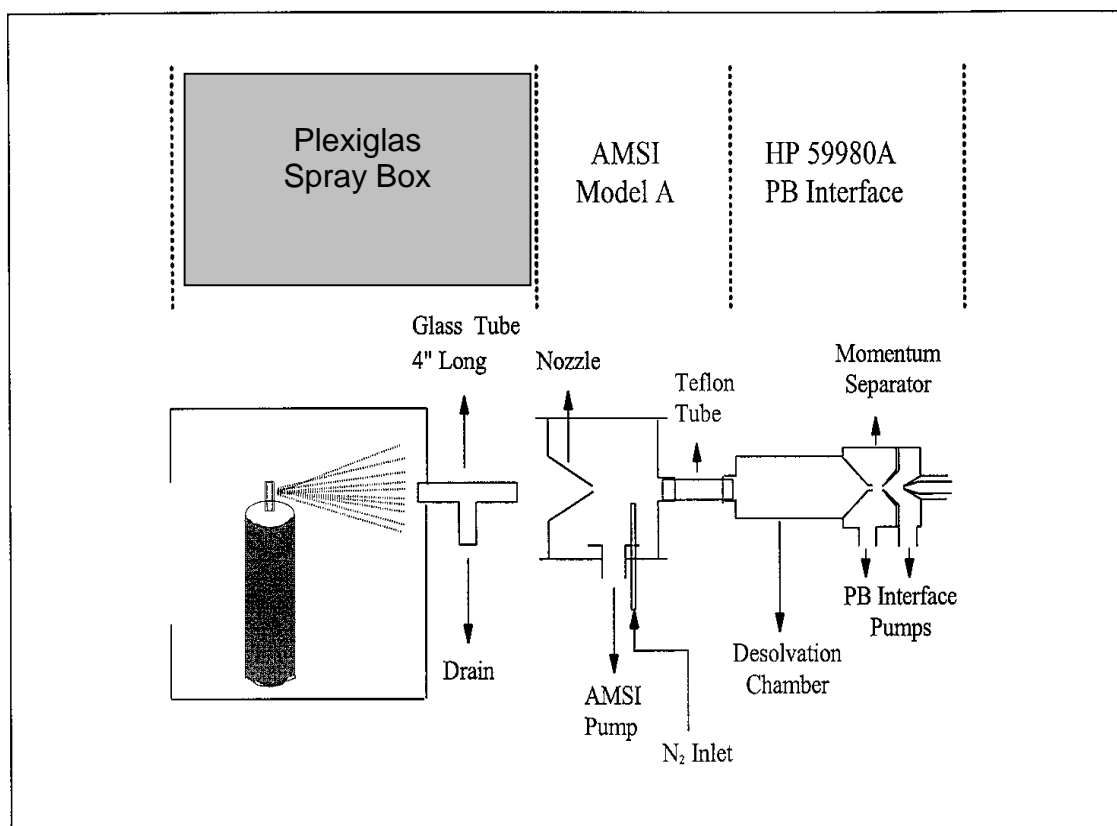
Tests were run to examine the potential that the transfer tube, between the spraying box
and AMSI, was not affecting the aerosol sample. The particles moving forward had enough
forward momentum to be unaffected by the transfer tube. This was due probably to a
combination of the vacuum of the MS drawing the particles forward and the force with which the
particles are ejected from the aerosol package.

5.2.5.2   Atmospheric Triple Quadrupole Mass Spectrometer (API)

A Sciex API III^{plus} triple quadrupole MS (API) equipped with a heated nebulizer was used. Each of the quadrupoles was individually calibrated using a mixture of polypropylene glycols. Then the MS was optimized for the aerosol products by tuning to SLS and BC via flow injections with the OCN. The interface temperature was set to 55°C, and the heated nebulizer was set at 500°C. The current gas was nitrogen, and the flow rate was 1.2 L/min. The nebulizer gas flow rate was 0.5 L/min, and the auxiliary gas flow rate was 1.2 L/min. The API source pressure was maintained at 400 to 500 torr with the AMSI operating.

The AMSI was coupled with the API (Figure 11) via a glass tube into the heated nebulizer. The schematic of the API coupling assembly is shown in Figure 12. The sprayed aerosol droplets were drawn into the AMSI with a vacuum pump into a heated glass tube (170°C). Upon exiting the glass tube, the sample was a mixture of dry particles and solvent vapors. The solvent vapors were pumped away, and the dry particles moved forward into the atmospheric entrance portion of the MS due to the high momentum of the particles. The dry particles were ionized by corona discharge. The generated ions entered the high vacuum portion of the MS for mass spectrometric detection.   Nitrogen was used as the steering gas for particle size selection. It was necessary to use a more complicated coupling with the API than with the PBMS, since the API entrance is at atmospheric pressure, so that there was no MS vacuum drawing sample through the AMSI into the MS.

Figure 11. Schematic of AMSI coupled to API.

25
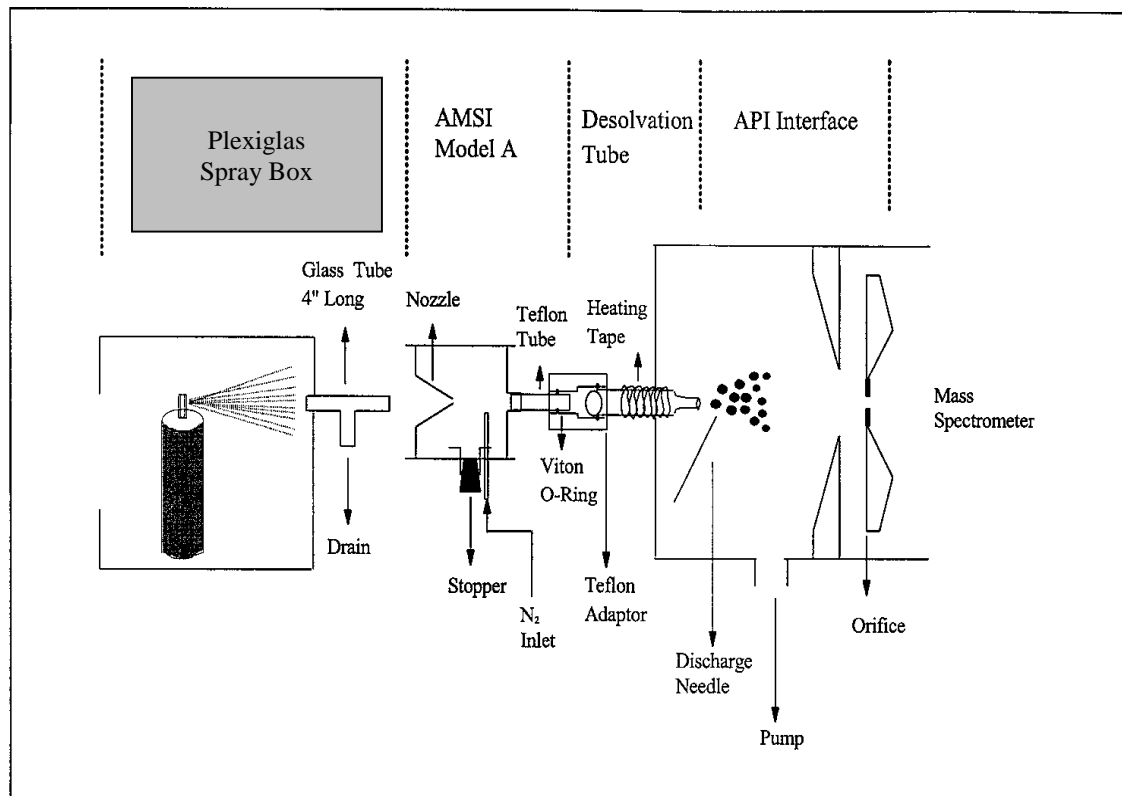
Figure 12. Interface coupling AMSI to heated nebulizer assembly.
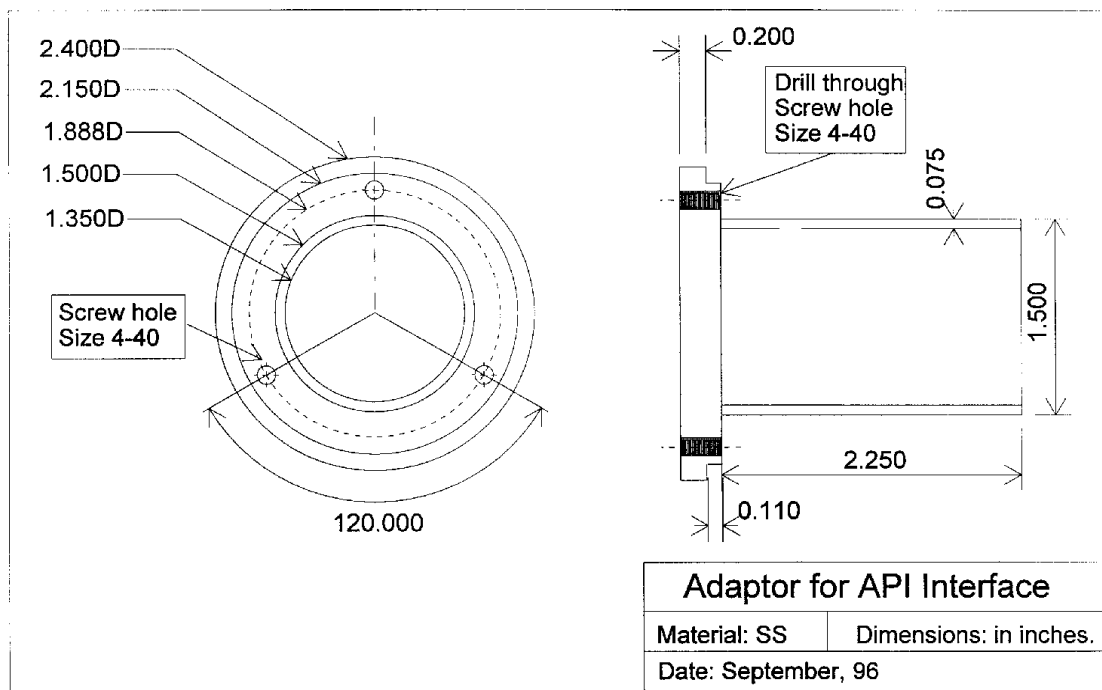
Daughter scans and parents scans were run to identify originating peaks for fragment ions. The ions m/z 119 and 169 were characteristic ions for BC and SLS, respectively. Two-second sprays were used to introduce the aerosol product into the AMSI.

5.2.6 Surrogate Aerosols Analysis

AMSI/MS analysis was performed on the surrogate aerosols and on blinded samples supplied by the Industry Partners. No information – such as type of product, formulation, ingredients, etc. – was provided with the blinded samples. These two samples only provided some actual samples against which to test the viability of the AMSI/MS to analyze real products.

The surrogate aerosols and two blinded aerosol products were analyzed using the AMSI interfaced with both the PBMS and the API. Both MS's were operated in the positive and negative ionization modes. Additionally, the PBMS was operated in both the EI and CI modes. The API is a very soft ionization technique resulting in CI-type spectra. The API was operated in the MS/MS mode.

SLS and BC bulk samples, obtained from the Industry Partners, and authentic standards, both individually and mixed, were analyzed using the OCN to generate the aerosol. The standards were first analyzed to determine the identification and quantitation ions for the surrogate aerosol components. The SLS bulk sample (Table 4) contained impurities that were detectable and which participated in ion/molecule reactions of the aerosol products. These

26

impurities were detected in the surrogate aerosols containing SLS. The characteristic SLS ion was m/z 169, which is the lauryl fragment that results from the loss of the sulfate fragment. The peak at m/z 197 is most likely the fragment $C_{14}H_{29}^{+}$, a fragment of the impurity. The identity of the impurity may be sodium myristyl sulfate. This impurity is present in only a trace amount in the standard obtained from the chemical supply house. The 169 ion was used for detection and quantitation of SLS in the surrogate aerosols. SLS, when analyzed by negative ion API, resulted in a more complicated mass spectrum than that obtained from positive ion API (Table 4).

Table 4. Peak assignments for API spectra of SLS (SLS, $C_{12}H_{25}NaSO_4$, MW=288). M represents the SLS molecule.

Ion Polarity	m/z	Assignments	Daughter Ions	Parents Ions
Positive	169	$C_{12}H_{25}^{+}$		
	197	$C_{14}H_{29}^{+}$		
Negative	80	SO_3^{-}		97, 98
	82	$(H_2SO_4+H-OH)^{-}$		
	97	HSO_4^{-}		177,185,217,228, 239,265,293,319,405
	99	$(H_2SO_4+H)^{-}$	82	
	119	$(NaSO_4)^{-}$		
	177	$(SO_3 \bullet HSO_4)^{-}$	97	
	199	$(SO_3 \bullet NaSO_4)^{-}$	119	
	217	$[2(HSO_4) \bullet Na]^{-}$	97	
	265	$C_{12}H_{25}SO_4^{-}=(M-Na)^{-}$	97	
	293	$C_{14}H_{29}SO_4^{-}$	97	
	297	$[SO_3 \bullet 2(HSO_4) \bullet Na]^{-}$	97,217	
	321	$C_{16}H_{33}SO_4^{-}$	97	
	385	$(M \bullet HSO_4)^{-}$	97,265	
	413	$[(C_{14}H_{29}NaSO_4) \bullet HSO_4]^{-}$	97, 293	
	487	$[M \bullet (SO_3 \bullet NaSO_4)]^{-}$	199, 265, 407	
	553	$(2M-Na)^{+}$	265	
	581	$[(C_{12}H_{25}SO_4) \bullet (C_{14}H_{29}SO_4) \bullet Na]^{-}$	265, 293	

Only the negative molecular ion (m/z 118) and the loss of one water fragment (m/z 136) were detected for BC by negative ion API. The fragmentation pattern was more complex when BC was analyzed by positive API (Table 5). The ion m/z 119 was chosen to identify and quantify BC in the surrogate aerosols.

Table 5. Peak assignments for APCI spectra of Butyl Cellosolve® (BC, $HO\text{-}CH_2CH_2\text{-}OC_4H_9$, MW=118). M represents the Butyl Cellosolve® molecule.

Ion Polarity	m/z	Assignments	Daughter Ions	Parents Ions
Positive	45	$(HO\text{-}CH_2CH_2)^+$		
	57	$C_4H_9^+$		
	63	$[(HO\text{-}CH_2CH_2\text{-}OH)+H]^+$		237
	89	$HO\text{-}CH_2CH_2\text{-}OC_4H_9$		219, 253, 281, 337
	101	$(M\text{-}H_2O+H)^+$	43, 57	176, 219, 237, 281, 337
	119	$(M+H)^+$	45, 57	
	145	$(2M\text{-}H_2O\text{-}OC_4H_9)^+$		
	163	$M \cdot (HO\text{-}CH_2CH_2\text{-}OH) \cdot H^+$	45, 57, 105	
	219	$(2M\text{-}H_2O+H)^+$	45, 47, 89, 101	
	237	$(2M+H)^+$	45, 57, 63	
	238	$(2M+2H)^{\cdot+}$	45, 57, 63	
	281	$M \cdot (M\text{-}H_2O) \cdot (HO\text{-}CH_2CH_2\text{-}OH) \cdot H^+$	45, 57, 89, 101, 107	
	337	$(3M\text{-}H_2O+H)^+$	45, 57, 89, 101, 107, 145, 163, 219	
Negative	118	M^-	72	
	136	$(M+H_2O)^-$		

The choice of m/z 119 and m/z 169 for BC and SLS detection and quantitation can be seen in the PBMS in CI mode analysis of SWA. The spectrum is shown in Figures 13 - 15. In Figure 13, the 119 and 169 peaks are easily detectable; therefore, ongoing ion molecule reactions are not a problem for aerosol compositional analysis. Figure 14 shows the spectrum of BC by API in the positive mode. Figure 15 shows the spectrum of SLS by API in the posit mode. Both of the spectra show that analysis by the selected ions is valid.

Although it appears that the ion/molecule reactions are not a major problem for aerosol chemical compositional analysis, it was important to determine if the source of ion/molecule reactions was the AMSI/MS analysis system or the aerosolization process itself. The two surface wipe surrogate aerosols were chosen to investigate this phenomena since they contained the surfactant SLS, and one of the surrogate aerosols was activated with a pump spray rather than a propellant system. The direct analysis without the AMSI of SWA indicated that the propellant-activated release of the product resulted in ongoing ion/molecule reactions, which did not occur in SWP. As can be seen in Table 6, all of the detected SWP peaks are fragments of SLS and BC. There were no reaction adducts of SLS and BC detected. The mass spectrum of SWA contains the same SLS and BC fragments (Table 5). The AMSI/PBMS in CI mode analysis resulted in similar data. The CI analysis of SWP resulted in only the detection of m/z 119 (BC + H$^+$), 169 (SLS – NaSO$_4$), and 197 (a fragment of an impurity in the SLS solution). The CI analysis of the SWA yielded the presence of ion/molecule reactions of SLS and BC, as well as fragments from BC and SLS (Table7). The ion/molecule reactions were not a result of aerosolization of a mixture of BC and SLS. A mixture of BC and SLS were analyzed using the OCN to aerosolize the mixture. No SLS-BC ion/molecule reaction adducts were detected. PBMS analysis is not known to result in ion/molecule reactions. Ion/molecule reactions do occur with API due to the ionization method by corona discharge. Since these ion/molecule reactions are occurring with PBMS spectra with propellant systems only, and not with pump sprays or the OCN, it is presumed that

these are occurring during the aerosolization process as the product is ejected from the package. In spite of this, as can be seen in Figure 13, it is possible to conduct the chemical compositional analysis of SWA by scanning the ions 119 and 169 for identification and quantitation.

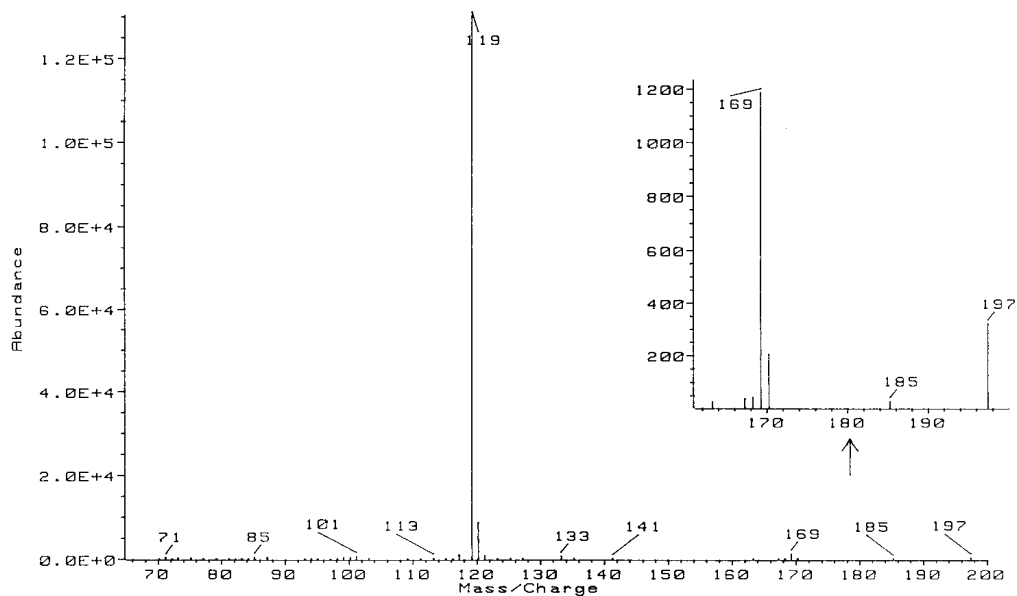Figure 13. PBMS in CI mode spectrum of SWA.

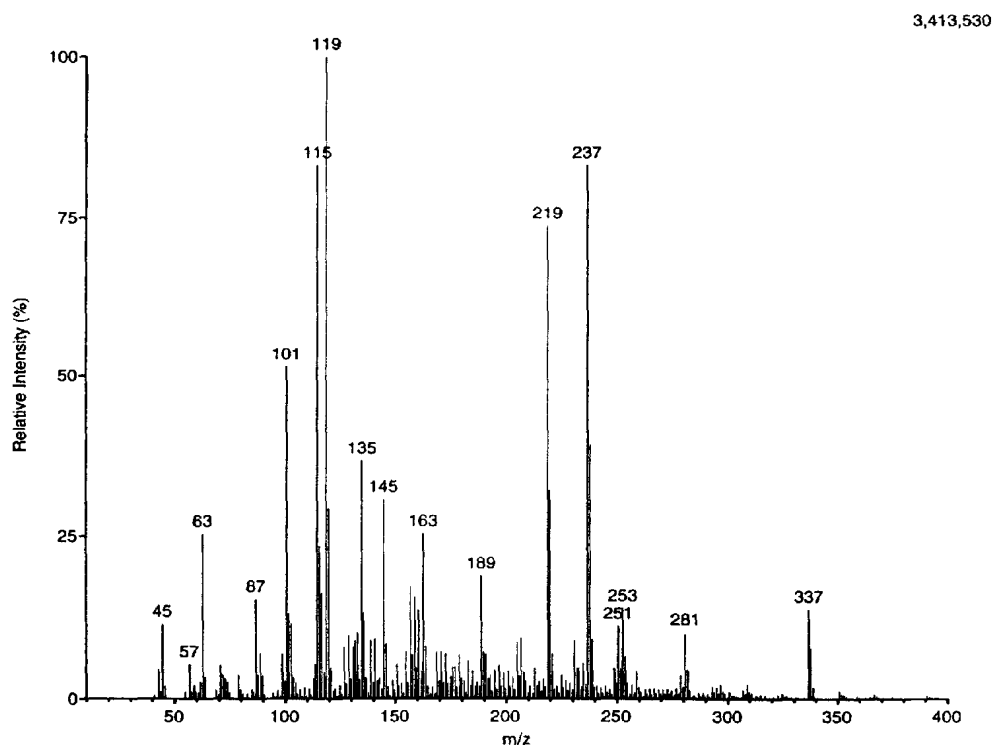Figure 14. API in positive mode spectrum of BC.

29

Table 6. Peak assignments for SWP and SWA analyzed by PBEI without the AMSI.

Surrogate Aerosol	M/z	Fragment Assignment	Originating Compound
SWP & SWA	41	$C_3H_5^+$	BC &/or SLS
SWP & SWA	45	$HOCH_2CH_2^+$	BC
SWP & SWA	57	$C_4H_9^+$	BC &/or SLS
SWP & SWA	69	$HOCH_2CH_2O$	BC
SWP & SWA	85	$C_6H_{13}^+$	SLS
SWP & SWA	87	$CH_2OC_4H_9^+$	BC
SWP & SWA	97	$CH_3C_4H_8CH=CH^+$	SLS
SWP & SWA	100	$BC=H_2O$	BC
SWP & SWA	111	$C_8H_{15}^+$	SLS
SWA	140	$C_{10}H_{20}^+$	SLS
SWA	147	$[(BC-H_2O) \bullet (BC-OC_4H_9)]^+$	BC
SWP & SWA	168	$C_{12}H_{24}$	SLS
SWA	207	$[(BC + OH) + C_5H_{12}]$	SLS & BC
SWA	221	$[(BC + OH) + C_6H_{14}]$	SLS & BC
SWA	281	$[(BC + OH) + C_9H_{20}]$	SLS & BC
SWA	295	$[(BC + OH) + C_{10}H_{22}]$	SLS & BC
SWA	355	$[(BC + OH) + C_{13}H_{28}]$	SLS impurity & BC

Table 7. Peak assignments for SWA analyzed by positive API with the AMSI

m/z	Fragment Assignment	Originating Compound
119	$BC + H^+$	BC
136	$BC + H_2O$	BC
150	$BC + CH_2OH$	BC
152	$BC + 2OH$	BC
169	$C_{12}H_{25}^+$	SLS
180	$[(BC + H^+) \bullet HOCH_2CH_2OH]$	BC
237	$2BC + H^+$	BC
254	$[(BC-OH) + C_{11}H_{23}]$	SLS & BC
269	$[(BC-H_2O) + C_{12}H_{25}]$	SLS & BC
279	$[(C_{14}H_{29}) \bullet CH_2CH_2OH+ 2H_2O$	SLS impurity & BC
286	$(C_{12}H_{25}^+) + BC$	SLS & BC
297	$[(BC-H_2O) + (C_{14}H_{29})]$	SLS impurity & BC
391	$[(BC + H_2O) + C_{14}H_{29} + C_4H_{10}]$	SLS, SLS impurity & BC

Figure 15. API in positive mode spectrum of SLS.
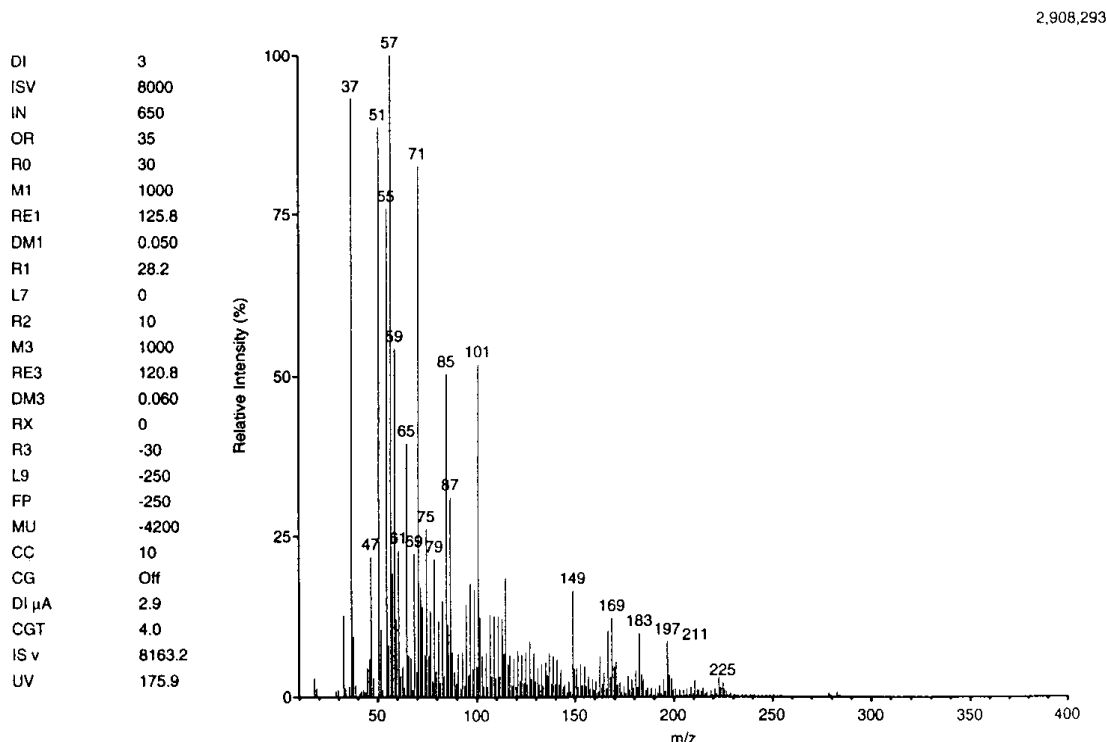
The silicon present in the surrogate surface non-wipe aerosols also resulted in ion/molecule reactions, this time between ethanol and silicone. The primary difference between the mass spectra of each of the analysis modes was in the abundance of the ions rather than in fragmentation patterns (Figures 16-18). There were no differences, other than ion abundance, between the EI and CI spectra. The soft ionization mode of the CI analysis did not reduce the formation of the ion/molecule reactants. This indicates that these reactions are occurring during the aerosolization process as the product is propelled from the aerosol package system. The silicone-ethanol adducts are given in Table 8. The only peak detected that was not a silicone-ethanol adduct was the molecular ion for ethanol.

Table 8. Peak assignments for silicone-ethanol adducts.

| m/z	Possible Structure	m/z	Possible Structure
45	$CH_3Si^+(H_2)$	327	$H_3Si[0Si(CH_3)_2]_3-O^+=Si(CH_3)_2$
73	$(CH_3)_3Si^+$	341	$CH_3SiH_2[0Si(CH_3)_2]_3-O^+=Si(CH_3)_2$
117	$CH_3Si(H_2)O(CH_2)_2OCH=CH_2$	355	$(CH_3)_2SiH[0Si(CH_3)_2]_3-O^+=Si(CH_3)_2$
133	$(CH_3)_2SiH-O^+=Si(CH_3)_2$	369	$(CH_3)_3Si[0Si(CH_3)_2]_3-O^+=Si(CH_3)_2$
147	$(CH_3)_3Si-O^+=Si(CH_3)_2$	401	$H_3Si[0Si(CH_3)_2]_4-O^+=Si(CH_3)_2$
207	$(CH_3)_2 SiH (CH_3)-OSi (CH_3)_2-O^+=Si (CH_3)_2$	415	$CH_3SiH_2[0Si(CH_3)_2]_4-O^+=Si(CH_3)_2$
221	$(CH_3)_3 Si (CH_3)-OSi (CH_3)_2-O^+=Si (CH_3)_2$	429	$(CH_3)_2SiH[0Si(CH_3)_2]_4-O^+=Si(CH_3)_2$
267	$CH_3Si(H_2)[0Si(CH_3)_2]_2-O^+=Si(CH_3)_2$	443	$(CH_3)_3Si[0Si(CH_3)_2]_4-O^+=Si(CH_3)_2$
281	$(CH_3)_2SiH[0Si(CH_3)_2]_2-O^+=Si(CH_3)_2$	517	$(CH_3)_3Si[0Si(CH_3)_2]_5-O^+=Si(CH_3)_2$
295	$(CH_3)_3Si[0Si(CH_3)_2]_2-O^+=Si(CH_3)_2$	591	$(CH_3)_3Si[0Si(CH_3)_2]_6-O^+=Si(CH_3)_2$

Figure 16. AMSI/PBMS in EI mode of SNW1.
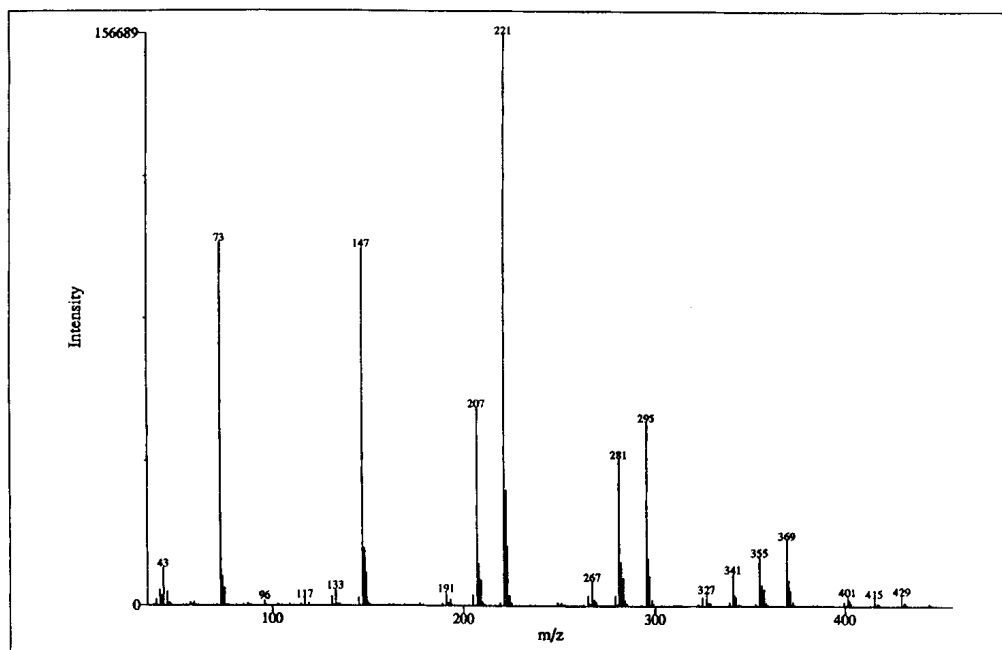
Figure 17. AMSI/PBMS in EI mode spectrum of SNW2.
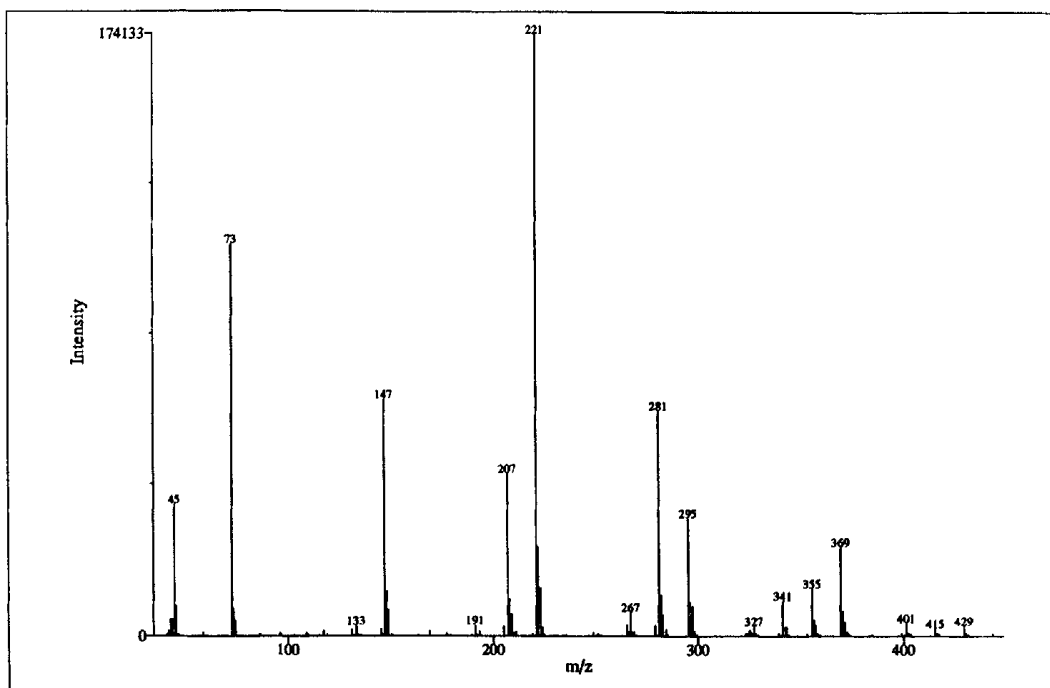
Figure 18. AMSI/PBMS in EI mode spectrum of SNWP.
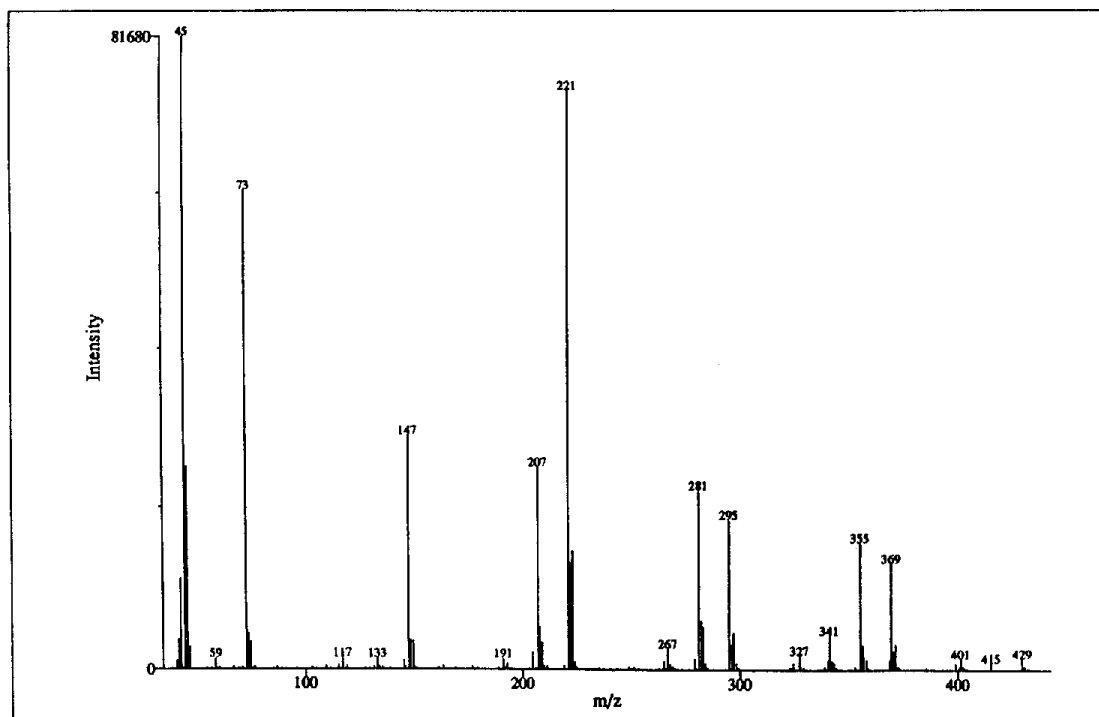
The air aerosol surrogates only contained water, ethanol, and propellant. The mass spectra of these surrogate aerosols indicated only the presence of ethanol in every case, except for the PBMS analysis without the AMS of AA1, which contained a few peaks from the propellant.

Since these ion/molecule reactions were detected, it was important to analyze actual samples containing active ingredients. The Industry Partners provided two blinded samples. No formulation, product type, etc. data were provided with the samples. These two samples were analyzed by API in the positive mode. The mass spectra for these two products, Product A and Product B are shown in Figures 19 and 20, respectively. It is not possible to identify these two products without building a library of aerosol products and their components. Product A (Figure 19) is a product containing essential oil fragrances, since molecular ions were detected for the essential oils: limonene, linalool, carvone, and caryophyllene. This product may be a polish or an air freshener. The product also contains BC as a volatile solvent, because m/z 119 was detected. Product B (Figure 20) is probably a personal care product, since the molecular ions for two cosmetic additives were detected: isopropyl myristate (m/z 271) and isopropyl palmitate (m/z 299). The product probably contains silicone since silicone clusters were evident.

An impurity was found in the Industry Partners' bulk SLS standard. This impurity was detectable in the surrogate aerosols containing SLS (Figure 21) by each of the MS analysis methods. This finding has important implications for pollution prevention strategy formulation. Tracking of impurities in aerosol consumer product formulations can reveal information about chemical source control and force chemical suppliers to provide more pure materials to their customers. This finding indicates how an impurity in a starting material for a product can be

33

Figure 19. Product A spectrum by AMSI/API in positive mode.
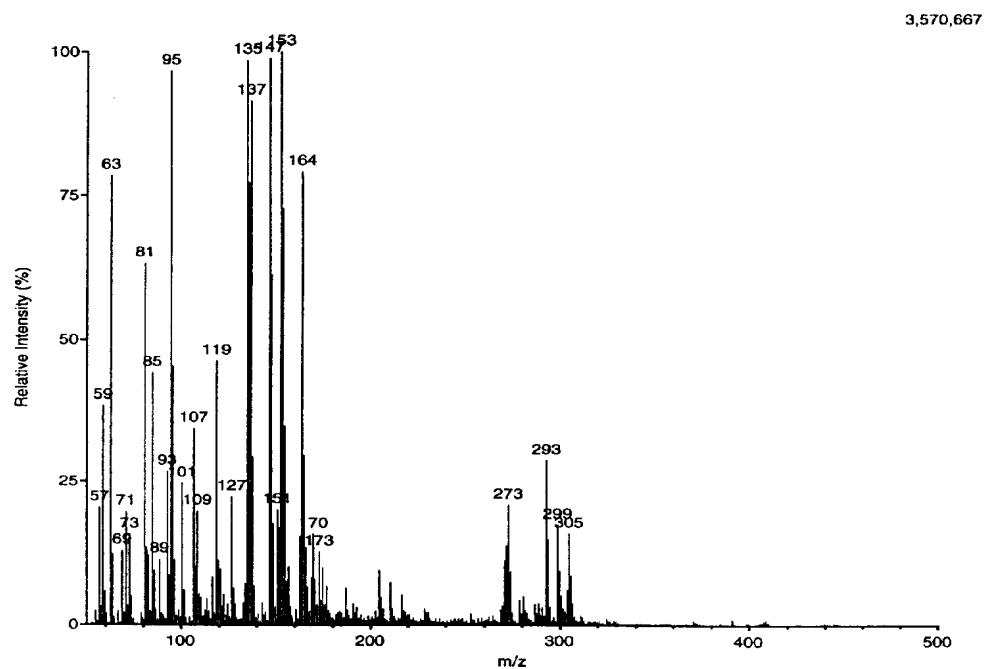
Figure 20. Product B spectrum by AMSI/API in positive mode.
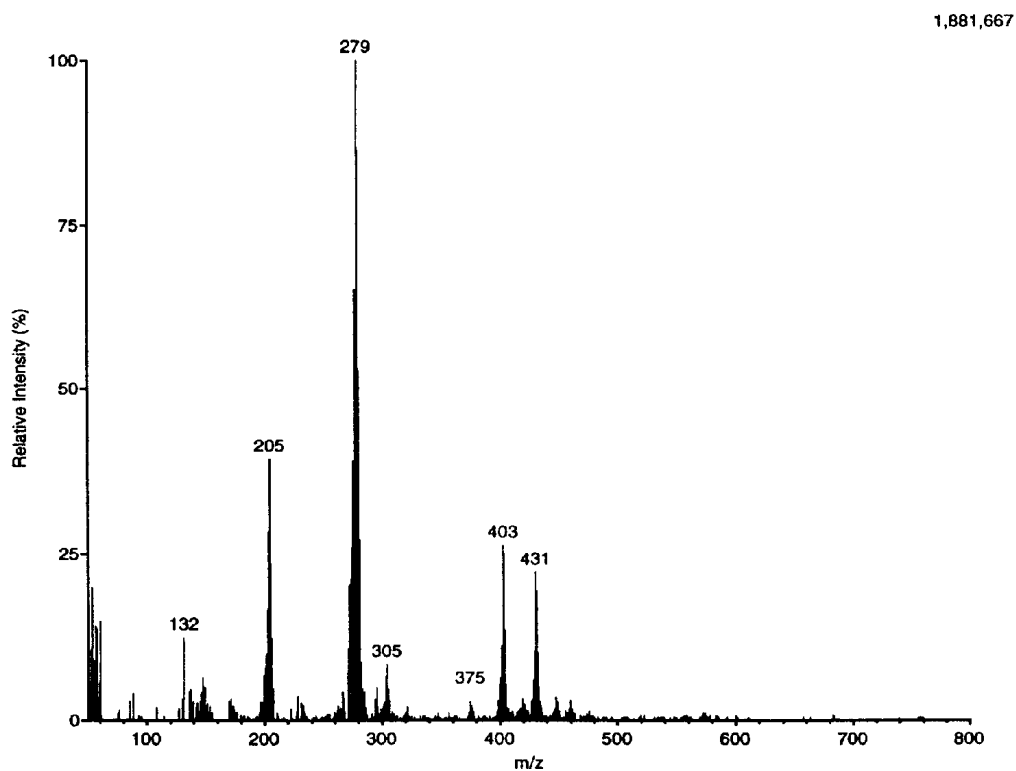
introduced unknowingly to the environment. The impurity is probably sodium myristyl sulfate (m/z 197).

Figure 21. SLS spectrum by AMSI/API in positive mode. M/z 197 is an impurity peak, which is probably sodium myristyl sulfate.
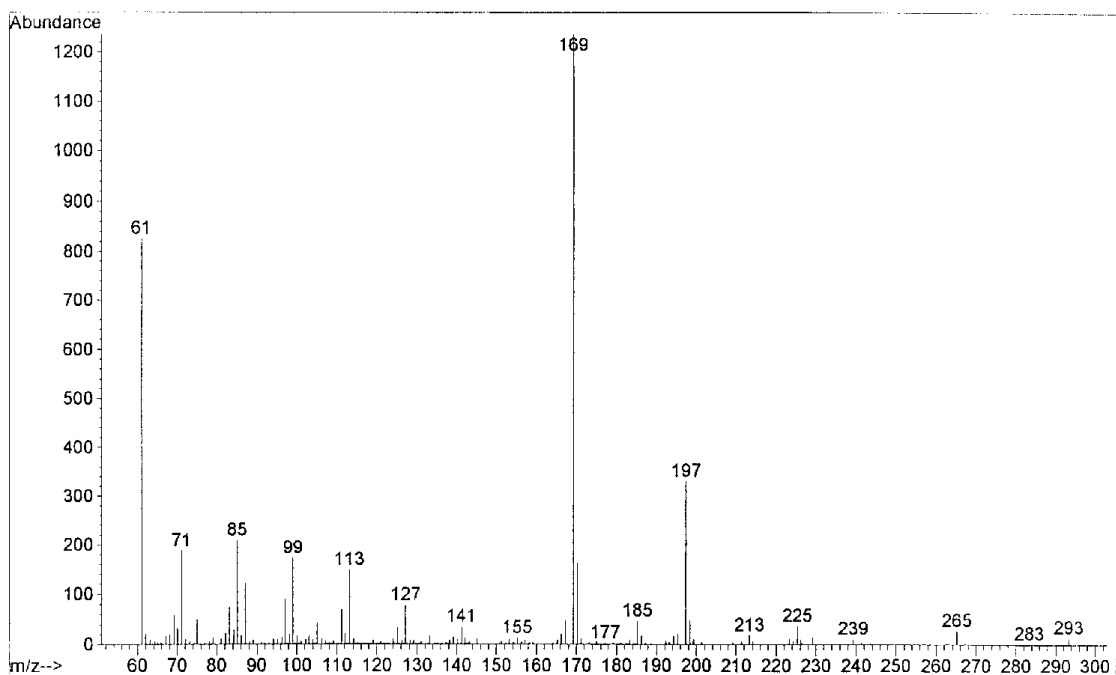
5.2.7 Chemical Composition Change Through Space

In order to meet the needs of the manufacturers in developing pollution prevention strategies, it was necessary to show experimentally that the AMSI/MS could be used to track chemical compositional changes through space. The results of this experiment are shown in Figure 22. In Figure 22, the m/z 119, the primary identification and quantitation ion for BC, can be detected in SWA with increasing distance of the spray actuator from the ASI inlet. The aerosol can was moved from 14.6 cm to 42.6 cm with SWA being sprayed into the AMSI at various points within this range. The BC in SWA was detectable at all points within this range. As the aerosol dispenser is moved farther from the AMSI entrance nozzle, the spray pattern expands and less of the sample reaches the AMSI entrance nozzle; therefore, the signal intensity decreases.

It was necessary also to show experimentally the potential of the AMSI/MS to quantitate the components of an aerosol consumer product. Figure 23 shows these results. During these experiments, the OCN was used to generate SWA mixtures in methanol. A constant particle size aerosol was generated by the OCN so that only the concentration of SWA was changing in this series of experiments. As detector saturation is reached, above 80% SWA, quantitative accuracy

35

decreases. Additional studies are needed to determine the accuracy of measurement and optimum operating conditions for quantitation.

Figure 22. Detection of m/z 119 ion for SWA by AMSI/MS with increasing distance from AMSI entrance nozzle.

Ion m/z 119, Increasing distance
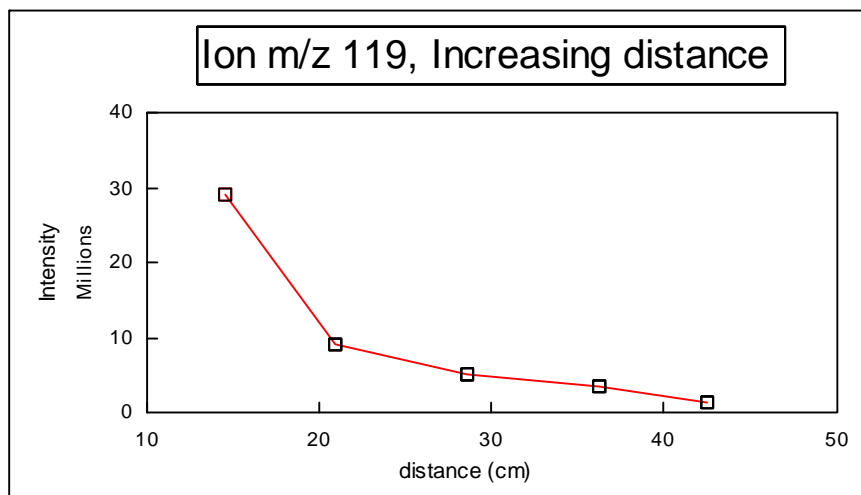
Figure 23. Depiction of signal intensity of m/z 119 with increasing SWA percentage.

Ion 119, Increasing concentation (%)
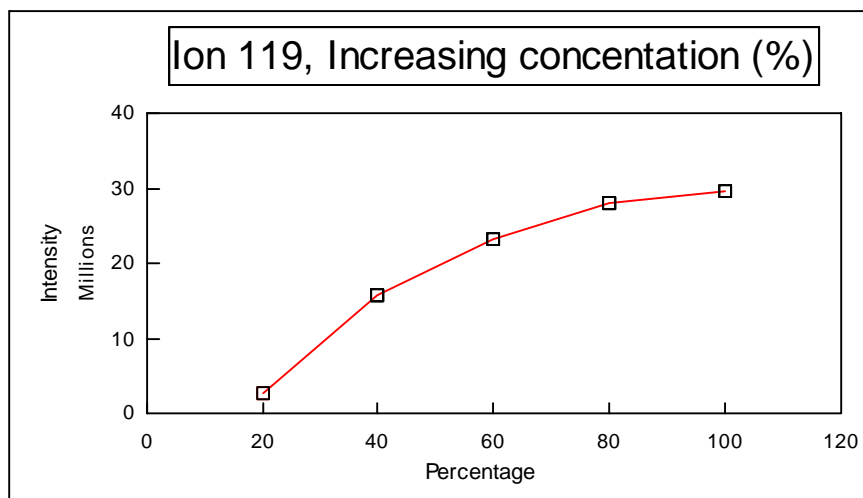
These series of experiments show that the AMSI/MS is able to determine quantitatively the chemical composition of aerosol consumer products during spatial dispersion. Changes in chemical composition and quantity are measurable with the AMSI/MS. The measurement of the changes in chemical composition as the aerosol moves through space can provide important data for formulation of products for pollution prevention. The composition of the product as it arrives at the use site determines the products efficacy. Knowing the actual composition of the product at

the use site will allow for formulating products with maximum efficacy with the least amount of chemical usage.

5.2.8 Particle Size Distribution Selection for Analysis via Steering Gas

Analysis of chemical composition as related to the particle size is dependent on selecting the particle size being sent into the MS. The AMSI uses a perpendicular gas stream to steer the particles away from the straight trajectory path. The momentum of the particles through the steering gas determines the pathway of the particles through the AMSI and whether or not the particles will pass into the MS. A stream of nitrogen or helium is introduced perpendicular to the aerosol beam axis so that the changes occur in the particle-size distribution entering the MS. Since larger particles have higher momentum and inertia, they stay on the original straight trajectory path, while the small particles are blown away. As the flow of steering gas is increased, the mean drop size of particles reaching the MS is increased. This means that the signal intensity should be greatest when the gas flow is lowest and the greatest number of particles with the widest particle-size distribution is travelling into the MS. Conversely, the measured signal intensity reduced as the gas flow is increased since only the larger-sized particles (decreased particle-size distribution) pass into the MS. This is depicted in Figure 24. With increasing gas flow (increasing chamber pressure) the signal intensity decreased. It is imperative to ascertain that the force of the gas not be so strong that the larger particles are splintered into small sized droplets. In its current form, the AMSI is not calibrated to relate gas flow to particle size distribution. It has been shown that the technique is viable, but no correlation with actual particle size versus chemical composition has been made.

The steering gas, with increasing gas flow, changes the aerosol particle-size distribution being transferred through the AMSI into the MS. Once the AMSI is calibrated so that the particle-size distribution versus the steering gas flow is known, pattern recognition techniques can be applied to determine particle size versus chemical composition data (24-27).

Figure 24. Depiction of particle-size distribution selection via increasing steering gas flow.
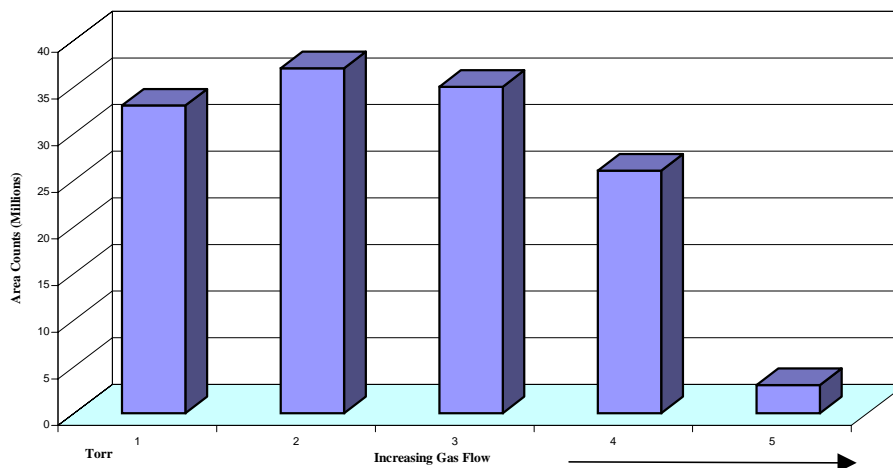
5.3 Particulate Spatial Dispersion

Particulate dispersional behavior, as well as the chemical compositional behavior, needs to be understood to design pollution prevention strategies for aerosol consumer products. A different set of tools and methodologies were developed to investigate the particulate dispersional behavior.

Particle transport in room air flow is influenced mainly by gravitation, convection, and turbulent (eddy) diffusion. These forces generate differences in particle concentrations and particle size distributions throughout a room. Movement of particles depends on the characteristics of the local air flow conditions and of the particle. Individual forces that influence movement of different sizes of particles are 1) the stopping distance, 2) settling velocity, 3) room air flow velocities, and 4) eddy diffusion resulting from fluctuating air flow velocities.

The stopping distance is the distance in still air that is penetrated by a particle with a certain initial velocity before falling to rest. The stopping distance for different particle sizes and an initial velocity of 2 m/s and 10 m/s is shown in Figure 25.

Figure 25. Distance in still air penetrated by particles with an initial velocity of 2 m/s and 10 m/s.
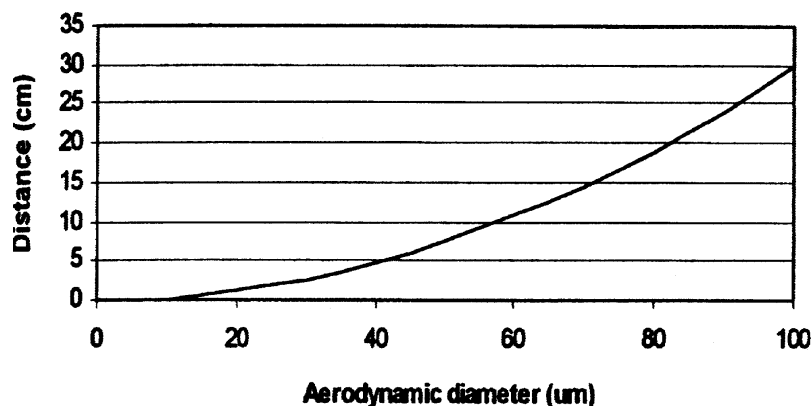
The settling velocity of particles suspended in still air is shown in Figure 26. If the air flow velocity is less than the settling velocity for a given particle of a given size, the particle will sediment out of the air flow. Settling velocity for particle sizes less than 10 μm will be less than 5 cm/s, and for particle sizes less than 100 μm will be about 23 cm/s.

Velocities in a room typically vary from zero to 20 cm/s in the occupied zone and up to 5 m/s at the room air diffuser. All particles with sizes greater than 100 μm will sediment out of the air flow in the occupied zone, certain fractions of particles with sizes between 20 and 100 μm also will sediment out, and particles smaller than 20 μm in size will remain in the air flow. This is illustrated in Figure 27, showing the steady state velocity for particles affected both by gravity and an upward air flow at different velocity levels.

38

Figure 26. Settling velocities for particles suspended in air.
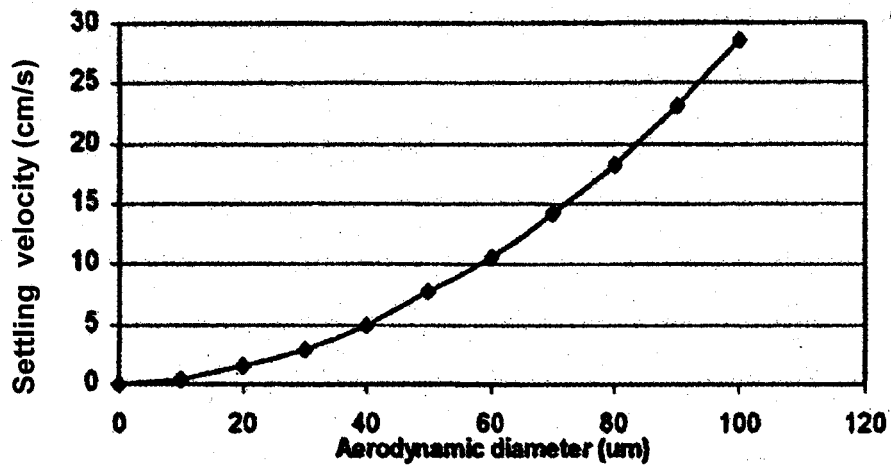
Figure 27. Steady state velocities of particles affected by gravity and different air velocities opposite to the direction of gravitational field (upward velocity is positive).
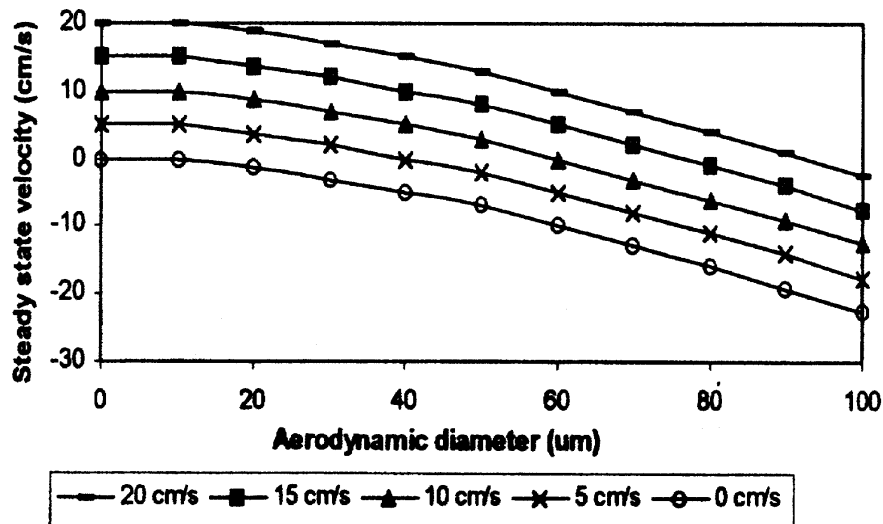
Eddy diffusion is another important force acting on particles in room air flow. Eddy diffusion is caused by fluctuating velocities in the air flow. Diffusion results in a net migration of particles from regions of high concentration to regions of low concentration. Eddy diffusion depends partially on air flow characteristics, such as air turbulent kinetic energy, dissipation rate of the turbulent kinetic energy and viscosity, and partially on particle characteristics, such as particle diameter and particle density. Eddy diffusion will be a constant for particles below 20 μm and will be decreasing for larger sized particles.

The spray cone of an aerosol consumer product is the dynamic three-dimensional projection of the liquid aerosol particles being ejected from the aerosol consumer product spray

39

nozzle into the air (33). The spray cone has a constantly changing length, particle size (and potentially changing chemical composition), and velocity distribution as the aerosol is dispersed through space. In the indoor environment, the spray cone is influenced by the localized air flow patterns in the space created by natural and mechanical ventilation. A basic understanding of this spray cone behavior is a critical factor in understanding product efficacy and in devising pollution prevention strategies.

The PIV system was used to determine the spray cone characteristics by measuring particle concentrations and velocity distribution. These techniques also were used in an environmental chamber to investigate the effect of localized air flow patterns on particle concentration distributions as the aerosols are transported through space in the indoor environment. A Malvern Particle Sizer was used to investigate the particle-size distributions to understand potential exposures during the use of aerosol consumer products.

5.3.1 Particle Size Distribution

Since the behavior of aerosol particles is dependent on their size and the nature of the propellant (carrier gas), particle size distribution data was needed to determine the impact of aerosol consumer products on the environment and consumers (34). This was done by using the Malvern light-scattering technique to measure the particle size distribution of the surrogate aerosols down to 1 μm particle size.

The Malvern 2600C Droplet and Particle Sizer has an accurate operating range of 1.2 – 1000 μm. The system consists of a helium-neon laser, a detector, and a computer system and operates on the Fraunhofer diffraction theory (35) (Figure 28). The Malvern system uses laser-induced light scattering to determine particle size distribution as a percentage by volume of each measured size range via mathematical models and calculations. This analysis provided data on the particle size (drop-size) distribution and the Sauter mean diameter (the diameter of a droplet with a surface to volume ratio equal to the mean of all the surface-to-volume ratios of the droplets in a spray distribution also referred to as the mean volume-surface diameter).

The particle size distributions, 13.6 cm from the nozzle (an arbitrarily chosen distance), of each of the surrogate aerosols are shown in Figures 29, 30, and 31. The results are summarized in Table 9 showing that the majority of the particles, for each of the surrogate aerosols, are above 25 μm. The Sauter Mean Diameter of each of the surrogate aerosols was above 50 μm. The figures graphically display these findings. These findings can have a significant impact on devising pollution prevention strategies to reduce user exposures. In general, these results indicate that there are few particles ranging in size below 25 μm as the aerosols left the aerosol package. The particle size distribution for the surrogate aerosols (representing different product-use types) were different (Figures 29, 30, and 31). Therefore, the dispersion of the aerosols through space can be expected to be different.

The design of the surrogate aerosols allowed for the comparison of the differences between hydrocarbon and compressed gas propellants. Examining Figures 29, 30, and 31, it appears that the compressed gas propellant yielded a larger particle size distribution than the hydrocarbon propellants. These data may not be statistically significant since multiple sample analyses on the surrogate aerosols were not conducted. Figure 29 depicts the results for the surrogate air aerosols AA1 and AA2. The only difference between these two aerosols is that AA1 uses a hydrocarbon propellant and AA2 uses a compressed gas propellant. Similar results are

Figure 28. Schematic of Malvern Particle Sizer for droplet size measurement.
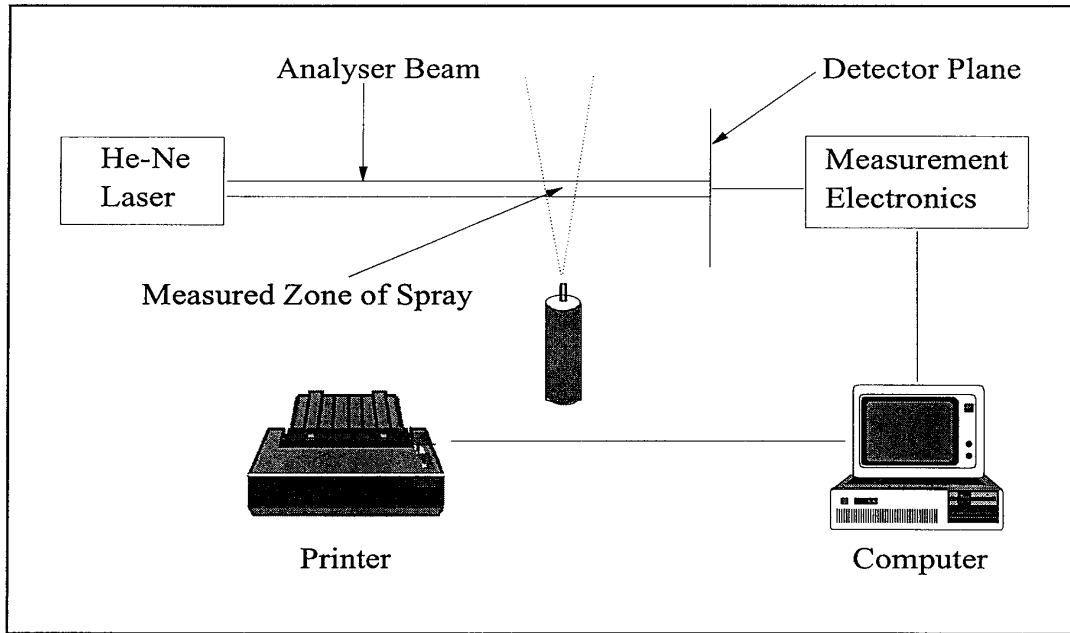
Table 9. Range of particle sizes of surrogate aerosols measured with Malvern particle sizer

Surrogate Aerosol	Propellant	Sauter Mean Diameter (µm)	Particles Size Range (µm)
AA1	A46	82.27	50 - 300
AA2	CO_2	179.74	50 - 550
SNWP1	A46	55.14	50 - 200
SNWP2	CO_2	64.93	25 - 200
SNWP	Mister	86.57	50 - 200
SWA	A31	117.37	50 - 350
SWP	Trigger	59.60	25 - 500

found in Figure 30 for the surface non-wipe surrogate aerosols. Figure 31 shows the difference between a hydrocarbon propellant (SWA) and a pump spray (SWP). The particle size distribution of SWP maximizes at a smaller particle size than SWA and over a broader range (Table 9). Similar results were found with the PIV techniques (discussed in Section 5.2.2). The PIV data revealed that the particle size distribution, determined via velocity measurements, is dependent upon the materials used in the aerosol; therefore, propellants can be expected to have a significant impact.

41

Figure 29. Particle size distribution measured with Malvern analyzer for surrogate air aerosols. A) AA1 and B) AA2. (AA1 has small Sauter mean diameter and AA2 has large Sauter mean diameter.)
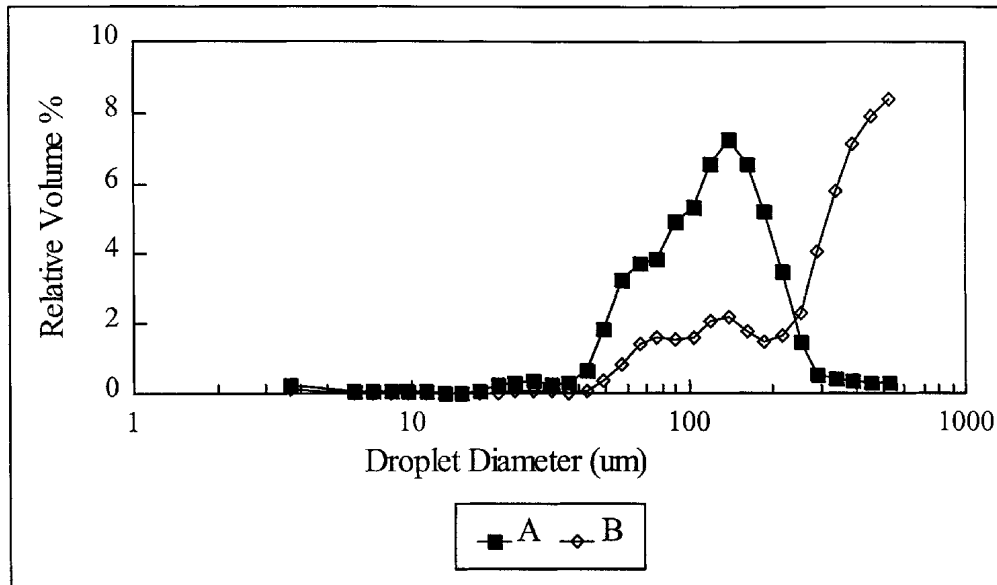
Figure 30. Particle size distributions measured with Malvern analyzer for surrogate surface non-wipe aerosols. A) SNW1, B) SNW2, and C) SNWP. (SNW1, SNW2, and SNWP have small Sauter mean diameters.)
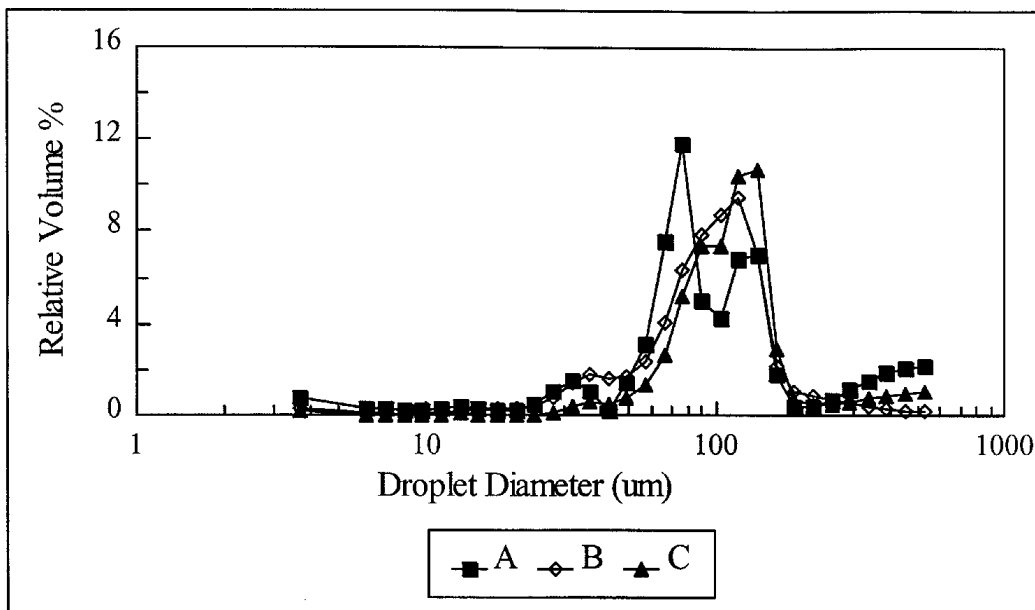
Figure 31. Drop-size distributions for (A) SWA and (B) SWP measured with Malvern system. (SWA has large Sauter mean diameter and SWP has small Sauter mean diameter.)
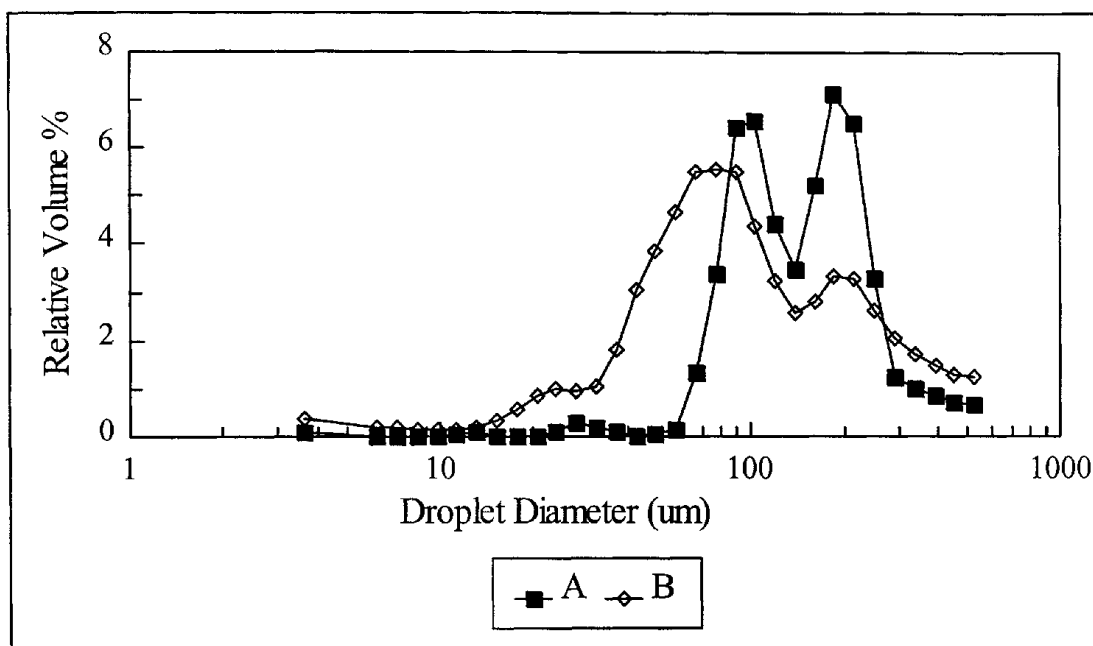
The particle size distribution in pressure-swirl nozzle spray cones, the type most commonly used for propellant-driven aerosol consumer products, is not the same throughout. Therefore, the particle size distribution across the spray cone's axial centerline can be dramatically different (9). For this reason studies were conducted across the spray cone of the surrogate aerosols, in order to investigate the importance of the position in the spray cone on particle size distribution. This was done by measuring the particle size of the released particles at different distances from the aerosol actuator nozzle and across the spray cone in two-dimensional space (Figure 32). The distances were chosen arbitrarily.

Figure 32. Depiction of spray cone particle-size distribution measurement scheme.
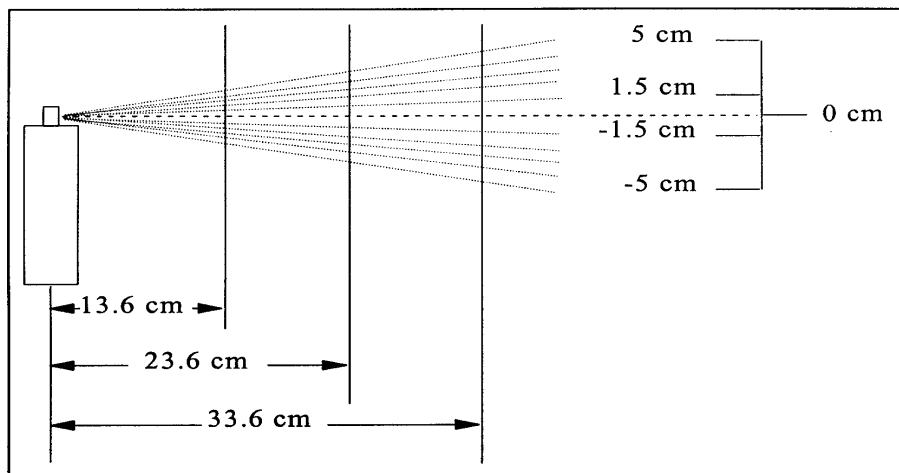
These studies were carried out on three different aerosols: 1) AA1, 2) SWA, and 3) ethanol using nitrogen as the propellant. These data provided information on the importance of the propellant gas on the particle size distribution (since aerosol velocity is dependent on the propellant gas) and the design of the aerosol package for final use.

There was not a significant difference in particle size distribution in the jet core as the distance from the spray nozzle was increased, although there appeared to be a tendency toward larger particles with increasing distance from the spray nozzle (Figures 33 and 34). This may indicate potential agglomeration of the particles with movement through space, but also may be the result of the particle size decreasing below the Malvern analyzer detectability due to evaporation. However, in the outer part of the jet, where the velocities are lower, there was a different particle size distribution in the aerosol jet. This can be explained by particle transport phenomena – larger particles, due to their larger initial momentum, travel farther than smaller particles, and diffusion of larger particles is less. Therefore, the particle size distribution is expected to change toward larger particles in the flow of the jet. This same situation also occurred in the jet centerline at a greater distance from the spray nozzle, where the velocities were less.

Centerline velocities for the surrogate aerosols as function of the distance from the spray nozzle are depicted in Figure 35. The velocities adjacent to the nozzle were higher than those in room air flow, however at a distance of less than 40 cm from the nozzle the velocities will be approximately the same. Therefore, flow conditions in surrogate aerosol jet adjacent to the nozzle are determined by nozzle design, and aerosol transport at distances greater than 40 cm from the nozzle are determined by the flow conditions in the room.

In Figure 36, the Sauter Mean Diameters are shown correlated with the position of the spray. The Sauter Mean Diameter for SWA is smallest at the centerline and 1.5 cm above the nozzle. When ethanol pressurized with nitrogen is tested, the Sauter Mean Diameter is smallest at 1.5 cm above the nozzle. The ethanol pressurized with nitrogen was investigated to see if a generic, no use designed, nozzle would change the results. There were no obvious advantages to analyzing the ethanol pressurized with nitrogen – the generic aerosol.

Another factor that could influence particle size distribution is the amount of product and propellant in the can, in other words, the "can-fullness". This can potentially be a problem with aerosol consumer products using compressed gases as the propellants. An experiment was conducted also to investigate particle size distribution as related to can-fullness. The amount of product remaining in the can was determined by weighing the can when full, when about half full, and when almost empty. The particle size distribution was measured with the Malvern system on a new, full can of AA1. The nozzle was depressed to release product until the can was approximately half full, as determined by weight. Then the particle size distribution was measured again. The nozzle was then depressed until the can was almost empty. The particle size distribution was determined again. The results are shown in Figure 37 showing that the particle size distribution does not dramatically change until the can is almost empty.

Figure 33. Particle-size distribution for AA1 at increasing distance from the laser beam.
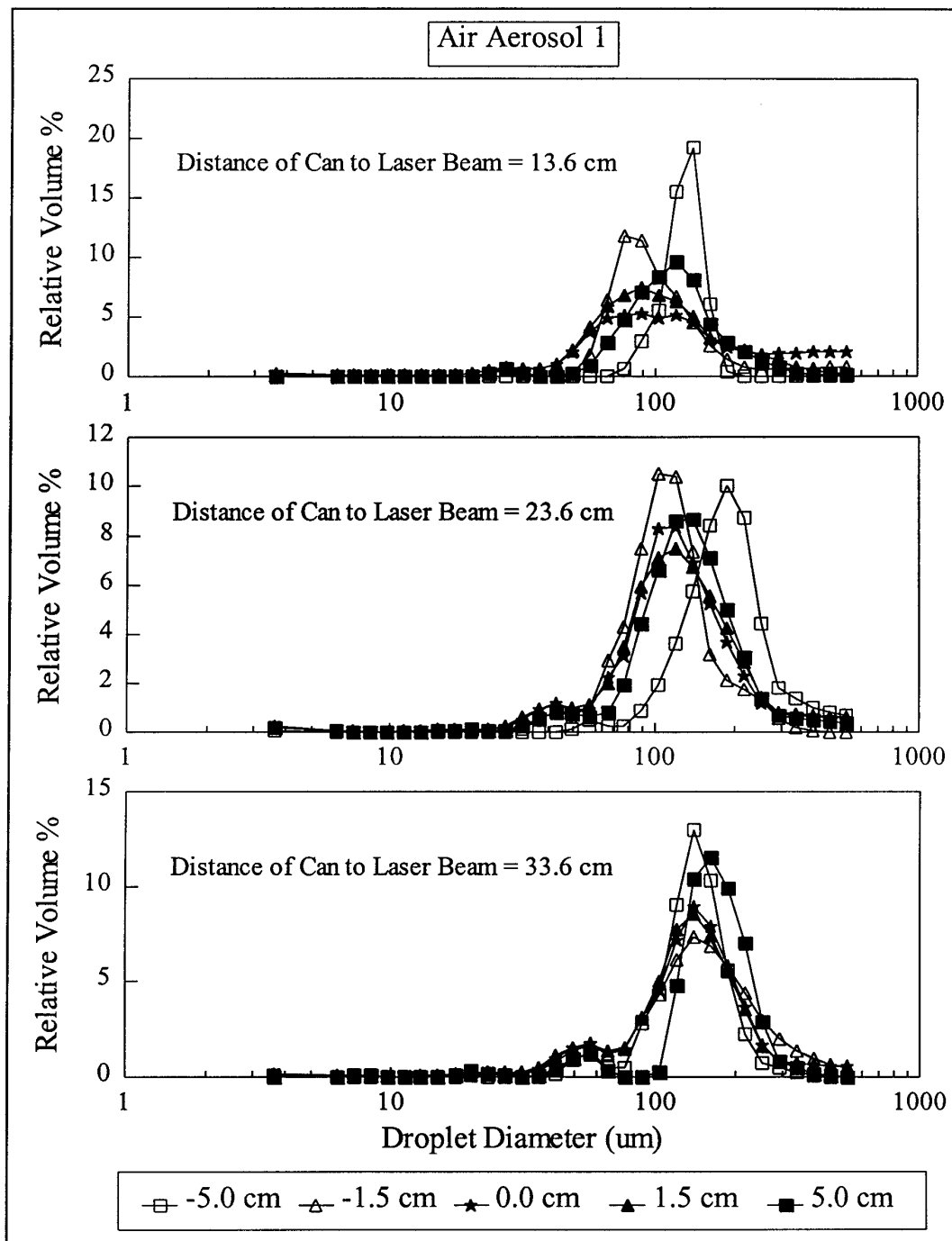
Figure 34. Particle size distribution for SWA at increasing distance from the laser beam.
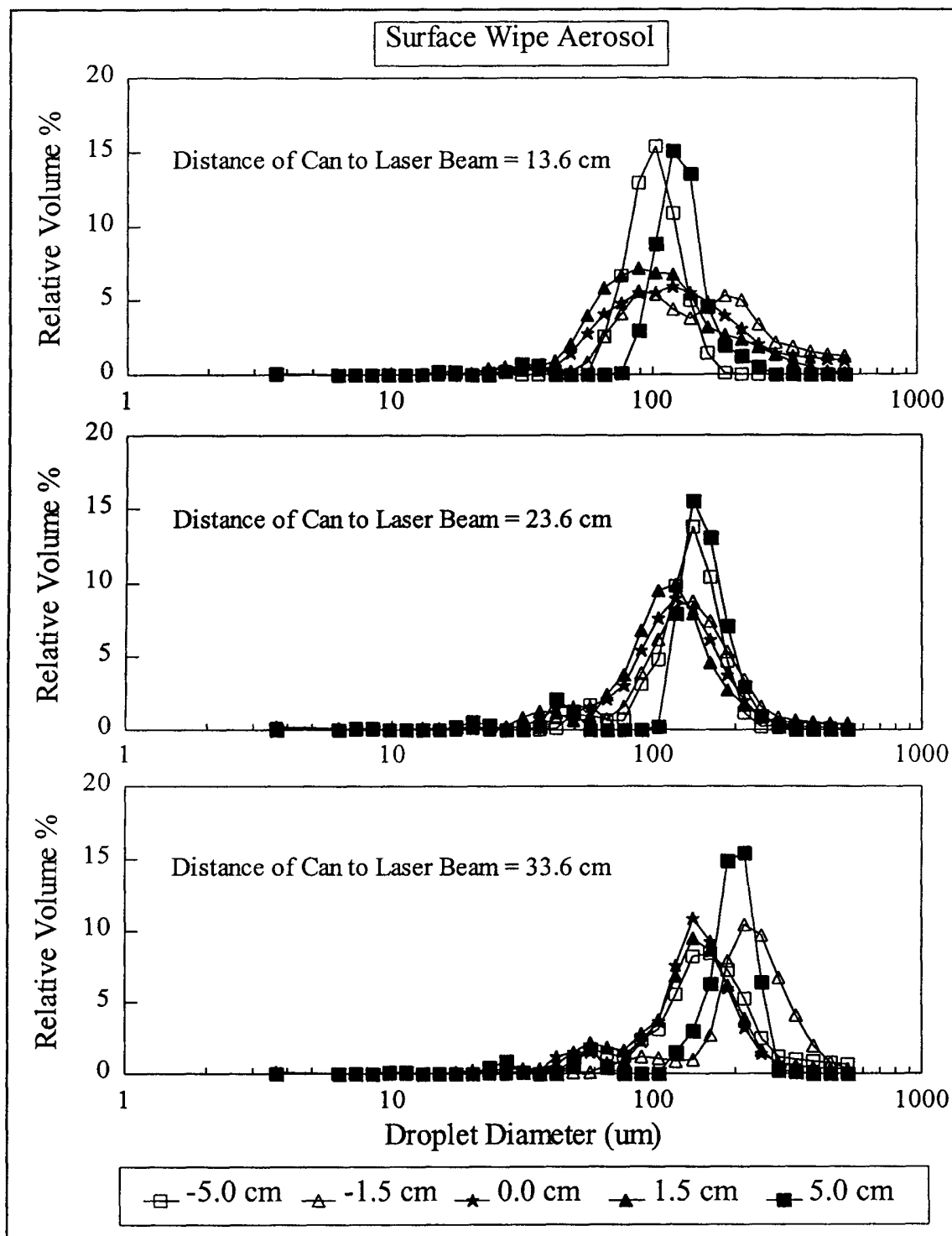
Figure 35. Velocity decay of surrogate aerosol particles along the jet centerline.
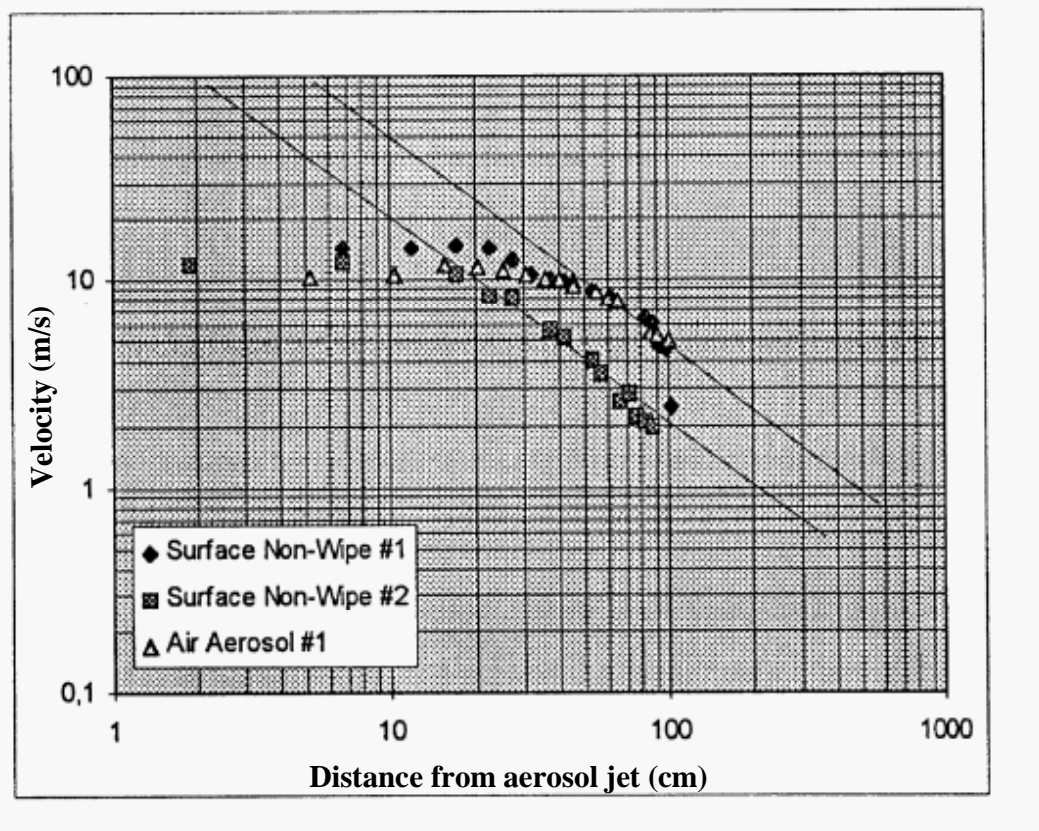
5.3.2 Aerosol Spray Cone Characterization

PIV (35-39) was used to characterize aerosol spray cones to determine the particle size distribution and particle concentrations via velocity determinations (40). With the PIV illumination and image acquisition systems, quantitatively dynamic structures of aerosol spray cones were visualized, producing contour plots of the aerosol particle concentrations and particle concentration profiles along the spray radial direction. Digital images were taken continuously during the entire spray period to determine the dynamic structures of aerosol sizes, concentrations and velocities of the random flow process of the aerosol spray jets. Using this method, the characteristics of aerosol sprays and the transport mechanism in rooms were studied. An environmental chamber facility equipped with a PIV was used during this project to investigate the transport mechanisms in a room, and how the transport is affected by room air ventilation. Since an aerosol spray is a random process, a large number of data points were needed to mathematically describe the process. The PIV was able to collect the data by rapidly and automatically recording the data.

The PIV imaging system was applied to analysis of the surrogate aerosol spray cone patterns. The temperature of the test environment was controlled at 21 $\pm$ 0.2°C. To ensure that the pressure inside the containers did not change more than $\pm$5%, the pressure in the aerosol cans was measured before and after the tests.

Figure 36. Sauter Mean Diameters correlated with distance from the spray.
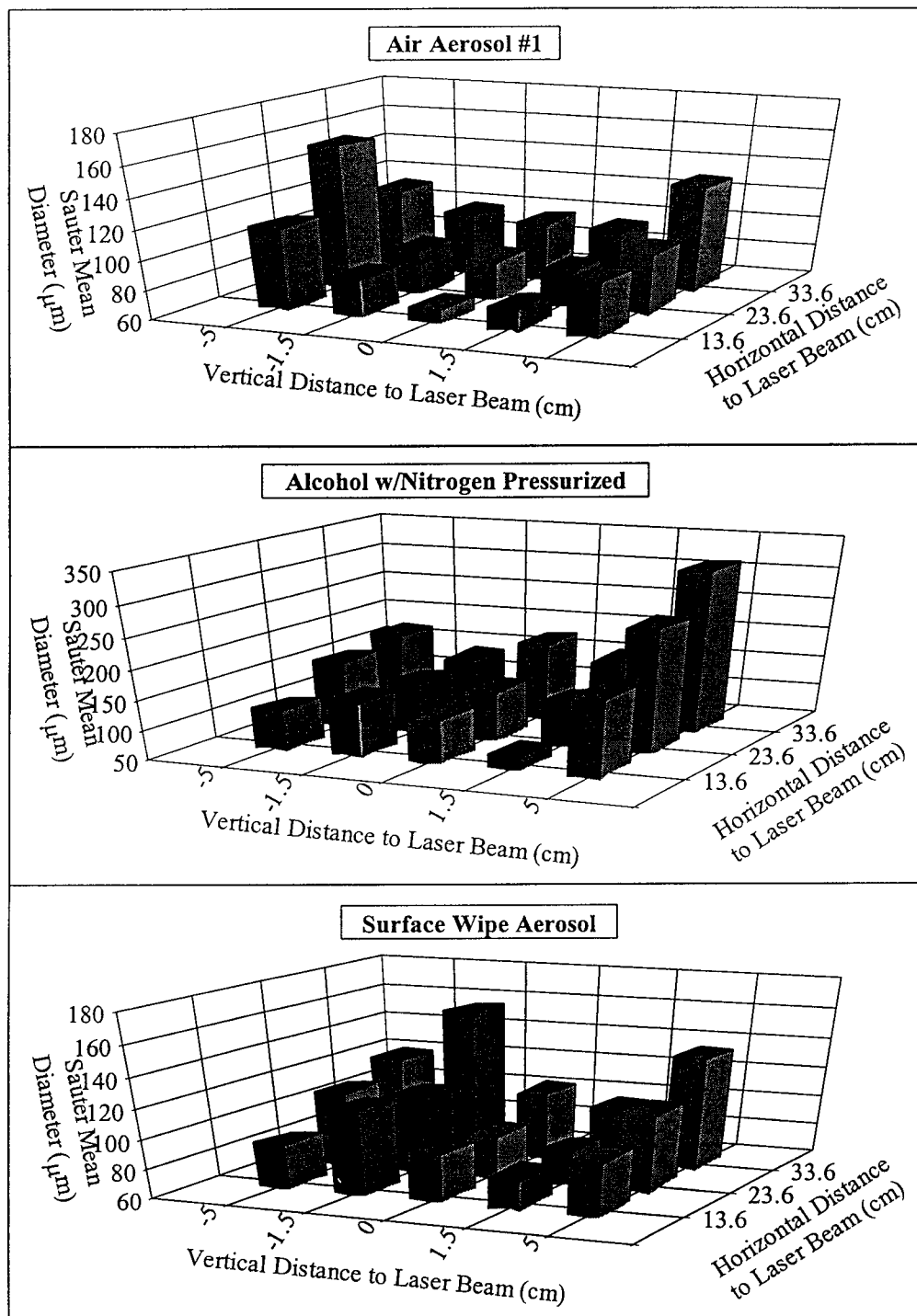
Figure 37. Particle size distribution related to can-fullness. A depicts a full can; B depicts < half full can; and C depicts an almost empty can.
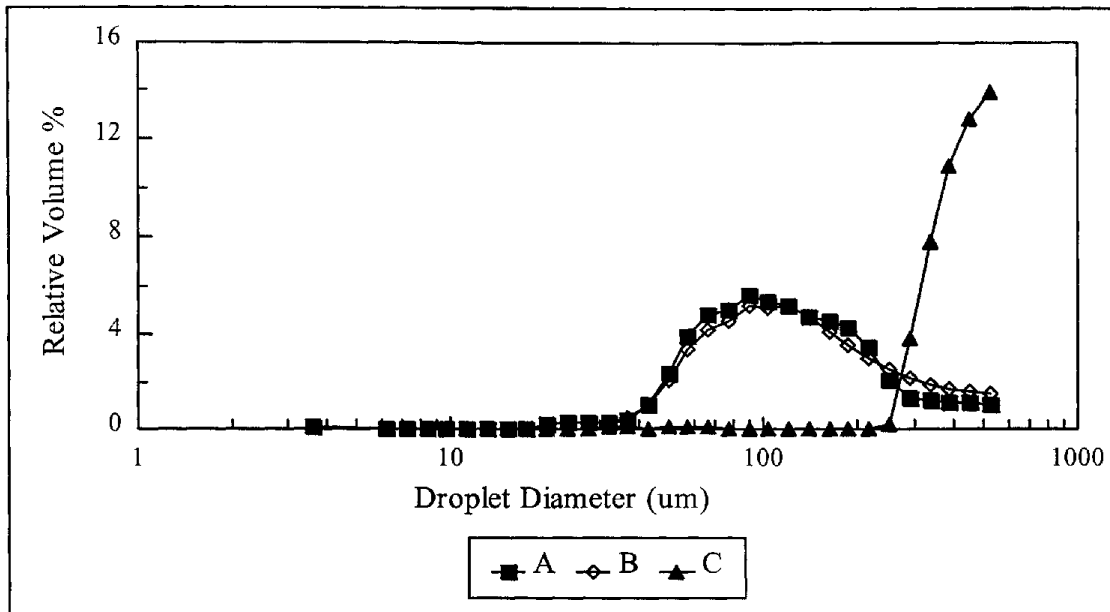
The PIV measurement system consists of an argon ion laser, a polygon mirror, sheet-forming optics, two charge-coupled device (CCD) cameras, two frame grabbers, and a host computer (Figure 38). The measurement system was used to measure particle size distribution, velocity and concentration, but different test procedures, image interrogation systems and calibration systems were required for each.

The argon laser provided a beam with constant intensity to illuminate aerosol sprays. The beam was swept through the view field with a rotating polygon mirror (Figure 39). A sweeping frequency of 30 frames per second was maintained via a motion controller. Each time the beam swept through the view field, a photodetector triggered the cameras. Images acquired by these cameras were sent to the host computer and saved on a hard disk for interpretation. Each group of data consisted of 120 to 240 images. The size and concentration distributions were obtained instantaneously. Particle size, concentration and velocity were calculated. These data then were compiled for calculations of statistical averaged values.

The measurement system capability covered the size range of the majority of particles in the surrogate aerosol products. Under current experimental conditions, particle sizes in the 20 μm range were measured in a view field of 200 x 150 mm. Two images covered the majority of the surrogate aerosol jets. Smaller view fields (11 x 7.5 mm), particles as small as 1 μm, can be detected; but due to funding and instrumentation limitations, this level was not achievable during this project. Measurement accuracy depended on the calibration system view field and particle size. Practical accuracy achieved was within 5% and was generally in good agreement with computer simulations.

49

Figure 38. PIV measurement system.
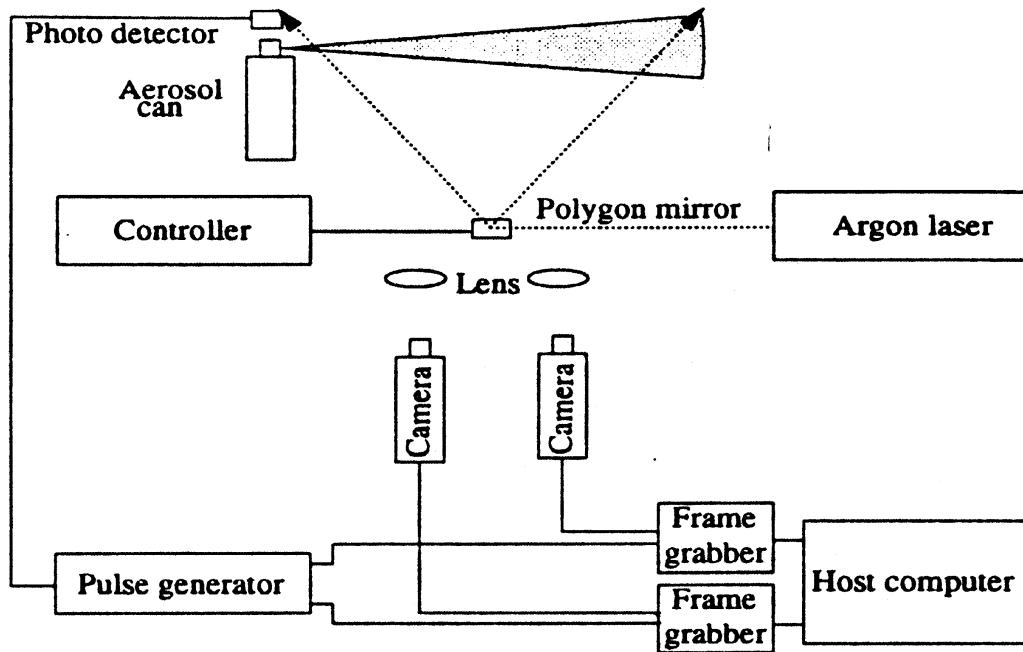
Figure 39. Schematic of beam sweeping over aerosol particles.
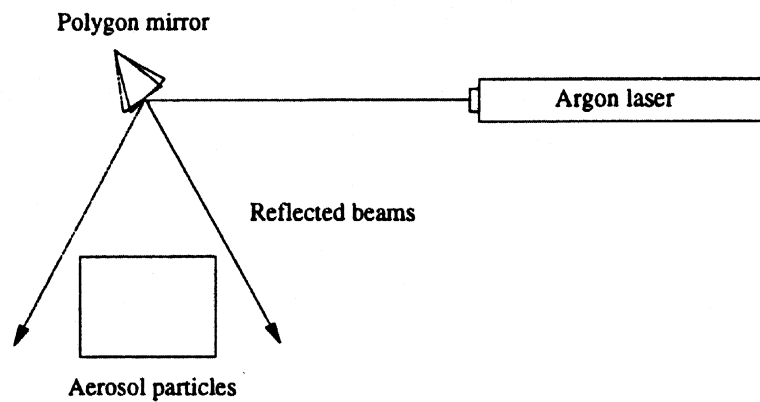
A small view field (Figure 40) was used for particle size distribution measurements. The whole flow field of the spray jet was divided into several smaller view fields allowing some overlap between the individual view fields in order to measure the overall size distribution information. A

50

computer-controlled step motor directed the camera position. Size distribution was calculated as the number of particles as a function of particle size. At the first stage, particle size was in pixels, the particle size in "image space". Particle size in "object space" was proportional to the size in "image space" and was calculated via a calibration curve.

Figure 40. Particle size distribution small view field schematic.
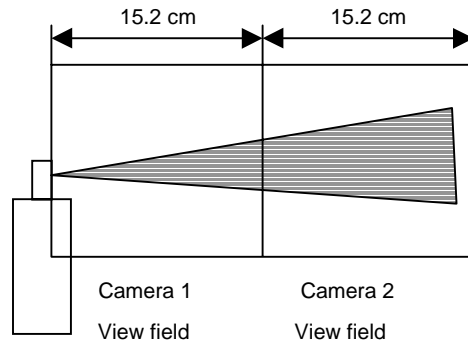
Only a relatively low-resolution image acquisition system was required for particle concentration measurements. The whole flow field was separated into two parts (Figure 41).

Particle images were recorded by two CCD video cameras and saved on computer hard disk for later interpretation. Particle concentrations were calculated from picture light intensity values. A particle counter (CI-7350) from Climet Instruments was used to calibrate the relationship between particle concentrations and the reflected light intensity.

Figure 41. Particle concentration measurements large view field schematic.
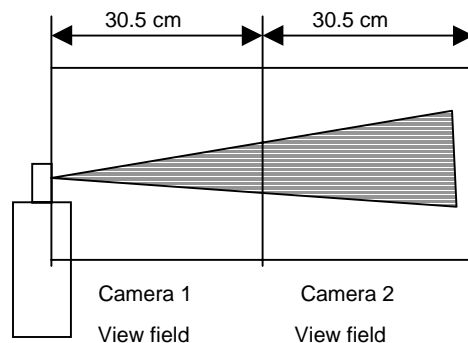
The two basic quantities used to describe the structure of aerosol sprays were aerosol particle concentration and velocity distribution. Since these two parameters are important in determining aerosol particle transport over space, they are important in the evaluation of aerosol product efficacy.

51

The concentration of particles is defined as the number of particles in a unit volume.

$$C = \frac{\Delta n}{\Delta V}$$

where C is the concentration, n is the particle number and V is the volume. In preliminary tests, volume was chosen to be 3.18 x 2.29 x 0.25 cm. Statistical averaged results are obtained by using a large number of data sets.

The particle concentration results were obtained in two different formats: 1) contour plots of the aerosol particle concentration (Figure 42), and 2) profiles of the particle concentration along the spray radial direction (Figure 43). The contour plots for the surrogate aerosols are shown in Figure 42. The contour plots are useful for visualizing particle trajectories and behavior of the aerosol jets.

The particle concentration profiles along the spray radial direction are useful for visualizing the size spectrum of the aerosol particles with increasing distance from the spray nozzle. The profiles of the particle concentration along the radius of the spray cone are shown in Figure 43 for the surrogate aerosols.

The particle concentrations varied markedly among the surrogate aerosols products. From Figure 43 and Table 10, it can be seen that the surrogate aerosols that used hydrocarbon propellants had a smaller particle concentration distribution than the compressed gas surrogate aerosols. The surrogate surface non-wipe aerosols, particularly SNW2, had the widest particle concentration distribution. These data may be useful for the development of pollution prevention strategies for product reformulation.

Table 10. PIV determined concentration distribution of surrogate aerosol particles at a distance from the spray nozzle.

Surrogate Aerosol	Propellant	Distance from Spray Nozzle of Peak Concentration Distribution (cm)
AA1	A46	0.00 – 3.18
AA2	CO_2	3.18 – 6.35
SNW1	A46	9.52 – 12.7
SNW2	CO_2	3.18 – 12.7
SWA	A31	3.18
SWP	Trigger	6.35

Figure 42. Contour plots of surrogate aerosol particle concentrations in the aerosol jets (1 in. = 2.54 cm):

53
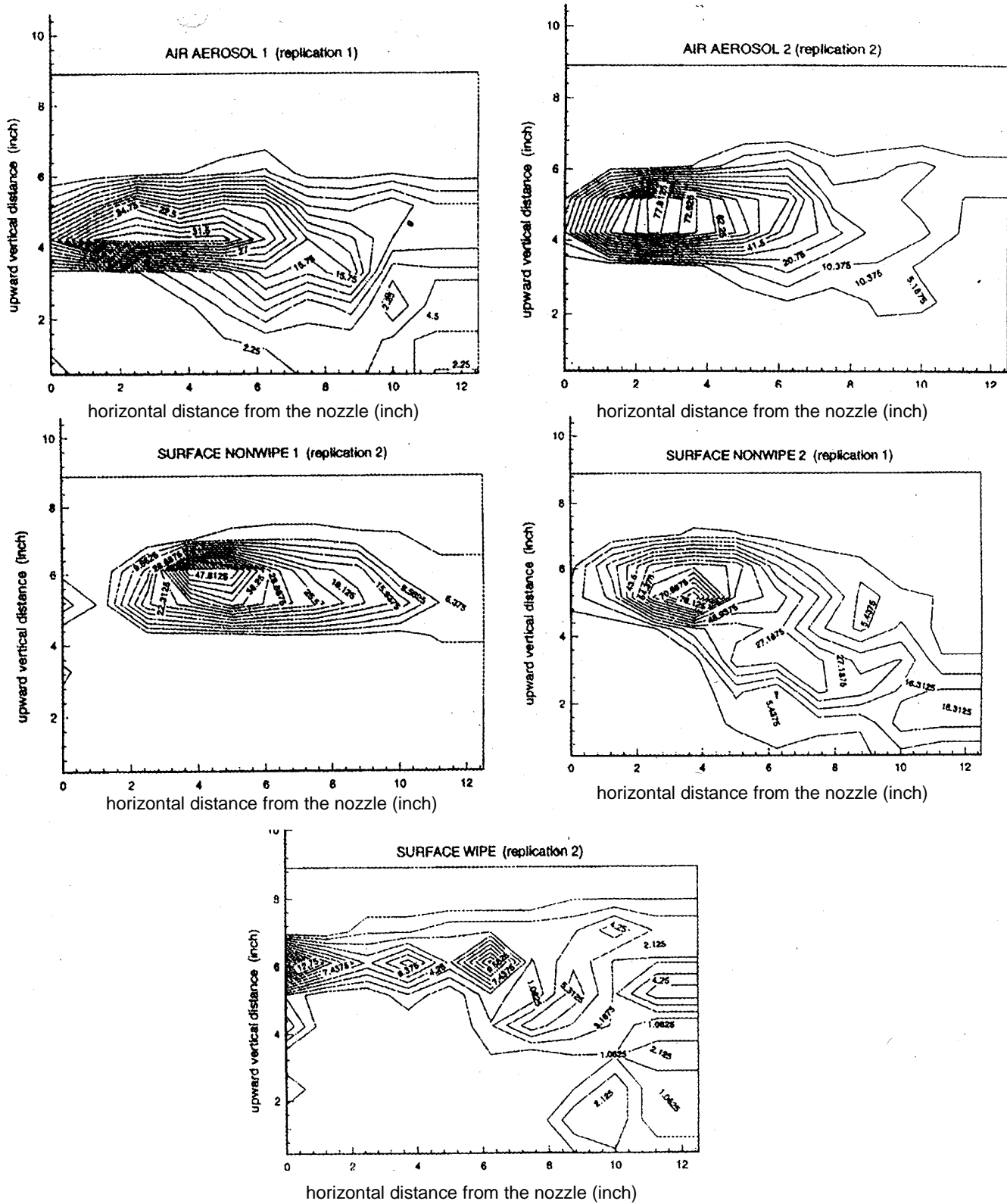
Figure 43. Surrogate aerosol particle concentration profiles along the radium of the spray cone.

A relatively high-resolution image acquisition system was required for particle velocity measurement in order to identify the individual particles in aerosol spray jets due to the high particle concentrations. Particle images were recorded either by video camera or photographic fil, sent to a PIV computer-based interrogation system, and digitized. The 1024 x 1024 pixel image was stored and divided into eight sub-images. Processing was performed in two array processor boards (mc860vs), each with four i860 microprocessors (Figure 44). After the interrogation procedure, velocity vector maps and velocity distributions were obtained.

Figure 44. Velocity measurement interrogation system hardware schematic.
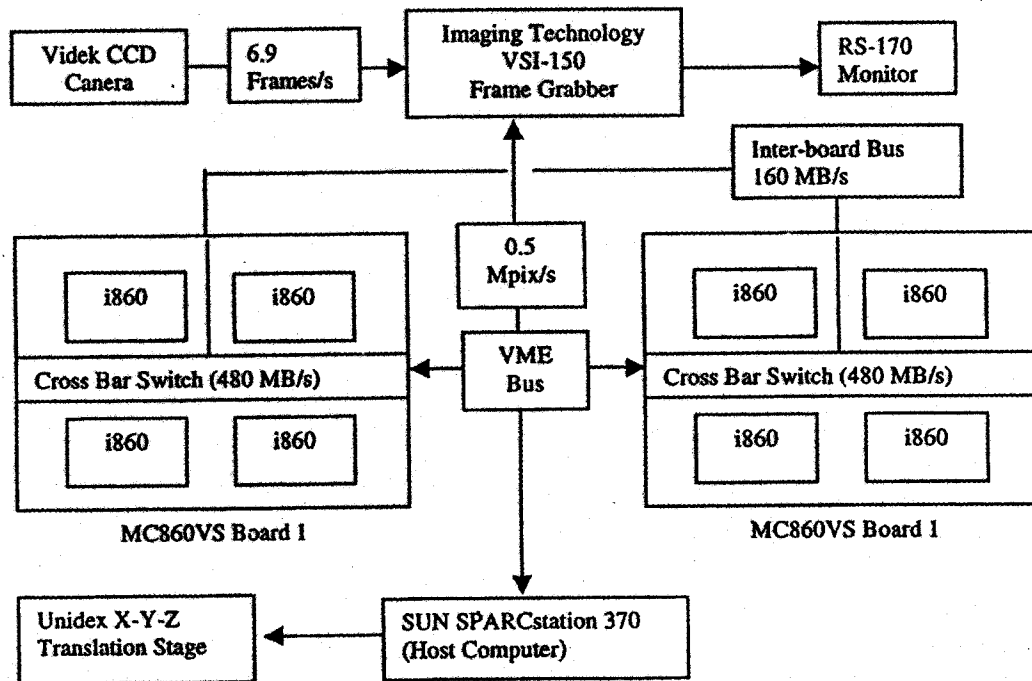
Laser Doppler Velocimetry (LDV) also was used to measure particle velocities; the comparison of results from the two different techniques determined the measurement accuracy. The LDV unit used in the test was a TSI SUREPOINT laser probe with an IFA550 signal processor operating on a host computer. For each data point, 8000 samples were used to calculate the averaged velocity value. The LDV data were found to be oin good agreement with the PIV data, within 5%.

The surrogate velocity data are depicted in Figure 45. These data are presented as a function of distance from the spray can nozzle. The velocities of the centerlines do not change significantly for the different surrogate aerosols. The velocity decreases as the distance from the nozzle increases. The range of the velocity is between 2 and 14 m/s when the distance from the nozzle changes from zero to 100mm.

55

Figure 45. Surrogate aerosol particle velocity distributions along the axis of the spray nozzle.
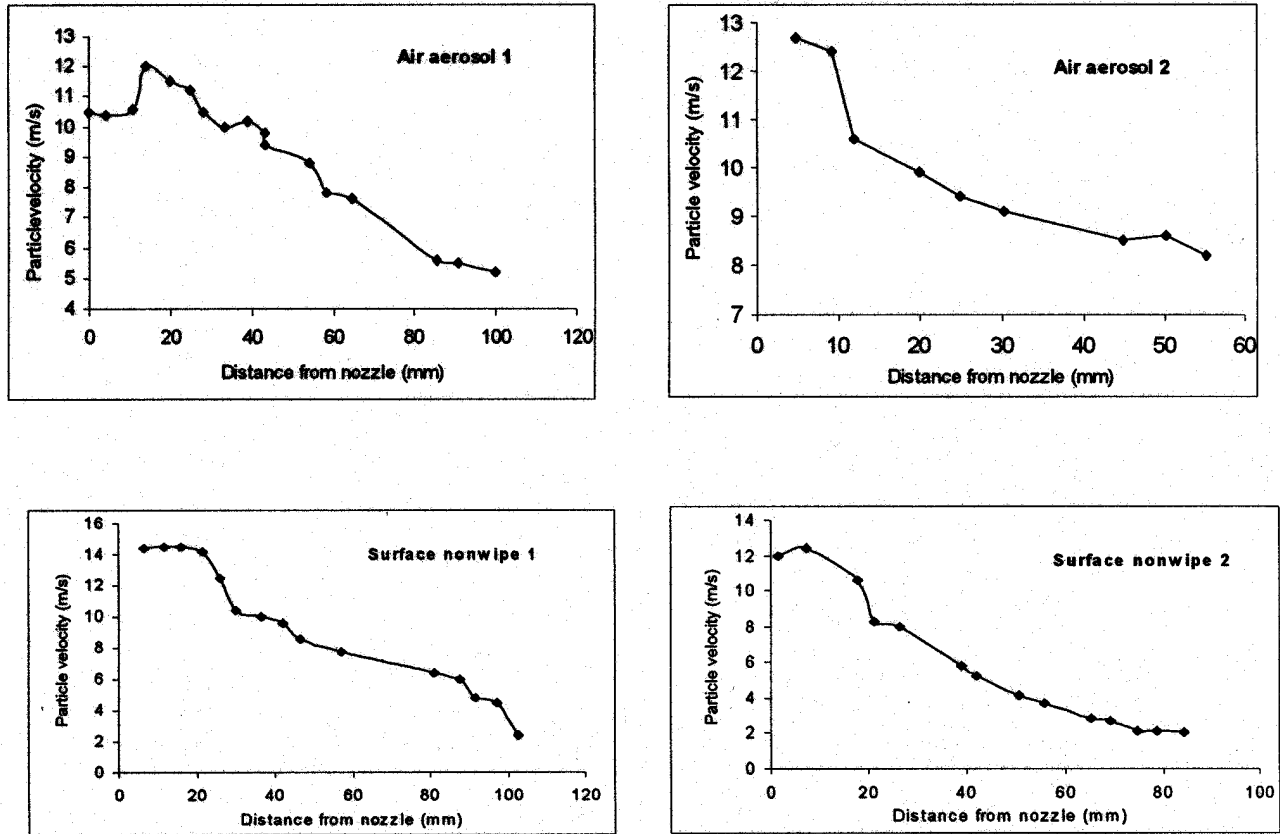
Model

A model, which can predict the major characteristics of aerosol spray patterns, can be useful to guide in the development of pollution prevention strategies. A simplified engineering model for aerosols was developed previously based on turbulent jets (42). This model assumes that 1) the jet emerges from a circular orifice into a stream of uniform velocity, U_s; 2) the flow of the mixtures of aerosol particles with air is turbulent with axis-symmetric mean values; 3) the jet velocity is larger than ambient stream velocity; and 4) the turbulent region is relatively narrow in the radial direction. Based on these assumptions, mass balance and momentum balance equations in a cylindrical coordinate system, (r,z) can be written:

$$\frac{\partial}{\partial z}\left(U_s + \overline{U}_z\right) + \frac{1}{r}\frac{\partial}{\partial r}\left(r\overline{U}_r\right) = 0$$

$$\frac{\partial}{\partial z}\left(U_s + \overline{U}_z\right)^2 + \frac{1}{r}\frac{\partial}{\partial r}r\overline{U}_r\left(U_s + \overline{U}_z\right) = \frac{1}{r}\frac{\partial}{\partial r}r\left(-\overline{u_r u_z}\right)$$

Where $\overline{U}_r$ and $\overline{U}_z$ are r and z components of the mean velocity of the mixture of aerosol and surrounding air, and u_r and u_z are r and z components of fluctuating velocity of the mixture of aerosol and surrounding air.

These equations can be solved numerically. This research project required the development of a simplified analytical model, which could be used easily in engineering practice; therefore similarity methods were chosen (33) to simplify the equations, and since the velocity and concentration profiles can be measured experimentally. These equations are outlined by Cui (34). Cui introduced a similarity variable, ξ_2, and several similarity functions, *f, g,* and *h.* The original variables, $\overline{U}_r$, $\overline{U}_z$, u_r, and u_z can be defined as functions of the similarity variable and functions.

To solve the balance equations, the following similarity relations are introduced:

$$\overline{U}_z = U_p \left(\frac{z+a}{d} \right)^p f(\xi_2),$$

$$\overline{U}_r = U_p \left(\frac{z+a}{d} \right)^r g(\xi_2),$$

Where $z = -a$ is the position of the "origin of similarity"; *d* is the diameter of the orifice; U_p is the issuing velocity of the mixture of the aerosol, propellant, and air; *f, g,* and *h* are the similarity

$$-\overline{u_r u_z} = U_p^2 \left(\frac{z+a}{d} \right)^{s_{21}} h(\xi_2),$$

functions; and

$$\xi_2 = \frac{r/d}{[(z+a)/d]^q}$$

Substituting the similarity relations into mass and momentum balance equations, the constants *d, r, q,* and , ξ_2 can be determined to be –1, -1, 1, and –2, respectively. If an eddy viscosity, ε_m, is introduced:

$$-\overline{u_r u_z} = \varepsilon_m \frac{\partial \overline{U}_z}{\partial r},$$

57

the velocity distribution can be obtained by setting the ambient stream velocity to zero, $U_s = 0$:

$$\frac{\overline{U}_z}{\overline{U}_{z,max}} = \left\{ 1 + \frac{\overline{U}_{z,max}(z+a)}{8} \varepsilon_m \xi_2^2 \right\}^{-2}$$

For the concentration distribution, the equation of transport can be written as:

$$\left(U_s + \overline{U}_z \right)\frac{\partial \overline{C}}{\partial z} + \overline{U}_r \frac{\partial \overline{C}}{\partial r} = -\frac{1}{r}\frac{\partial}{\partial r}\left(r\overline{u_r c} \right)$$

where

$$C = \overline{C} + \gamma = C_p + \overline{C_1} + \gamma,$$

C_p is the value for C for the issuing fluid, and γ is the fluctuating part of the concentration.

Cui (34) introduced a similar relationship involving a diffusion tensor:

$$\frac{\overline{C_1}}{C_p} = \frac{d}{z+a} k(\xi_2),$$

where k is the similarity function:

$$\xi_2 = \frac{r}{z+a},$$

$$-\overline{u_c} = \varepsilon_c \frac{\partial \overline{C}}{\partial r},$$

Cui then determined the concentration profile:

$$\frac{\overline{C}}{C_{1,max}} = \exp\left\{ \int_0^{\xi_2} d\xi_2 \frac{\varepsilon_m}{\varepsilon_c} \frac{d}{d\xi_2}\left(\ln\frac{\overline{U}_z}{\overline{U}_{z,max}} \right) \right\},$$

58

Cui applied Prandtl's mixing-length hypothesis to further simplify the result:

$$\frac{\varepsilon_m}{U_p d} = l_m^2 \left| \frac{d}{d\xi_2} \frac{\overline{U}_z}{\overline{U}_{z,max}} \right|,$$

$$\frac{\varepsilon_c}{U_p d} = l_c^2 \left| \frac{d}{d\xi_2} \frac{\overline{U}_z}{\overline{U}_{z,max}} \right|,$$

where l_m and l_c are mixing lengths.

The expression of concentration distribution of aerosol particles can be written as:

$$\frac{\overline{C}}{\overline{C}_{1,max}} = \left(\frac{\overline{U}_z}{\overline{U}_{z,max}} \right)^{l_m^2 / l_c^2},$$

where the velocity distribution and the constants ε_m, ε_c, l_m, and l_c depend on the material properties of the aerosols.

Once the similarity functions are applied to the model, the mass, the momentum, and energy fluxes can be determined by using the velocity and concentration distribution for the aerosol. The amount of effective materials carried by the aerosols to the use site can be calculated from these quantities. The uniformity of the materials distributed at the use site also can be evaluated. The characterization of the aerosols in this manner may guide in the development of pollution prevention strategies and more efficacious products.

Applying the model to the surrogate aerosol data, Cui (33) found that the spray pattern correlated with the material properties of the liquids. The velocity of the aerosol particles in the propellant driven sprays appeared to be increasing near the spray nozzle. This may have been caused by the evaporation of the liquid propellants near the nozzles. The velocities peaked at a distance of 20 mm from the nozzle and decreased as the distance from the nozzle increased. This was probably due to air drag. This mechanism appeared to control the atomization process near the spray nozzle.

5.3.3 Aerosol Transport in Rooms

When the PIV was combined with large-scale environmental chamber technology, the effects of room air ventilation, both natural and mechanical could be measured. The PIV/environmental chamber system also allowed for the measurement of particle velocities in a whole room. This allows for the calculation of changes in particle size distributions in the indoor environment. Both understanding the effect of ventilation and the particle size distribution throughout a room can lead to valuable data for development of more efficacious, less toxic, and

59

more user friendly products. These data may guide manufacturers to design effective pollution prevention strategies.

The PIV/environmental chamber system primarily has three subsystems which illuminate flow structure, acquire images and interrogate the images. These three subsystems allow calculation of velocity and particle-concentration distribution in the indoor environment (27). The whole field is illuminated with light, either laser or white, to visualize particle flow. Films or electronic media record images of visualized particles. The recorded images are interrogated by a computer system to obtain positions, displacements and concentrations of particles. If particles are neutrally buoyant and small, the particle velocity will be the same as air velocity. Otherwise, the particle velocity will be different from velocity of the carrying media and the distribution of particles will deviate from the distribution of the air.

The PIV/environmental chamber system consisted of a test room (28); heating, ventilation and air-conditioning (HVAC) system; illumination system; image shift technique; flow seeding technique using particles; image interrogation and statistic data analysis technique.

The aerosol test room was constructed in the Room Ventilation Simulator (Figure 46), which consists of an adjustable inner room and an outer room for controlling ambient environmental conditions of the inner test room. The outer room is an insulated building used to simulate climatic conditions. The front and left side of the aerosol test room (Figure 47) are made of clear, tempered glass permitting optical access to the room interior. The other two walls are made of black painted wood for an optimal optical environment. The aerosol test room was designed and constructed to allow for easily changing room configurations, such as types and locations of diffusers and returns. The supply air to the room enters through a closed loop fan system.

Figure 46. Test room for ventilation simulator.

1. OUTER ROOM
2. OUTER ROOM AMBIENT SIMULATOR
3. OUTER ROOM SUPPLY AIR DUCT
4. OUTER ROOM SUPPLY AIR DIFFUSER
5. OUTER ROOM RETURN AIR
6. INNER ROOM
7. INNER ROOM EXHAUST TO BE DUCTED TO INNER ROOM A/C SYSTEM
8. CONDENSING UNIT FOR INNER ROOM AIR CONDITIONING SYSTEM
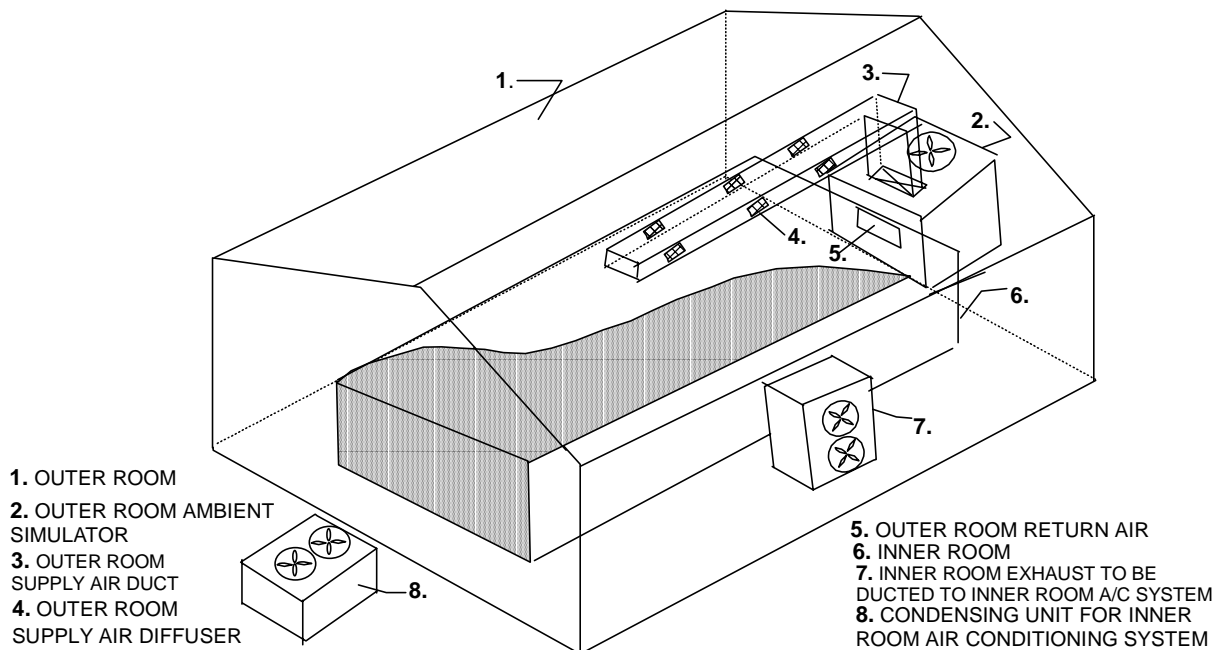
Eight halogen lamps were used to illuminate the aerosol test room so that the particle flow patterns were visualized and recorded. The light was controlled by eight cylindrical lenses installed in front of 1500 watt light bulbs. These lenses changed the five point light sources to a line light source. The lens focal length was 90 mm. the depth of the field was calculated as:

$$\delta = 4(1 + M)^2 \, f^2 \lambda$$

where δ is the depth of field, M is the camera magnification, f is the camera f-number, and λ is the wave length of the illumination light.

Figure 47. PIV/environmental chamber system schematic.
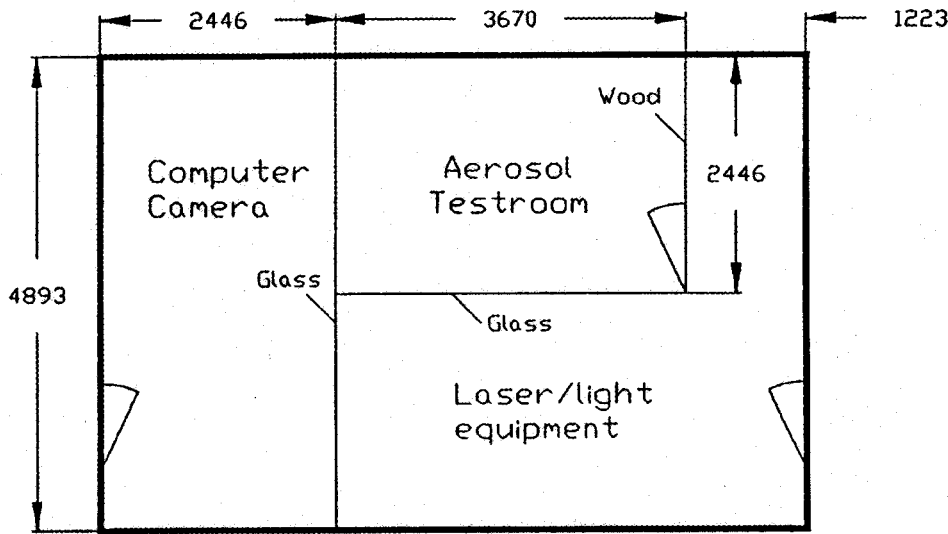
Room Ventilation Simulator (all dimensions are in mm).

To maximize the light intensity, the minimum value of the f-number was used in the experiments. The thickness of the light sheet was uniform and was chosen to be 50 mm as the depth of field. To reduce light scattering from the space around the lens, lamps were placed in an air ventilated box. The light resolution images of the flow patterns were captured with a Nikon N8008 AF35 mm camera. Light intensity, shutter speed, exposure time, and lens aperture were optimized so that relatively small particles were illuminated in the aerosol test room. The best exposure time determined experimentally was 1/30 sec.

Since room air flows have large inverse velocities, image shift techniques were used to determine the direction of velocity. The shift velocity was calibrated, using both stationary images and measurements of shift velocity. The velocity of shift (U_s) was determined by camera magnification (M) and maximum flow velocity (0.9 m/s) near the diffuser and by analysis of test images; minimum shift speed was determined. The camera was shifted by a step motor moving a constant speed of 0.2 m/s.

For velocity measurements, the acquired images were interrogated to obtain a velocity vector map. The images were processed by a computer system for the PIV. The PIV photograph

was divided into a high resolution grid of interrogation spots. Each spot contained a sufficient number of particle images defining a local, instantaneous velocity. The photographic analysis was done automatically with a DEC Microvax computer with an attached Numerix 432 array processor using a 2-D Fast Fourier Transform algorithm. A velocity vector map resulted from the image interrogation. From the velocity vector map, the flow pattern, velocity, turbulence of the flow field was calculated. The velocity vectors were sufficiently accurate to differentiate instantaneous out-of-plane vorticity fields. The velocity statistics obtained with the PIV system were in good agreement with those obtained by computer simulation and LDV measurements.

Three different types of particles were used to investigate aerosol transport in rooms. The first type was neutral, buoyant helium-filled bubbles, 1 mm in diameter, and generated by a bubble generation system. Since these bubbles behave as a low pass filter, the flow structure that was obtained is applicable only to particles greater than or equal to 1 mm. Flow structures smaller than 1 mm in diameter were extrapolated from the helium bubble results as average effects. The second type of particles used was plastic microspheres. These particles were heavier than air and ranged in size between 10 and 50 µm. The third type of particles was from the surrogate aerosols. The size ranges of these products were found to be between 25 and 500 µm. These particles also were heavier than air.

The HVAC system was operated for 30 minutes at each air change rate to ensure that room airflow had reached steady state conditions. Helium bubbles or the plastic microspheres, or the surrogate aerosols were seeded into the test room. When the density of particles reached the required value (5 to 7 bubbles/mm^2 for the helium bubbles), the light was switched on, the image shifting step motor started, and simultaneously the image was acquired. The step motor controlled by the computer triggered the camera automatically. The light was on only during image acquisition, 0.5 minutes. If a large number of images was needed for statistical analyses, the process was split into a few short sessions. The acquired images were analyzed by a completely automatic system incorporating a DEC Microvax computer with an attached Numerix 432 array processor. Velocity vector maps were obtained after the interrogation procedure. Statistical analysis was used to analyze the large amount of data.

Concentration measurements were done with a CCD camera, obtaining images of scattered light intensity from particles, an optical particle counter (CI-7350 from Climet Instruments) for system calibration, and a host computer for storing and analyzing the images (Figure 48). Because light intensity scattered by particles is proportional to their concentration, it was not necessary to resolve individual particles. The test was started with uniformly distributed particles. The image was acquired after the HVAC system was turned on. The time intervals between the images were kept constant. The particle images were first saved on hard disk and processed later. The particle concentration measurement was calibrated by using the optical particle counter to quantify the relationship between the particle concentration and the reflected light intensity.

Experiments were done for two dimensional, isothermal airflow conditions with air change rates of 5 and 10 air changes per hour (ACH). Depending on room structures, air flows and seeding particle density, 2000 to 8000 vectors were obtained for the size of the given two-dimensional view field. The small-scale structures of airflow are depicted in Figure 49. This capability is critical for the study of diffusion effects dominated by small structures in the indoor environment, which in turn is important for aerosol particle transport. From the obtained instantaneous airflow patterns, it can be demonstrated that room airflow is turbulent with low

Figure 48. PIV/environmental chamber measurement system schematic.
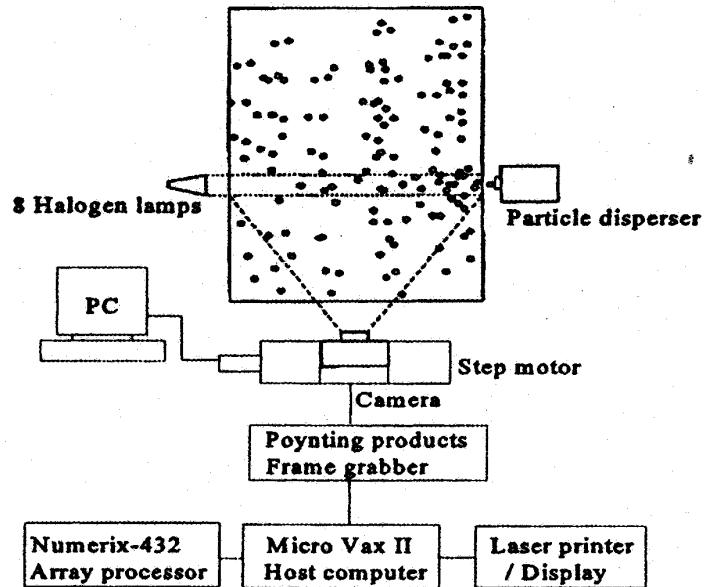
Figure 49. Vector map of instantaneous room air velocities at an air change rate of 5 ACH. The image is taken in the middle of the room.

63
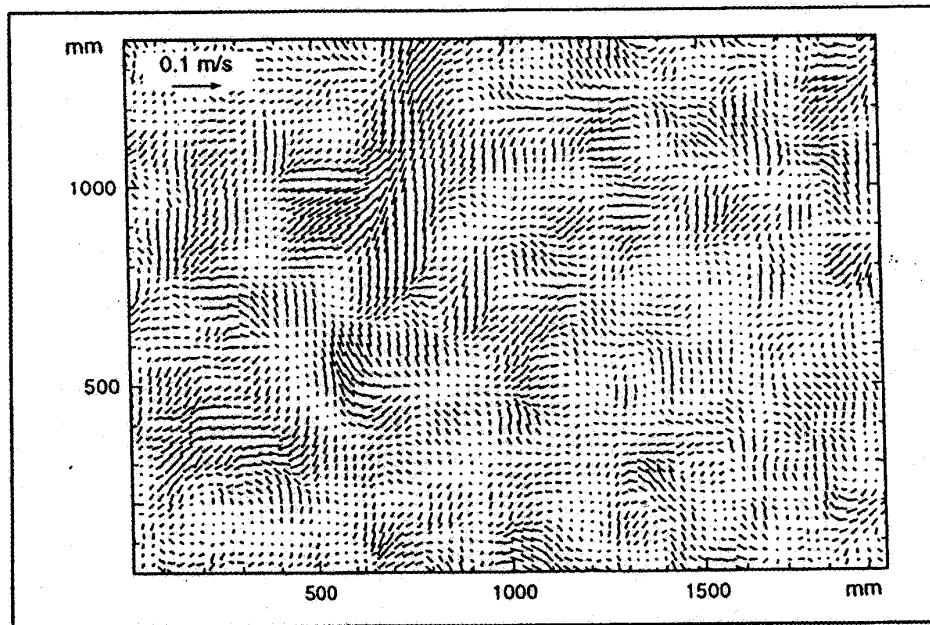
mean velocities and high velocity fluctuations. The system measures instantaneous and time-averaged velocity distribution in a view field of 2000 x 1500 mm with 1 mm seeded particles. Velocity statistics from PIV ensemble averaged vector maps show resemblance and good agreement with computer simulations and LDV measurements. The particle velocity was measured with an accuracy of 5%.

A contour plot of the particle concentration at 5 ACH are shown in Figure 50. Numbers in the plots are thousand particles per cubic feet. Although the concentration distribution of the particles was found to be complicated, the particle concentrations were denser in the lower part of the room and more dilute in the upper part of the room. This phenomenon is difficult to see in Figure 50, but could be visually observed and is evident in the concentration measurements (Figure 42). This is an important finding for designing products with the greatest efficacy. If the use site for the product is high in the room, less of the product will reach the use site; and therefore, more of the product will be required for satisfactory results. Nozzle designs can be evaluated and optimized using this technique.

The HVAC system and its design has an impact on the particle distribution and settling rate in rooms. The shape of the diffusers used to distribute the air in indoor space can affect the particle concentrations and settling within a room. Figure 51 shows what the impact of a circular diffuser has on particle concentrations. The concentration of particles in the air closer to the spray nozzle, decreased from time 0 to 4 minutes, but increased at greater than 1.6 m from the spray nozzle. This is probably due to the turbulent airflow suspended the particles. The data show that the particle movement is influenced by local airflow conditions.

Figure 50. Contour plot of instaneous particle concentration at an air change rate of 5 ACH. The images were taken in the middle of the room. (1 ft. = 3 m).

64
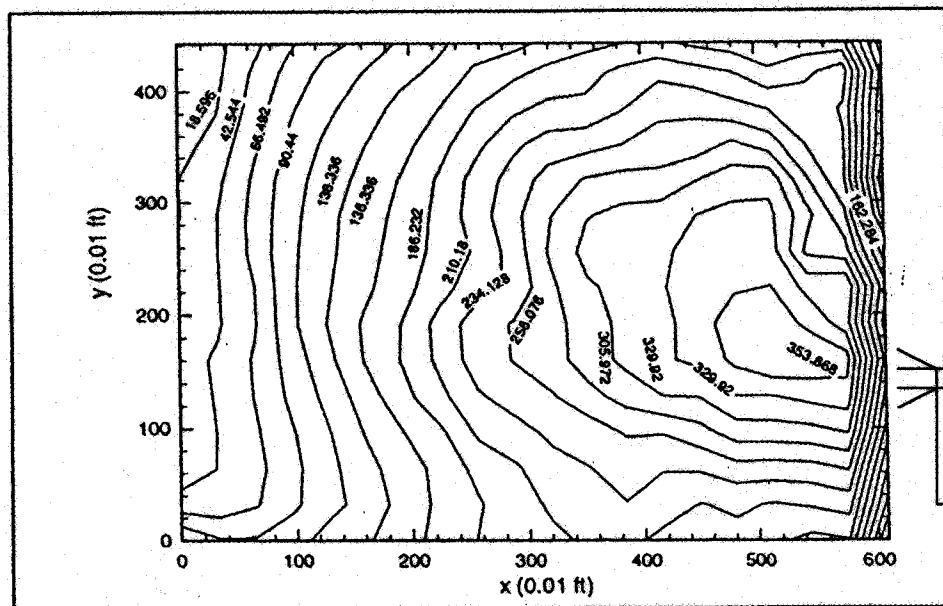
Figure 51. Normalized particle concentration in environmental chamber with a circular diffuser distributing the air.
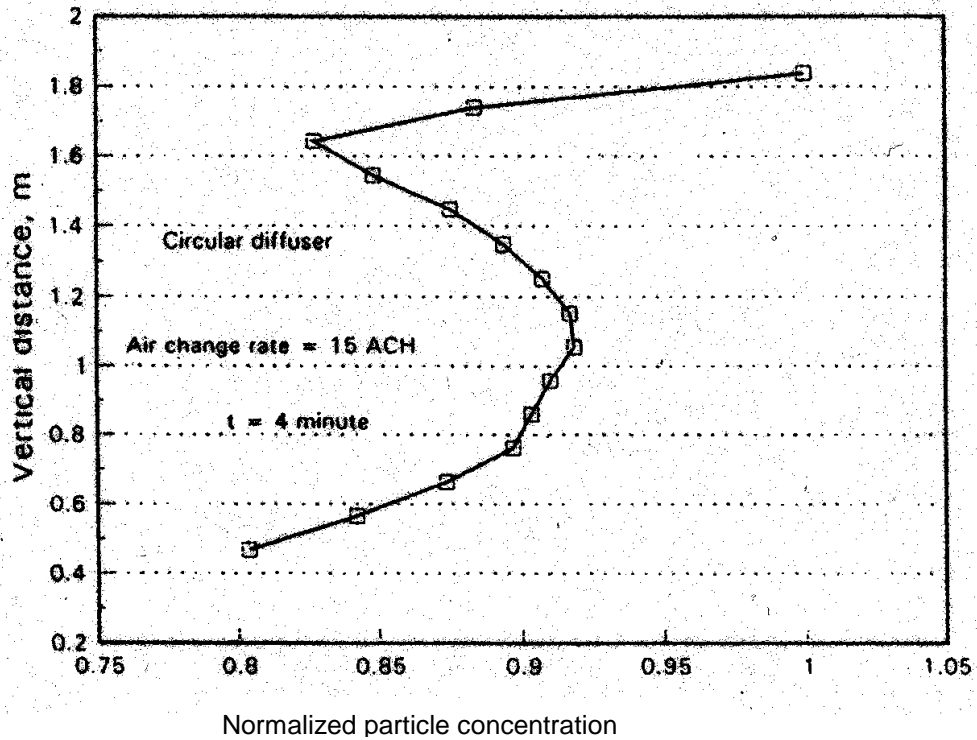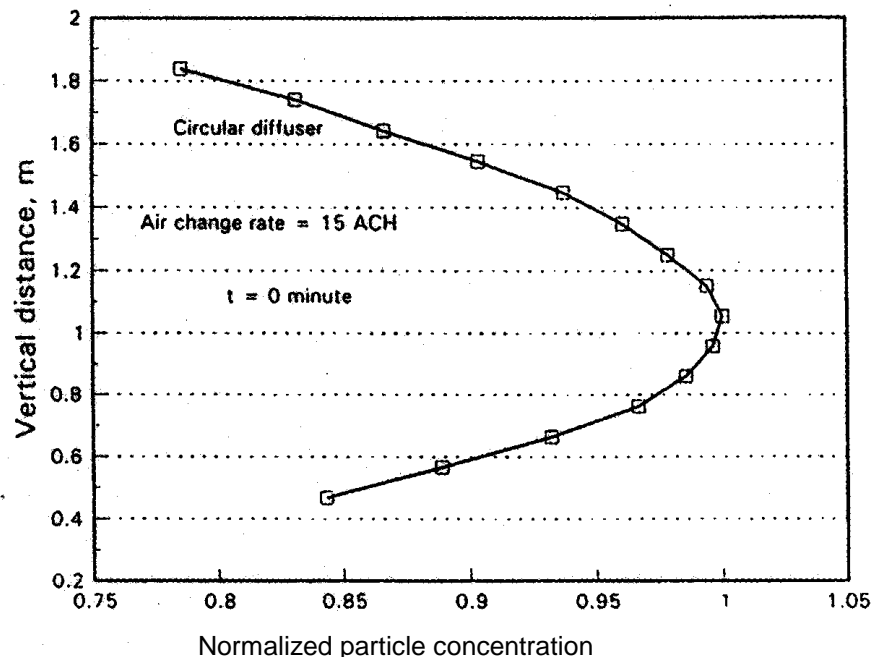
6.0 Technology Costs to Industry or Other Researchers

6.1 AMSI

Since the AMSI is not commercially available and must be machined, the costs are dependent upon the particular machine shop. In general the cost of the AMSI should be below $1000. The AMSI, in its current form, must be interfaced with a MS with particle beam or electrospray (or ion spray) capabilities, preferably with MS/MS capabilities. These systems range from $150,000 to $500,000 depending on the sophistication. Once the AMSI/MS system is operating, the analytical costs will range from a few tens to a few hundreds of dollars per sample. Analysis requires a few minutes of time per sample. Data interpretation requires the greatest amount of time and is dependent upon the skill and knowledge of the operator. As a laboratory builds a database of aerosol products, data interpretation can be cut down to a few minutes of time.

6.2 Aerosol Spray Pattern Characterization

The expense of the PIV imaging system is decreasing with the rapid developments of computer hardware and software techniques. There are considerable price and feature variations among companies manufacturing these systems. Table 11 and Table 12 show typical prices for the components needed. The argon laser, pulse generator, photo detector and peripheral instruments can be used in both velocity measurement and concentration measurement. These components cost $21,000-$23,000.

Table 11.   Aerosol particle concentration and size distribution in spray jets--PIV system costs.

Component	Quantity Needed	Price / Component
Video Camera	2	$2000-$3000
Frame Grabber	2	$4500-$5000
Argon Laser	1	$10000-$12000
Host Computer	1	$5000-$6000
Software	1	$2500
Pulse Generator	1	$5000
Photo Detector	1	$1000
Peripheral Equipment		$5000
Particle Counter	1	$10,000
TOTAL	10	$51,500 - $57,500

Table 12.   Aerosol particle velocity distribution in spray jets -- PIV system costs.

Component	Quantity Needed	Price / Component
Video Camera	1	$20000-$25000
Frame Grabber	1	$15000-$16000
Argon Laser	1	$10000-$12000
Host Computer	1	$10000-$15000
Software	1	$10000
Pulse Generator	1	$5000
Photo Detector	1	$1000
Peripheral Equipment		$5000
TOTAL	7	$76,000-$89,000

(A more expensive camera will be required for measurement of smaller particle sizes. Additional equipment and instrumentation will be required for three-dimensional analysis.)

The measurement frequency was 24 frames per second. For each surrogate aerosol product 240 frames were taken for concentration measurement and 24 frames for velocity measurements. After image acquisition procedure, the data are interpreted to extract velocity, size and concentration distribution information. This process requires about 6 hours for concentration information and 12 hours for velocity distribution information test.

The component costs for the PIV/environmental chamber system are decreasing with rapid development and costs vary for each component. Tables 13 and 14 approximate the current component prices.

During the velocity measurement procedure, 3 to 5 minutes are needed for each frame image. During concentration measurements, 10 frames of images can be taken in 1 second. For each type of surrogate aerosol product, 250 frames of images were taken for the concentration measurements, and 24 frames were taken for velocity measurements. For each aerosol test, the imaging time is about 1 hour for concentration distribution measurements and 3 hours for velocity measurements.

After the image acquisition procedure, the data are analyzed to obtain velocity, size and concentration distribution information. Normally, for concentration measurements, 10 frame images are taken as 1-minute transfers for average data, and as 10-minute transfer for concentration distribution data. For velocity measurements, one interrogation spot requires 0.3 second and one frame image containing nearly 10,000 vectors. Approximately 1 hour is required for a relative velocity vector map.   Therefore, it takes approximately 6 hours to obtain concentration information, and 26 hours to obtain velocity distribution information.

Table 13.   Aerosol particle concentration distribution in environmental chambers -- PIV system costs.

Component	Quantity Needed	Price / Component
Video Camera	1	$2000-$3000
Frame Grabber	1	$4500-$5000
Halogen Lamp	5	$20-$30
Host Computer	1	$5000-$6000
Software	1	$2500
Peripheral Equipment		$5000
Particle Counter	1	$10000
TOTAL	10	$29,100-$31,650

Table 14. Aerosol particle velocity distribution in environmental chambers -- PIV system costs.

Component	Quantity Needed	Price / Component
Sinar p2 4x5 Camera	1	$ 5000
Lens	1	$1400
Frame Grabber	1	$15000-$16000
Halogen Lamp	10	$ 20-$30
Host Computer and Software	1	$20000-$25000
Optical Instrument and Table	1	$20000
Peripheral Equipment		$5000
Position Control Motor	1	$10000
Negative Reading Video	1	$1000
Light Instruments		$5000
TOTAL	17	$82,600-$88,700

In order for a PIV system to detect smaller particle sizes and in three-dimensions, a more sophisticated camera is required. Table 15 estimates the cost of new PIV system.

Table 15. New PIV system costs for aerosol particle distribution measurement in an environmental chamber.

Component	Quantity Needed	Price/Component
Digital Camera	1	$15,000 - $20,000
Laser	1	$15,000 - $20,000
Host Computer	1	$10,000 - $15,000
Software	1	$10,000
Peripheral Equipment		$1,000
Pulse Generator	1	$5,000
Photo Generator	1	$1,000
TOTAL	6	$57,000 - $72,000

7.0. Quality Assurance

Quality assurance activities were an integral part of this research program. The work was conducted under the principles outlined in the U.S. Environmental Protection Agency's *AEERL Quality Assurance Procedures Manual for Contractors and Financial Assistance Recipients* (November 1991 Draft) and specifically applied to this research project through the "Quality Assurance Project Plan for "Application of Pollution Prevention Techniques to Reduce Indoor Air Emissions from Aerosol Consumer Products". The quality assurance plan was prepared, revised, and approved prior to onset of the laboratory portions of the research project.

This project is a Category IV project, a research and development project in support of a proof of concept. In this project tools and methods were developed for real-time characterization of aerosol consumer products. Since this was a developmental research project, specific quality objectives were developed during the project for each task based on the experimental objectives and good laboratory practices.

7.1 Project Description

This research project was a cooperative agreement among academia, government, and a group of Industry Partners (listed in Appendix 1). The primary objective of the project was to develop characterization tools and methodologies that can be used by manufacturers to develop pollution prevention strategies for aerosol consumer products. The Industry Partners stated that the tools would be used to "develop the most efficacious and least toxic" products. This objective was met by:

1. Designing the AMSI for spatial chemical compositional characterization of aerosol consumer products;
2. Application of PIV and PIV/environmental chamber technology to particulate characterization of aerosol consumer products; and
3. Transferring of the technology among industry, governmental agencies, and researchers.

The tools from this research project are the starting point for development of standard methods for aerosol analysis by the aerosol industry. Once these standard methods are developed, pollution prevention strategies can be formulated.

7.2 AMSI Development

The AMSI had to provide spatial chemical compositional data. The ability of the AMSI to provide quantitative data also had to be shown. In order to meet these requirements, standard aerosols were generated from authentic standard compounds of SLS, BC, ethanol, and water so that comparisons to the MS data from the surrogate aerosols and the authentic standards could be made. This ascertained that the MS identifications were accurate. Results from authentic standards obtained from a chemical supply house and from bulk standards obtained from the Industry Partners were compared. The bulk SLS standard from the Industry Partners contained a traceable impurity. This impurity was detected in the surrogate aerosols containing SLS. The spectra obtained from the surrogate aerosols had to match the spectra obtained from the authentic standards.

The standard aerosols were also used to generate a series of standards of known composition so that the potential for quantitation could be assessed, and to understand the limits

of the analytical system (Figure 2). These were generated in aerosol form with the OCN. The AMSI/MS was found to go out of linearity, severely affecting quantitation accuracy at greater than 80% aerosol composition.

Reproducibility of response was an additional issue for the AMSI. Multiple sprays of the surrogate aerosols into the AMSI/MS (Figure 16) determined reproducibility. Reproducibility was found to be within 5% of the standard deviation from the mean peak area. The greatest source of error was found to be the operator pushing the aerosol actuator button. With practice, an operator can achieve the 5% reproducibility. Reproducibility was determined by comparing the area counts from replicate analyses. The relative standard deviation was calculated from a minimum of five repetitive injections.

7.2.1 OCN Calibration

The particle size generated by the OCN was calibrated using the Malvern analyzer, which was calibrated using a standard calibrated glass graticule. The graticule was referenced to optical microscopy measurements, referenced to NIST standards. The chemical composition of the OCN generated aerosol was determined by comparison to flow injection of the authentic standards of SLS, BC, ethanol, and water. Flow injection was accomplished by using a syringe pump to flow the standard solution into the MS. All authentic standards were prepared in HPLC-grade methanol.

7.2.2 MS Calibration

The PBMS and API systems were tuned to manufacturers' specifications. (All instrument operators are trained in the tuning specifications of the instrument. The tuning instructions are available in the instrument manuals, which are stored in the rooms housing the MS's.) The PBMS systems used PFTBA to calibrate with tuning algorithms supplied with the instruments. The API was tuned to manufacturers' specifications for a mixture of polyethylene glycols. The tuning parameters of each MS were adjusted for maximum sensitivity for detection of SLS by flow injection of an SLS authentic standard. (Authentic standards were analyzed for each of the analytes in the surrogate aerosols, but tuning with SLS optimized the analytical system for the aerosol analyses. SLS had the lowest instrumental response of the surrogate analytes. By maximizing on SLS, maximum sensitivity was achieved.) Instrument calibrations were performed daily for each day of operation for multiple points. The instruments had to achieve calibration within 5% of the tuning specifications before analyses were performed. These specifications included peak height, peak shape, and isotopic abundance of at least four ions in the calibration compounds. If an instrument did not achieve the specified response, corrective maintenance procedures were taken prior to sample analyses.

7.3 PIV Analyses

The PIV and PIV/environmental chamber systems had to provide accurate velocity measurement data for the calculation of particle concentration distribution data. Table 16 summarizes the capability and accuracy of the PIV measurement system. The velocity measurements obtained from the PIV were compared, whenever possible, to LDV data, a more conventional method of analysis. Particle concentration measurements were calibrated with an optical particle counter, which is calibrated by the manufacturer. These data were compared with aerodynamic particle sampler data. The experimental derived velocity statistics were compared to computer simulations and LDV measurements. The laser generator, controller, pulse generator, photodetector, cameras, frame grabbers, and host computer were tested according to the manufacturers' specifications. Each operator was trained in the proper operation and testing of the instrumentation. The system was referenced to known standards.

Precision of the measurements was obtained by collecting the samples in replicate to reduce experimental error. For the velocity measurements, 24 replicates were done and the data were averaged. Ten to 12 replicates were performed for the concentration measurements. The number of replications was based on an analysis of variance based on the F-test among the replications.

Statistical data analysis techniques were used to process the measurement data. This reduced the measurement errors to within 5% limits and established confidence in accuracy of the analytical results. Standard data processing programs were used to obtain the concentration contour plots, velocity vector maps, and the size distribution curves as a function of time and spatial location.

7.3 Surrogate Aerosols

The surrogate aerosols were supplied in two batches to the university researchers. Stability, based on chemical composition, was monitored by MS analysis. Early in the project, it was found that the surrogate aerosols using carbon dioxide as the propellant were unstable, since corrosion prohibitors were not included in the surrogate aerosols. These surrogate aerosols were used within a few days of receipt and then not used again during the project. Replicate analyses were used to monitor the stability of the other surrogate aerosols. Differences between the surrogate aerosol batches were less than 10%, and were considered to be insignificant, since this was a method development project. The surrogate aerosols were merely a means to develop the tools and methodologies, rather than being exact measurements. Uniformity between batches sent to the two university laboratories was not an issue since each laboratory developed tools for different characterization issues.

Table 16. Summary of PIV system capability and accuracy.

AEROSOL JET MEASUREMENT SYSTEM					
	View Field	**Capability**	**Accuracy**	**Evaluation**	**Alternate Measurement Methods**
Size Distribution	11.0 x 7.5 mm 200 x150 mm	>1 μm > 18 μm	Varies inversely with particle size	Approximates a point measurement technique	Particle Counter, Malvern Analyzer No alternate whole field method
Concentration	200 x 150 mm	Depends on calibration system. Accuracy of relative concentration measurement is high			
Velocity	200 x 150 mm	> 18 μm	5%	Capable of measuring air & particle velocity as a function of particle size & density	No alternate whole field method
ROOM AIR MEASUREMENT SYSTEM					
Concentration	200 x 150 mm 2000 x1500 mm	Depends on calibration system. Accuracy of relative concentration measurement is high		Cannot resolve individual particles	
Velocity	200 x 150 mm	> 18 μm > 180 μm	5%	Capable of measuring air & particle velocity as a function of particle size & density Capable of measuring velocities of room air & large particles in large flow fields	No alternate whole field method

8.0 References

1.   U.S. EPA. *Unfinished Business: A Comparative Assessment of Environmental Problems*, EPA-230/2-87-025a-e (NTIS PB88-127030). Office of Policy, Planning and Evaluation, Washington, DC, 1987.

2.   U.S. EPA. *Reducing Risk: Setting Priorities and Strategies for Environmental Protection*, SAB-EC-90-021. Science Advisory Board. Washington, DC, 1990.

3.   Pollution Prevention Act of 1990, Public Law No. 0-508, Vol. 42 U.S.C. Sec 13101-13109. (West Supp. 1991). 1990.

4.   Habicht, Henry F., II. *Memorandum: EPA Definition of Pollution Prevention*. U.S. EPA, May 28, 1992.

5.   Chemical Specialties Manufacturers Association. *The Consumer Products Handbook*. Inc., Washington, DC, 1992.

6.   Spurny, K.R. *Physical and Chemical Characterization of Individual Airborne Particles*; K.R. Spurny, Ed.; Halsted, a division of John Wiley & Sons, New York, NY, 1986; p. 17.

7.   Lehtimaki, M., and Willeke, K. "Measurement Methods." In *Aerosol Measurement: Principles, Techniques, and Applications*, ed. K. Willeke and P.A. Baron, Van Nostrand Reinhold, New York, NY, 1993, p. 112-145.

8.   White, A.W.C., Martin, R., and Lowe, J.A. The importance of particle size analysis in spray systems. *Spray Technology, Product Development/International*, 1993.

9.   Graynor, A. Spray Pattern Duality: A Scientific Dilemma. *Research & Development*, 1993.

10.   Spagnolo, G.S., and Paoletti, D. Automatic system for three fractions sampling of aerosol particles in outdoor environments. *J Air & Waste Management Assoc* **44**: 702-706 (1994).

11.   Chemical Specialties Manufacturers Association. *Aerosol Guide*, 7th edition, Washington, DC, 1981, p. 119-120.

12.   Chemical Specialties Manufacturers Association. *Aerosol Guide*, 7th edition, Washington, DC, 1981, p. 121-123.

13.   Chemical Specialties Manufacturers Association. *Aerosol Guide*, 7th edition, Washington, DC, 1981, p. 77-78.

14.   Nordmeyer, T., and Prather, K.A. Real-time measurement capabilities using aerosol time-of-flight mass spectrometry. *Anal Chem* **66:** 3540-3542 (1994).

15.   Prather, K.A., Nordmeyer, T., and Salt, K. *Anal Chem* **66:** 1403-1407 (1994).

16.   Winkler, P.C., *et al. Anal Chem* **66**: 1403-1407 (1994).

17.   Lui, D.Y., Rutherford, D., Kinsey, M., and Prather, K.A. Real-time monitoring of pyrotechnically derived aerosol particles in the troposphere. *Anal Chem* **69**: 1808-1814 (1997).

18.   Qian, M.G., and Lubman, D.M. *Anal Chem* **67:** 234A-242A (1994).

19.   Dorman, S. Spray Technology & Marketing's 10th annual new product roundup. *Spray Technology & Marketing*, August: 24-40 (1993).

20.   Creaser, C.S., and Stygall, J.W. Particle beam liquid chromatography-mass spectrometry: Instrumentation and applications. *Analyst* **118**: 1467-1480 (1993).

21.   Noble, C.A., *et al.* Aerosol characterization using mass spectrometry. *Trends in Analytical Chemistry* **13**: 218-222 (1994).

22.   Bayer, C.W., *et al.* Design of an aerosol mass spectral interface. *Engineering Solutions to Indoor Air Quality Problems*, Air & Waste Management Association, **1997**, in press.

23.   Veltkamp, P.R., *et al. J Geophy Res* **101 (D14)**: 19495-19504 (1996).

24.   Henry, R.C., *et al. Atmos Environ* **18:** 1507-1515 (1984).

25.   Breiman, L., *et al. Classification and Regression Trees*, Wadsworth Int. Group, Belmont, CA, 1984.

26.   Breiman, L. *Automatic Identification of Chemical Spectra*, Technical Report, Technology Service Corporation, Santa Monica, CA, 1978.

27.   Huang, E.C., *et al.* Atmospheric pressure ionization mass spectrometry. *Anal Chem* **62**: 713A-724A (1990).

28.   Wachs, T., *et al.* Liquid chromatography-mass spectrometry and related techniques via atmospheric pressure ionization. *J of Chromatog Sci* **29**: 357-369 (1991).

29.   McLuckey, S.A., Glish, G.L., and Grant, B.C. Simultaneous monitoring for parent ions of targeted daughter ions: A method for rapid screening using mass spectrometry/mass spectrometry. *Anal Chem* **62**: 56-61 (1990).

30.   Wiloughby, R.C., and Browner, R.F. *Anal Chem* **56**: 2626 (1984).

31.   Ho, S.Z. *Aerosol sample introduction mass spectrometry*. Ph.D. Dissertation, Georgia Institute of Technology, Atlanta, GA. August 1997.

32.   John, W. "The Characteristics of environmental and laboratory-generated aerosols." In *Aerosol Measurement: Principles, Techniques, and Applications*, ed. K. Willeke and P.A. Baron, Van Nostrand Reinhold, New York, NY. 1993, p. 60.

33.   Cui, M.M., *et al.* A study of structure of spray cones utilizing digital particle image velocimetry. *Engineering Solutions to Indoor Air Quality Problems VIP-51*, Air & Waste Management Association, **1995:** pp. 214-225.

34.   Lee, R.E., Jr. *Science.* **178:** 567-575, 4061 (1972).

35.   Wiener, B.B. "Particle and droplet sizing using Fraunhofer diffraction." In *Modern Methods of Particle Size Analysis*. Ed. H.G. Barth, John Wiley & Sons, New York, NY, 1984.

36.   Adrian, R.J. Particle-imaging techniques for experimental fluid mechanics. *Annual Review of Fluid Mechanics* **23**: 261-304 (1991).

37.   Keane, R.D., and Adrian, R.J. Optimization of particle image velocimeters. Part II: Multiple pulsed systems. *Measurement Science and Technology* **2:** 1202-1215 (1990).

38.   Meinhart, C.E., Prasad, A.K., and Adrian, R.J. A parallel digital processor system for particle image velocimetry. *Measurement Science and Technology* **4**: 619-626 (1993).

39.   Cui, M.M., *et al.* A novel, whole-field, non-intrusive diagnostic technique for improvement of indoor air quality. *Engineering Solutions to Indoor Air Quality Problems VIP-51*, Air & Waste Management Association, **1995**; pp. 95-99.

40.   Wu, J., *et al.* Adjustable room ventilation simulator for room air and air contaminant distribution modeling. *Indoor Air'90. Proceedings of the Fifth International Conference on Indoor Air Quality and Climate* **4**b: 237-242 (1990).

41.   Bayer, C.W., and Browner, R.F. Characterization of aerosol consumer products. *Engineering Solutions to Indoor Air Quality Problems VIP-51*, Air & Waste Management Association, **1995**; pp. 205-207.

42.   Hinze, J.O. *Turbulence*, 2nd ed., McGraw-Hill, New York, NY, 1975, p. 790.

9.0. Appendix 1

Industry Partners

1. Armin Clobes, Ph.D. (Chair)
   SC Johnson Wax
   1525 Howe Street, MS 145
   Racine, WI 53404
   414-631-2351   FAX: 414-631-4428

2. G.P. Ananth
   SC Johnson Wax
   1525 Howe Street, MS 145
   Racine, WI 53404
   414-631-2113   FAX: 414-631-4015

3. Ron M. Davis
   CCL Custom Manufacturing
   1 West Hegeler Lane
   Danville, IL 61832
   217-442-1400   FAX: 217-442-0902

4. John DiFazio
   Chemical Specialties Manufacturers Association, Inc.
   1913 Eye Street, NW
   Washington, DC 20006
   202-872-8110   FAX: 202-872-8114

5. Douglas Dykstra
   Guardsman Products, Inc.
   2960 Lucerne, SE
   Grand Rapids, MI 49546
   616-285-7857   FAX: 616-285-7870

6. William A. Frauenheim III
   Diversified CPC International, Inc.
   PO Box 490
   Channahon, IL 60410
   815-423-5991   FAX: 815-423-5627

7. Larry Jacobs
   Procter and Gamble
   5299 Spring Grove Avenue
   Cincinnati, OH 45217
      513-627-6090   FAX: 513-627-6668

8. Carleen Kreider
   Seaquist Valve
   1160 N. Silver Lake Road
   Cary, IL 60013
      708-639-2124   FAX: 708-639-1186

9. Robert P. Paulein
    Chemical Specialties Manufacturers Association, Inc.
    1913 Eye Street, NW
    Washington, DC 20006
    202-872-8110   FAX: 202-872-8114

10. Douglas Raymond
    Sprayon Products
    26300 Fargo Avenue
    Bedford Heights, OH 44141
    216-498-6049   FAX: 216-498-6140

11. Bryan R. Ruble
    SC Johnson Wax
    1525 Howe Street, MS 122
    Racine, WI 53403
    414-631-2443   FAX: 414-631-3752

12. Dennis Stein
    3M Company
    3M Center Building, 225-3N-02
    St. Paul, MN 55144-1000
    612-736-1596   FAX: 612-736-9278

13. Laura Vaccaro
    Reckitt and Colman
    1 Philips Parkway
    PO Box 425
    Montvale, NJ 07645-0425
    201-573-636   FAX: 201-573-6046

14. Theodore Wernick
    Gillette Company
    401 Professional Drive
    Gaithersburg, MD 20879
    301-590-1543   FAX: 301-590-1535

15. Jesse Williams
    Bissell, Inc.
    PO Box 1888
    Grand Rapids, MI 49501
    616-791-7740   FAX: 616-453-1383